

# Who Bears Rising Commercial Property Insurance Costs?

July 2, 2026

Minjoo Kim

Prateek Mahajan

Zirui Wang

McCombs School of Business

University of Texas at Austin

## Abstract

Using a novel set of property-level operating statements for multifamily properties, we document a large and widespread rise in commercial property insurance costs, with annual growth exceeding 15% since 2019, and study who bears these costs along three margins. First, the burden varies across locations: regions with greater local disaster risk, higher exposure to reinsurance-market shocks, and greater homeowners insurance regulatory frictions experience larger increases in commercial insurance costs. Second, the burden is shifting from tenants toward owners. Rent increases initially offset nearly all insurance-cost increases, but this response has weakened sharply over time; larger and more recent shocks are increasingly associated with lower profitability and lower transaction prices. Third, the burden is uneven across owners. Larger owners and those with lower-risk portfolios obtain more favorable pricing, even for the same property and especially in high-risk locations; these advantages have grown over time and are associated with the reallocation of high-risk assets toward larger owners. Together, the results show that commercial insurance repricing is not merely a cost shock: because coverage is required and owner identity affects pricing, it also shapes cash-flow incidence, asset values, and the allocation of climate-exposed real assets.

The authors thank Aydoğ̃an Altı, William Fuchs, Shan Ge, Caitlin Gorback, Richard Green (discussant), John M. Griffin, Joseph Gyourko, Samuel Kruger, Xiang Li (discussant), Yifei Li (discussant), Kevin Mei, Jon Moreno-Medina, Philip Mulder, Simon Oh, Adriano Rampini, Glenn Rudebusch, Parinitha Sastry (discussant), Yang Shi (discussant), Clemens Sialm, Laura Starks, Tim Stumhofer, Lin Tang (discussant), Ana-Maria Tenekedjjeva, Sheridan Titman, Alex Van De Minne (discussant), Nancy Wallace, Charles Yang (discussant), Yiyuan Zhang (discussant), and conference and seminar participants at the American Finance Association (AFA) Annual Meeting (PhD Poster Session), American Real Estate and Urban Economics Association (AREUEA) Conference, Baruch-JFQA Climate Finance and Sustainability Conference (Poster Session), Boca Finance and Real Estate Conference, Brookings Insurance Task Force Meeting, Conference on Sustainable Finance at Deakin University, Financial Intermediation Research Society (FIRS) Conference (PhD Session), Financial Management Association (FMA) Annual Meeting, Georgia Tech & Atlanta Fed Household Finance Conference (Young Scholar Poster Session), MRS International Risk Conference, Southern Finance Association (SFA) Annual Meeting, USC Marshall PhD Conference in Finance, UT Dallas Fall Finance Conference (PhD Poster Session), the University of Texas at Austin, and the University of Texas at San Antonio for their helpful comments. They gratefully acknowledge financial support through two research grants, from (1) the Brookings Institution as part of the Hutchins Center on Fiscal and Monetary Policy's project on the "Challenges Climate Change Poses to U.S. Property-Casualty Insurance and Housing Markets" and (2) the Real Estate Research Institute. This paper was previously circulated as "The Rise in Insurance Costs for Commercial Properties: Causes, Effects on Rents, and the Role of Owners." *First version: November 19, 2024.*

The Brookings Institution is committed to quality, independence, and impact. We are supported by a [diverse array of funders](#). In line with our [values and policies](#), each Brookings publication represents the sole views of its author(s).

# 1 Introduction

Property insurance is a cornerstone of real estate markets. By transferring risk away from property owners and lenders, it stabilizes cash flows and supports credit provision in the face of rare but costly disasters (Sastry and Sen, 2025). That stabilizing role is under growing strain. As the frequency of billion-dollar disasters in the United States has surged, rising from roughly 3 per year in the 1980s to an average of 23 per year since 2020, commercial property insurance has undergone a dramatic repricing.<sup>1</sup> Since 2019, average insurance costs have grown by more than 15% annually, peaking at nearly 30% in 2023. This pattern points to a persistent increase in the cost of insuring commercial real estate, with far-reaching consequences for tenants, property owners, operating cash flows, asset values, and credit markets. Yet despite the scale of the commercial real estate sector, we know relatively little about how the burden of rising insurance costs is distributed across locations, between tenants and property owners, across owners, and through changes in the ownership of climate-exposed properties.<sup>2</sup>

In this paper, we use a large, novel set of property-level operating statements from Agency Commercial Mortgage-Backed Securities (CMBS) deals to study who bears rising insurance costs in multifamily housing along three margins. First, we document three supply-side dimensions along which insurance-cost increases differ across locations: insurers place greater weight on local disaster exposure after the large 2017–2018 loss years, rising reinsurance costs amplify price increases in states with greater reinsurance exposure, and regulatory frictions in the homeowners insurance market spill over into commercial policies. Second, we examine how the burden is divided between tenants and property owners. Early in the sample, nearly all of the insurance-cost increase is reflected in rents; as shocks become larger in recent years, however, most of the increase is associated with lower net operating income (NOI), lower transaction prices, and higher cap rates, consistent with markets capitalizing persistent NOI compression. The rent response is also systematically stronger in markets with more inelastic supply, among owners with greater local market share, in areas with greater moving frictions, and in areas with fewer tenant outside options. Third, we study how the burden differs across property owners. Larger owners and those with lower-risk portfolios obtain more favorable insurance pricing, even for the same property and especially in high-risk locations. As these advantages intensify over time, high-risk properties held by smaller owners become more likely to be sold and, conditional on sale, are increasingly acquired by larger buyers, linking insurance repricing to ownership reallocation. Thus, our central contribution is not simply to document rising commercial insurance costs, but to show how repricing is associated with differences in the burden borne across locations, between tenants and property owners, and across property owners, including through ownership reallocation.

The commercial sector provides a particularly informative setting for studying climate-risk repricing. Commercial lines are less constrained by state rate regulation than homeowners insurance (Born and Klimaszewski-Blettner, 2013; Kim, Leverty, and Liu, 2025), and Agency CMBS loan covenants require comprehensive insurance coverage, limiting the scope for borrowers to respond by reducing coverage or self-insuring. The setting also allows us to study spillovers across insurance lines: commercial pricing is shaped not only by local physical risk and reinsurance markets, but also by regulatory frictions in the homeowners insurance market. Finally, multifamily properties separate owners from tenants and allow ownership to change while the physical asset remains fixed, making it possible to go beyond whether climate risk is priced and study how a mandatory insurance shock is reflected in rents, NOI, asset values, and ownership allocation.

We begin by documenting that the rise in insurance costs is large, national, and not unique to multifamily properties. The largest increases appear in coastal states such as Florida, Texas, Louisiana, and California, but substantial increases also appear in inland markets exposed to non-coastal hazards such as flood, wildfire, hail, and convective storms. The increase is therefore broader than a coastal-climate story. This establishes the aggregate shock and the substantial regional heterogeneity that motivate the rest of the analysis.

---

<sup>1</sup> Disaster damage estimates are from the National Centers for Environmental Information (NCEI) and have been adjusted for inflation to 2024 dollars using the CPI. See [here](#) for more details.

<sup>2</sup> The CRE market is valued at \$22.1 trillion as of 2026 (Board of Governors of the Federal Reserve System, 2026). While the rise in homeowners insurance premiums is now well documented (e.g., Keys and Mulder, 2025), we know much less about insurance dynamics in the commercial real estate sector. Sastry and Sen (2025) highlight that “understanding the exposures of firms and the extent to which commercial insurance markets help mitigate exposures is largely unexplored.”

The first margin is how the rise in insurance costs varies across locations. We document three supply-side patterns. First, insurance pricing increasingly reflects exposure to local natural disaster risk. Using tract-level data from FEMA’s National Risk Index, we find that properties in high-risk areas experience significantly larger increases in insurance costs, particularly after 2018. Before 2018, insurance costs are relatively insensitive to local risk measures. From 2018 onward, however, they become much more sensitive to risk exposure.<sup>3</sup> The same break appears when we use realized disaster damages rather than forward-looking risk measures, indicating that insurers place substantially greater weight on local climate risk after 2018.

Second, rising reinsurance costs amplify this repricing by increasing the cost of supplying insurance in places more exposed to correlated catastrophe risk (Keys and Mulder, 2025). We show that the increased pricing of local risk closely tracks the rising price of reinsurance and that states with greater ex ante exposure to reinsurance markets, such as Florida, Louisiana, and Texas, experience significantly larger cost increases when reinsurance prices rise. A common increase in national reinsurance costs therefore does not affect all properties equally; it has the largest effect in riskier locations within states whose insurers rely more heavily on reinsurance markets. In our triple-interaction design, a 10-index-point increase in national reinsurance costs has an effect on insurance cost per unit that is roughly 2.5 times as large in high-exposure states as in low-exposure states, holding local risk fixed.

Third, comparing commercial property insurance to homeowners insurance, which has been the primary focus of the existing literature, we find that commercial insurance costs have risen substantially faster in nearly every county. Specifically, from 2019 to 2022, 95% of the population lives in counties where the increase in commercial insurance costs is at least twice as large as the increase in homeowners insurance costs. This widening gap is consistent with homeowners-market frictions muting observed repricing in residential lines through both direct rate constraints (Oh, Sen, and Tenekedjieva, 2025) and changes in effective coverage, while commercial insurance pricing is better able to adjust. In line with this interpretation, the relative-pricing wedge between commercial and homeowners insurance widens with local risk in states with high homeowners-market frictions, but not in low-friction states. We also show that after major disasters, commercial insurance cost growth is roughly 19–22 percentage points (ppt) larger on the high-friction side of a state border, consistent with cross-product subsidization from constrained homeowners lines into commercial policies.

The second margin is how rising insurance costs are divided between tenants and property owners. Although higher insurance expenses create pressure to raise rents, our estimates point to increasing constraints on owners’ ability to do so. In the baseline specification, roughly 49% of the increase in insurance costs is reflected in rents on average; more demanding CBSA-by-class-by-year specifications imply smaller shares of roughly 37–39%. The rent response is stronger in markets with more inelastic housing supply, for owners with higher local market share, in areas with greater moving frictions, and in areas with fewer tenant outside options, while the corresponding NOI declines are larger where the rent response is weaker. Further, there is substantial time-series variation: the rent response is concave and has declined sharply over the last decade. By 2024, the marginal rent response to insurance cost increases is near zero. A 10% increase in insurance costs that is associated with a 0.35% increase in rents in 2014 is associated with only a 0.02% increase by 2024. Conversely, the NOI decline associated with a 10% increase in insurance costs grows to more than 0.95% by 2024. Taken together, the estimates point to pass-through limits that leave a larger share of the insurance-cost burden on owners through lower NOI, especially in the most exposed markets.

By combining these time-varying response estimates with the distribution of annual insurance-cost growth, we quantify the implied cumulative effects on rents and profitability. The average impact over 2014–2024 is relatively modest, amounting to a 0.9% increase in rents and a 5.1% decline in NOI. In the areas most affected by rising costs, however, the implied effects are substantial. At the 95th percentile of the insurance-cost-increase distribution, the estimates imply an 11% increase in rents and a 26% decline in NOI over this decade-long period. These profitability effects are also reflected in transaction markets: riskier properties trade at lower transaction prices and higher cap rates relative to the pre-2018 period.

<sup>3</sup> As shown in Figure IA.11, property damages spike around 2017–2018, indicating a discrete increase in realized exposure around the timing of the repricing break. This period also coincides with a broader hardening of property insurance and reinsurance markets. We interpret the post-2018 shift in pricing behavior as consistent with insurers placing greater weight on catastrophe exposure after these large loss years.

Thus, insurance repricing is reflected in current cash flows and in the capitalization of climate risk into asset values.

The third margin is how the burden varies across property owners. Larger property owners pay lower per-unit insurance costs than smaller owners, a pattern consistent with economies of scale, stronger insurer relationships, risk-management differences, or greater bargaining power in insurance procurement. This advantage is particularly pronounced in high-risk areas, where insurance repricing is most severe and scale appears most valuable. Insurance costs also vary with the owner’s broader portfolio risk. Higher-risk properties face lower insurance costs when held in lower-risk owner portfolios, even after controlling for the risk of the focal property. This relationship varies sharply by owner size: small owners experience little cost advantage from holding lower-risk portfolios, while large owners with lower average portfolio risk secure significantly lower insurance costs. These findings therefore point to portfolio composition mattering most when coupled with scale.

These relationships are not solely cross-sectional. Within continuing ownership relationships, increases in owner size are associated with lower insurance costs for incumbent properties, while increases in portfolio risk are associated with higher costs, especially for higher-risk assets. Insurance costs also fall discretely following portfolio-level mergers and acquisitions (M&A), with the largest post-acquisition savings appearing when the acquirer-target owner-size gap is largest, acquired properties are riskier, and the acquisition produces a larger reduction in portfolio risk.

These owner-level pricing advantages increasingly coincide with a reallocation of high-risk properties toward larger owners with apparent advantages in managing mounting expenses. Through the late 2010s, the cost advantage large owners enjoy is relatively uniform across risk categories. Since 2020, as insurance-cost growth accelerates, this advantage narrows for low-risk properties while expanding significantly in high-risk locations. After 2018, high-risk properties owned by smaller owners become more likely to change hands and, conditional on sale, are increasingly acquired by larger buyers. Consistent with these patterns, ownership of high-risk properties shifts toward larger entities that appear better able to obtain favorable insurance pricing and manage higher costs.

This reallocation margin distinguishes insurance from many other operating-cost shocks, such as property taxes: owner identity affects the insurance cost itself, rather than only the ability to absorb a given cost. The result is a growing role for large owners in high-risk markets and a direct link between climate-risk repricing, profitability, and the ownership structure of high-risk assets.

While recent work has focused primarily on homeowners insurance (e.g., [Oh, Sen, and Tenekedjjeva, 2025](#); [Keys and Mulder, 2025](#); [Sastry, Scharlemann, Sen, and Tenekedjjeva, 2025](#)), our findings show that commercial insurance markets are a central channel through which climate risk affects real estate outcomes. Because insurance is a required input for multifamily finance, repricing is reflected not only in insurance expenses, but also in rents, NOI, property valuations, required yields, and ownership patterns. By raising operating expenses and compressing NOI, rising insurance costs may weaken the income-return component that has historically made commercial real estate attractive to institutional capital.

**Related Literature.** Our paper contributes to four main strands of literature, speaking directly to the agenda outlined in [Sastry and Sen \(2025\)](#) by providing asset-level evidence on who bears rising commercial insurance costs: which locations face larger increases, how costs are divided between tenants and property owners, how the burden varies across owners, and how ownership of exposed assets changes. First, we add to the literature on insurance supply and pricing, which has focused primarily on homeowners insurance and climate risk. Recent studies emphasize the role of regulation, information, and insurer balance-sheet constraints in shaping premiums and supply. For instance, [Oh, Sen, and Tenekedjjeva \(2025\)](#) highlight the role of regulation and cross-subsidies in homeowners insurance, while [Boomhower, Fowlie, and Plantinga \(2023\)](#) emphasize how information asymmetries complicate the alignment of premiums with underlying risk. Similarly, [Ge \(2022\)](#) uses evidence from weather and life insurance to study how financial constraints affect pricing strategies, and [Sen \(2023\)](#) and [Sen and Humphry \(2020\)](#) show that insurance regulation can alter risk management, underwriting, product composition, and market concentration. We build on foundational work on capital constraints in reinsurance markets and financial frictions in insurance ([Froot, 2001](#); [Kojien and Yogo, 2015](#)).<sup>4</sup>

<sup>4</sup> Our reinsurance results also connect to classic work on insurance-market capacity and catastrophe pricing, which emphasizes that shocks to intermediary capital can generate cyclical hard markets and sharp increases in the price of bearing catastrophe risk

Commercial real estate insurance remains relatively understudied, even though it offers a useful complement to the homeowners setting. Commercial lines are less constrained by rate regulation (Born and Klimaszewski-Blettner, 2013), and lender-mandated coverage requirements limit endogenous take-up responses: unlike homeowners facing rising premiums, who may reduce coverage or self-insure (Cookson, Gallagher, and Mulder, 2025; Sastry et al., 2025), CMBS borrowers are subject to comprehensive, “all-risk” insurance requirements. Our supply-side tests show that mechanisms emphasized in homeowners insurance markets—risk repricing, reinsurance exposure, and regulatory frictions—also matter in commercial lines. We then trace how these insurance-market forces are reflected in commercial real estate cash flows, asset values, and the reallocation of properties across owners.

Second, we contribute to the literature on climate finance and real estate by identifying insurance as a central transmission channel through which climate risk affects property cash flows. Prior studies show that climate risk influences a broad range of real estate and financial market outcomes, including property values, mortgage terms, borrower composition, credit outcomes, and corporate bond pricing (Bakkensen and Barge, 2021; Bernstein, Gustafson, and Lewis, 2019; Murfin and Spiegel, 2020; Sastry, 2026; Seltzer, Starks, and Zhu, 2026; Ge, Johnson, and Tzur-Ilan, 2026). Other work shows that climate risk affects mortgage delinquency and commercial real estate valuations, including through physical-risk penalties and realized-disaster effects (Holtermans, Kahn, and Kok, 2024; Foerster, Ryan, and Scheid, 2025; Fang, Li, Scofield, and Yavas, 2024). Sastry, Sen, and Tenekedjieva (2026) study how mispricing of climate risk distorts mortgage credit supply and shifts climate-related losses to taxpayers. Buschbom, Eastman, Wang, and Zhou (2025) study commercial property insurance across major CRE sectors and emphasize the pricing of realized climate risk in CMBS settings.<sup>5</sup> We show that climate-risk repricing in insurance markets is associated with higher operating costs, lower profitability, lower property values, and reallocation across owners in multifamily housing, connecting insurance repricing directly to the broader climate-finance question of who bears climate risk and how that burden propagates through real estate markets.

Third, we extend our understanding of the incidence of insurance cost increases. Prior work, focused primarily on homeowners, links premium increases to house price declines, household relocation, and heightened mortgage and credit card delinquency (Hino and Burke, 2021; Ge, Lam, and Lewis, 2024; Ge, Johnson, and Tzur-Ilan, 2026). Sastry et al. (2025) study rising homeowners insurance prices through the coverage margin, showing that households reduce discretionary coverage while lender-mandated coverage remains relatively inelastic. We examine the multifamily market, where insurance costs are paid by property owners but may be reflected in rents, owner profitability, and asset values. By documenting both a partial rent response and a sharp decline in that response over time, we provide evidence consistent with climate-risk repricing increasingly shifting the burden of insurance costs onto owners through lower NOI. The transaction evidence further shows that the heightened pricing of climate risk is increasingly capitalized into property values, with riskier properties trading at lower prices per unit and higher cap rates relative to the pre-2018 period.<sup>6</sup>

Finally, we contribute to research on the role of ownership structure in real estate markets. Previous studies have primarily examined the long-term rental market, showing how large institutional owners influence rents and asset quality (Mills, Molloy, and Zarutskie, 2019; Austin, 2022; Coven, 2023; Gorbach, Qian, and Zhu, 2024). Kojien, Shah, and Van Nieuwerburgh (2026) show that buyer and seller identities matter for commercial real estate prices and trading. We extend this line of inquiry by showing that owner scale and portfolio composition matter for insurance pricing and the reallocation of high-risk assets.<sup>7</sup> Larger owners obtain lower insurance costs, especially in high-risk areas, and owners with lower-risk portfolios obtain lower insurance costs even for otherwise similar high-risk properties. These owner-side advantages are not

---

(Gron, 1994; Winter, 1994; Froot and O’Connell, 1999; Jaffee and Russell, 1997; Eastman and Kim, 2024).

<sup>5</sup> Kalda, Sharma, Soni, and Wenning (2025) show that climate-related stress in homeowners markets can spill over across locations and can appear in premiums as well as in non-price margins such as claim rejections. Relative to Buschbom et al. (2025), our paper focuses on multifamily properties and contributes new evidence on supply-side amplification through reinsurance, spillovers from homeowners-market frictions, the division of costs between tenants and owners, heterogeneity across owners, and the reallocation of risky assets toward larger owners.

<sup>6</sup> Our results complement the literature on the incidence of property taxes (Carroll and Yinger, 1994) and interest rates (Lee, 2024). A key distinction is that insurance costs can vary with owner identity, creating an ownership-reallocation margin that is less natural for shocks whose costs are tied primarily to the property rather than to owner characteristics such as size or portfolio diversification.

<sup>7</sup> More broadly, these results connect to the corporate demand-for-insurance and risk-management literatures, which study why firms insure and how insurance demand covaries with financing constraints, investment, underinvestment frictions, debt covenants, and organizational structure (Mayers and Smith, 1990; Hoyt and Khang, 2000; Aunon-Nerin and Ehling, 2008).

merely cross-sectional: they also appear within continuing ownership relationships, are reflected in discrete insurance-cost declines following M&A events, and increasingly coincide with a reallocation of risky assets toward larger owners. Our results therefore connect ownership structure to rents and profitability, as well as to who holds risky assets and how climate risk is allocated in commercial real estate.

## 2 Data

Our primary dataset covers multifamily properties with loans securitized through the Agency CMBS market, specifically Freddie Mac and Fannie Mae, which collectively owned or guaranteed roughly 40% of the \$2.2 trillion in outstanding multifamily mortgage debt as of September 2023 (Heeb, 2024). Regulatory disclosure mandates require both entities to release comprehensive loan performance data for the properties underlying their CMBS offerings. This dataset includes key metrics such as insurance costs,<sup>8</sup> rent, and NOI, along with property-level details such as address, number of units, year built, and year of last renovation. Our hand-collected dataset comprises 455,922 property-year observations across 102,995 unique properties.<sup>9</sup>

An important feature of the Agency CMBS setting is that the GSEs impose strict insurance coverage requirements on borrowers. Freddie Mac and Fannie Mae both require property-damage coverage on a replacement-cost basis equal to at least 90% of insurable value, and 100% for single-building properties, and both cap allowable deductibles.<sup>10</sup> For property-specific policies, the maximum per-occurrence deductible is \$50,000 for properties with insurable value below \$10 million and \$100,000 for properties with insurable value of \$10 million or more. The Agencies allow blanket policies covering multiple properties under a shared per-occurrence limit, but such policies must provide coverage at least as comprehensive as a stand-alone policy and are subject to a \$250,000 maximum deductible. These requirements limit borrowers' ability to respond to rising premiums by reducing coverage or self-insuring.

We supplement this data with similar property-level data for hospitality, office, industrial, and retail properties obtained from Bloomberg. For most of our analysis, however, we focus on multifamily properties in Agency CMBS deals for three reasons: (1) other property types are frequently subject to triple-net leases ("NNN"), under which tenants cover both rent and certain operating expenses, complicating the incidence analysis; (2) loans in Agency CMBS deals are subject to more standardized insurance coverage requirements; and (3) multifamily properties constitute the largest share of our sample, and restricting the analysis to a single asset class facilitates cleaner comparisons and simplifies interpretation.

To measure natural disaster risk, we use two datasets: the Spatial Hazard Events and Losses Database for the United States (SHELDUS) and the National Risk Index (NRI). SHELDUS provides county-level data on historical natural hazard events and associated losses, capturing realized disaster impacts across multiple peril types. The NRI provides a forward-looking assessment, with expected loss estimates and risk scores at the census tract level for multiple hazards, including coastal and riverine flooding, hurricanes, wildfire, hail, and severe storms. To analyze the role of geographic location, we geocode all property addresses using the U.S. Census Geocoder and calculate each property's elevation and distance to the nearest coast using data from the National Elevation Dataset and Natural Earth, respectively.

We obtain insurer-level information from the National Association of Insurance Commissioners (NAIC) Annual Statement's State Page (Exhibit of Premiums and Losses) and Schedule P for the period from 2010 through 2023. The State Page reports state-level premiums and losses by line of business, while Schedule P reports reinsurance activity. We focus on non-liability commercial lines and extract annual measures of direct written premiums, direct earned premiums, incurred losses, and reinsurance transactions.

For comparisons with homeowners insurance, we use ZIP-year homeowners premium data from U.S. Department of the Treasury (2025), which reports average homeowners insurance costs from 2018 to 2022.<sup>11</sup>

<sup>8</sup> We observe realized insurance expenses rather than premiums per dollar of coverage. These expenses may reflect changes in coverage amounts, replacement values, deductibles, policy limits, or other contract terms, which we do not observe separately. Our estimates should therefore be interpreted as evidence on the realized insurance-cost burden faced by financed multifamily properties.

<sup>9</sup> Figure IA.1 shows that the CMBS sample expands substantially over time and tracks the cross-sectional distribution of multifamily units across MSAs reasonably well.

<sup>10</sup> See [here](#) for the insurance requirements for Fannie Mae and [here](#) for Freddie Mac.

<sup>11</sup> The 2018–2022 period in this comparison reflects Treasury data availability. For robustness, we also use county-year data going back to 2014 from [Keys and Mulder \(2025\)](#).

We aggregate this data to the county-year level and combine it with the state-level homeowners-market friction measure from [Oh, Sen, and Tenekedjieva \(2025\)](#). This allows us to compare commercial and homeowners insurance growth and to test whether homeowners-market frictions spill over into commercial insurance pricing.

Finally, to identify property ownership, we use Real Capital Analytics (RCA). Ownership identification is often complicated by variation in recorded names, including subsidiaries, holding companies, and non-standard naming conventions. RCA addresses this issue by standardizing ownership names and identifying the ultimate parent owner. Using these data, we calculate the total number of multifamily units owned by each entity annually across the United States as a proxy for owner size.<sup>12</sup>

Together, these datasets allow us to study who bears rising insurance costs along three margins: which locations face larger increases, how the costs are reflected in rents, NOI, and property values, and how the burden varies with owner characteristics and is associated with ownership reallocation.

### 3 The Rise in Commercial Property Insurance Costs

We begin by documenting the substantial rise in commercial property insurance costs over time and across markets. This section establishes three facts that motivate the rest of the paper. First, the rise has been rapid and sustained, with average annual growth exceeding 15% in every year since 2019. Second, it is broad-based, extending across commercial asset classes and reaching well beyond the highly exposed coastal markets typically associated with climate-related insurance stress. Third, the rise is large relative to property cash flows: by 2024, insurance expense has become a meaningful share of rent and operating expenses, with important implications for incidence, profitability, and owner-side adjustment, which we examine in later sections. Figure 1 presents the time-series evidence, and Figure 2 presents the cross-sectional evidence.

#### 3.1 Time-Series Variation

Figure 1, Panel A plots insurance costs for multifamily properties as shares of rent and total operating expenses (OpEx). Both measures are stable before 2019, averaging below 2.7% of rent and 5.7% of total operating expenses. By 2024, they rise to 4.7% and 9.9%, respectively—roughly a doubling in five years. This increase transforms insurance from a modest line item into a meaningful component of property cash flows.<sup>13</sup> The widening of the 25th–75th percentile band after 2019 further indicates that the rise has become more dispersed across properties, foreshadowing the heterogeneity in incidence and owner-side adjustment that we examine later in the paper.

Figure 1, Panel B (left) shows the median and average annual percentage change in insurance costs from 2011 to 2024. Average annual growth exceeds 15% in every year since 2019 and peaks at nearly 30% in 2023.<sup>14</sup> Figure 1, Panel B (right) plots the annual percentage change in the ratio of insurance costs to operating expenses, benchmarking insurance growth against broader growth in operating costs. The same pattern emerges: the insurance-to-OpEx ratio rises by at least 8% annually from 2019 onward, including a surge of nearly 20% in 2023.

Figure 1, Panel C replicates the analysis in Panel B (left) for non-multifamily commercial property types using Bloomberg data. A similar time-series pattern appears across hospitality, industrial, mixed-use, mobile home, office, and storage properties, although the magnitude of the increase varies by asset class. The series move together most strongly after 2019, suggesting a common commercial-insurance repricing component rather than an asset-class-specific shock. The recent rise in insurance costs is therefore not unique to multifamily properties but instead reflects a broader repricing across commercial real estate. For the remainder of the paper, we focus on multifamily properties because they constitute the largest share of our

<sup>12</sup> Figure IA.2 shows that RCA provides broad coverage of the multifamily market, closely tracking the number of units over time and across MSAs. Figure IA.3 shows that, relative to the broader RCA multifamily universe, properties matched to the CMBS sample tend to be larger, have fewer floors, be newer, be less expensive, and have higher cap rates, while still broadly tracking the geographic distribution of multifamily units across MSAs.

<sup>13</sup> Figure IA.4 shows the same pattern when insurance costs are scaled by NOI and debt service. By 2024, average insurance costs equal roughly 8% of NOI and 18% of debt service.

<sup>14</sup> The mean is persistently above the median during the post-2019 surge, especially in 2023, indicating that the increase is broad-based and right-skewed, with a subset of properties experiencing very large shocks.

sample and provide a setting in which we can examine how rising insurance costs affect rents, net operating income, and ownership structure.

### 3.2 Cross-Sectional Variation

Figure 2, Panel A compares median annual insurance costs per unit in 2022–2024 with the 2010–2017 baseline, where the baseline period predates the post-2018 shift in local-risk pricing documented below. Each bubble represents a CBSA, sized by the number of sample properties and colored according to the magnitude of the cost increase. Across CBSAs, median insurance costs per unit rise by a factor of 1.94. In 37% of CBSAs, containing 34% of the properties in our sample, median insurance costs at least double. These large relative increases are not confined to CBSAs with high initial insurance costs: many markets with only moderate pre-period insurance costs still experience roughly two- to three-fold increases. The rise is therefore widespread across local commercial property markets rather than driven by a small set of outliers.

Figure 2, Panel B plots the percentage change in insurance costs between 2022 and 2023 across CBSAs. The largest increases occur in coastal states, including Florida, Texas, Louisiana, and California, but substantial increases also appear in inland markets, including Oklahoma, Colorado, Tennessee, and Indiana, where exposure can come from hazards such as hail, severe storms, wildfire, and flooding rather than only coastal risk. Only 12% of CBSAs, containing just 1% of sampled properties, experience increases of less than 10%, and only 29% of CBSAs, containing 9% of sampled properties, experience increases of less than 20%. Thus, although climate-related insurance stress is often associated with a narrow set of highly exposed coastal markets, the recent repricing is better understood as a pervasive national phenomenon.

### 3.3 Commercial vs. Homeowners Insurance Cost Growth

The preceding subsections show that the rise in commercial property insurance costs is large, broad-based, and economically meaningful. Before turning to how the increase varies across locations, we benchmark commercial insurance against homeowners insurance. This comparison is informative because prior work shows that homeowners insurance pricing is often constrained by state-level regulation (Oh, Sen, and Tenekedjieva, 2025), whereas commercial lines are generally less tightly constrained by rate regulation.<sup>15</sup>

To construct this comparison, we use homeowners insurance premium data from U.S. Department of the Treasury (2025). These data are available at the ZIP-year level and report average homeowners insurance costs per policy annually from 2018 to 2022. We aggregate them to the county-year level and compute annual percentage changes, then compare those changes with county-year changes in commercial insurance costs from our property-level dataset. The analysis in this subsection therefore focuses on the post-2018 period because that is the period for which comparable homeowners premium data are available.

Figure 3, Panel A presents scatterplots comparing annual percentage changes in commercial and homeowners insurance costs across counties for 2019–2020, 2020–2021, and 2021–2022. From 2021 to 2022, 72.3% of the population lives in counties where commercial insurance costs grow more than five times faster than homeowners insurance costs, or increase while homeowners costs decline. More broadly, 98.1% of the population lives in counties where commercial insurance costs increase at least as much as homeowners insurance costs, and 94.8% lives in counties where commercial insurance costs increased at least twice as much.<sup>16</sup> Thus, the recent rise in insurance costs has been far more pronounced in commercial lines than in homeowners lines, and this gap is pervasive across local markets. The pattern is visible in all three subperiods shown in the figure: the wedge is already pronounced in 2019–2020, narrows somewhat in 2020–2021, and then widens again in 2021–2022. As a robustness exercise, Figure IA.5 repeats this comparison using the county-year homeowners insurance data from Keys and Mulder (2025), which are available from 2014 to 2024. From 2019 to 2024, more than 72% of the U.S. population lives in counties where the cumulative increase in commercial insurance costs is at least twice as large as the cumulative increase in homeowners insurance costs.

<sup>15</sup> This distinction is also consistent with recent evidence that compliance costs associated with insurance contract regulation have become less important in commercial lines than in personal lines as commercial markets have deregulated (Kim, Leverty, and Liu, 2025).

<sup>16</sup> Counties where commercial insurance costs decline are omitted from the figure for clarity.

This pronounced wedge between commercial and homeowners insurance cost growth suggests that frictions could be suppressing observed repricing in residential lines, raising the question of whether those same frictions spill over into commercial pricing—a sharper implication we test directly in Subsection 4.3.

## 4 Burden Across Locations

The previous section documents that commercial property insurance costs rise sharply and broadly and shows that the increase far outpaces homeowners insurance growth. This section examines which locations bear larger increases than others. We document variation driven by three supply-side mechanisms. First, insurers price local climate risk much more aggressively after 2018, following large catastrophe-loss years and the hardening of property insurance and reinsurance markets. Second, rising reinsurance costs amplify this repricing, especially in states where insurers have greater ex ante exposure to reinsurance markets. Third, commercial premiums rise disproportionately in states with high homeowners insurance-market frictions, consistent with cross-product subsidization. These patterns are not intended to provide a complete decomposition of the aggregate increase. Other factors, including changes in replacement costs, coverage terms, deductibles, insurer markups, or property characteristics, may also affect measured insurance expenses. Instead, the tests aim to identify distinct dimensions along which commercial insurance becomes more expensive in some places than in others.

### 4.1 Repricing of Local Risk

The first test asks whether the sensitivity of insurance cost growth to local climate risk changes over time. We use two complementary sets of measures. The first is FEMA’s National Risk Index (NRI), which provides census tract-level risk scores and expected annual building losses—forward-looking assessments of the disaster exposure insurers face when pricing coverage. The second is SHELDDUS county-level property damage data, which captures realized historical losses. Using both allows us to test whether the post-2018 shift appears in forward-looking risk measures, backward-looking loss experience, or both.

Figure 4, Panel A shows a clear regime shift in the pricing of expected local risk. The annual coefficients on both tract-level risk scores and expected annual building losses are small through 2017, then rise sharply after 2018, with the largest effects appearing in the most recent years.<sup>17</sup> The timing follows the large catastrophe-loss years of 2017–2018 and coincides with the hardening of property insurance and reinsurance markets documented below. The evidence therefore does not reflect insurers simply continuing a pre-existing pattern of risk-based repricing. Rather, they place substantially greater weight on local climate risk after 2018, consistent with a broader shift toward forward-looking catastrophe modeling and risk selection in insurance markets, where model uncertainty and correlated disaster losses can make risk repricing nonlinear rather than purely actuarial (Ibragimov, Jaffee, and Walden, 2009; Wagner, 2022; Boomhower, Fowlie, and Plantinga, 2023).

Panel B shows the same post-2018 break using realized disaster damages from SHELDDUS. The left subpanel reports positive relationships between insurance cost growth and average property damages per capita across one- to five-year damage horizons. The right subpanel shows that this relationship is driven by the post-2018 period: before 2018, historical damages have little predictive power for insurance cost growth, while after 2018 the coefficients are positive and statistically significant across horizons.<sup>18</sup>

The consistency across forward-looking risk scores, expected losses, and realized damages points to a clear post-2018 regime shift in the pricing of local disaster risk. At the same time, the broad and heterogeneous increase in insurance costs even outside high-risk or high-damage areas suggests that local risk does not capture the full cross-sectional variation, motivating the second dimension: exposure to reinsurance markets.

<sup>17</sup> Figure IA.6 and IA.7 map county-level risk scores and expected annual losses, respectively. Figure IA.8 shows analogous annual effects for percentage changes in insurance costs. Figure IA.9 shows the corresponding full-sample binscatters and pre/post-2018 splits, and Figure IA.10 reports similar patterns using alternative FEMA NRI risk measures. The figures in this subsection include year fixed effects, so they examine differential repricing of expected risk or realized damages within the same year.

<sup>18</sup> Figure IA.11 reports the national time series and county-level geography of realized property damages, and Figure IA.12 shows the binscatter relationship between insurance cost growth and five-year average property damages per capita.

## 4.2 Reinsurance Amplification

Reinsurance functions as insurance for insurers, transferring catastrophic risk to global reinsurers that specialize in absorbing large-scale losses and allowing primary insurers to remain solvent through extreme events such as hurricanes and wildfires. Because reinsurance is priced in global markets, movements in reinsurance prices capture changes in the price of systematic catastrophe risk. If primary insurers differ in how heavily they rely on reinsurance, then a common increase in reinsurance costs should coincide with larger cost increases in states where insurers are more exposed to reinsurance markets. This interpretation is consistent with theories of catastrophe-risk intermediation in which the supply of reinsurance capital is less than perfectly elastic, so that correlated losses raise the marginal cost of bearing risk (Froot, 1997; Froot and O’Connell, 2008).

In recent years, the cost of reinsurance has increased substantially. As shown in Figure 5, Panel A, the Guy Carpenter Rate-On-Line Index, a widely used benchmark for reinsurance pricing, has risen steadily since 2018, with a particularly sharp increase from 2021 to 2023. Panel A also plots the estimated effect of local disaster risk on insurance costs over time. The two series closely co-move, with both rising sharply in recent years. This co-movement points to reinsurance exposure as a second dimension of variation: cost increases are larger where insurers rely more heavily on reinsurance, even holding local disaster risk fixed. This motivates tests that separate national reinsurance shocks from local risk repricing.

To quantify how insurance cost increases vary with reinsurance exposure, we follow Keys and Mulder (2025) and construct a state-level measure of how much insurers operating in a given state depend on reinsurance to manage risk:

$$ReinsuranceExposure_s = \frac{\sum_{i \in I} DirectPremiumsWritten_{i,s} \times PctCeded_i}{\sum_{i \in I} DirectPremiumsWritten_{i,s}}, \quad (1)$$

where  $DirectPremiumsWritten_{i,s}$  is the total direct insurance premiums written by insurer  $i$  in state  $s$  and  $PctCeded_i$  is the share of insurer  $i$ ’s total direct premiums ceded to unaffiliated reinsurers.<sup>19</sup>

Figure IA.13, Panel A maps the resulting state-level reinsurance exposure. Darker shades indicate a larger share of total direct premiums ceded to unaffiliated reinsurers. States along the Gulf Coast and in the Southeast—including Florida, Louisiana, and Texas—exhibit the highest exposure, exceeding 20% in some cases, consistent with elevated hurricane risk and heavier reliance on reinsurance. Many states in the Midwest and parts of the Northeast have substantially lower exposure, often below 10%.

To test whether cost increases are larger in high-exposure states when reinsurance prices rise, we estimate the following triple-interaction regression model in level changes in insurance costs per unit:<sup>20</sup>

$$\begin{aligned} \Delta(Insurance/Unit)_{i,s,t} = & \beta \times \Delta(ReinsuranceCost)_t \times ReinsuranceExposure_s \times RiskScore_i \\ & + \delta_t \times ReinsuranceExposure_s + \zeta_t \times RiskScore_i + \gamma_i + \tau_t + \varepsilon_{i,s,t}, \end{aligned} \quad (2)$$

where  $\Delta(Insurance/Unit)_{i,s,t}$  is the change in insurance costs per unit for property  $i$  in state  $s$  during year  $t$ ,  $\Delta(ReinsuranceCost)_t$  is the change in the Guy Carpenter Rate-On-Line Index,  $ReinsuranceExposure_s$  measures insurers’ reliance on reinsurance markets in state  $s$ , and  $RiskScore_i$  is the tract-level disaster risk score of property  $i$ . The specification includes property fixed effects ( $\gamma_i$ ) to control for time-invariant property characteristics, year fixed effects ( $\tau_t$ ) to account for macroeconomic shocks or broader trends affecting insurance costs, and controls for the time-varying effects of reinsurance exposure ( $\delta_t \times ReinsuranceExposure_s$ ) and local risk ( $\zeta_t \times RiskScore_i$ ). Identification therefore comes from whether properties with similar local risk experience larger insurance cost increases when national reinsurance costs rise if they are located in states with greater ex ante reinsurance exposure.<sup>21</sup>

<sup>19</sup> We construct this measure using 2017 data so that it captures exposure before the sharp rise in reinsurance costs. Figure IA.13, Panel B shows that both insurer-level cession rates and state-level exposure are broadly stable over time.

<sup>20</sup> Because the reinsurance mechanism operates through a common national pricing shock, we estimate this specification in level changes in insurance costs per unit so that the marginal effects can be interpreted directly as dollar increases associated with rising reinsurance costs.

<sup>21</sup> The estimates capture amplification through reinsurance-market exposure, rather than decomposing whether the Rate-On-Line index reflects expected catastrophe risk, reinsurance-capital scarcity, or reinsurer markups.

The Florida–Georgia border illustrates the identifying variation. Figure IA.13, Panel A plots reinsurance exposure, while Figure IA.6 displays the corresponding county-level risk scores. State-level reinsurance exposure changes sharply at the border even though local risk varies relatively smoothly across the region. More generally, the empirical strategy exploits analogous cross-state variation throughout the full sample rather than this particular border alone. Property fixed effects absorb time-invariant differences across properties, while the interactions with local risk and year effects allow us to distinguish common reinsurance shocks from differences in baseline disaster risk. Thus, identification comes from whether properties with similar local risk experience larger insurance cost increases when national reinsurance costs rise in states that are more exposed to reinsurance markets.

The left subpanel of Figure 5, Panel B shows the marginal effect of a 10-index-point increase in reinsurance costs, plotted across risk scores with separate lines for reinsurance exposure ranging from 10% to 25%. To interpret the results, we focus on a risk score of 80, marked by the dotted vertical line. For a property located in a census tract with a risk score of 80 and reinsurance exposure of 10%, a 10-index-point increase in reinsurance costs implies a \$19 increase in insurance cost per unit. For the same level of local risk but with reinsurance exposure of 25%, the same increase in reinsurance costs implies a \$47 increase in insurance costs per unit. Thus, the effect of a common reinsurance shock is roughly 2.5 times as large in high-exposure states as in low-exposure states, holding local risk fixed. Since insurance costs have increased more in areas with higher local risk, as shown in the previous subsection, the dollar effect is substantially larger in higher-risk areas. Replacing the risk score with  $\log(\text{Expected Building Losses per Capita})$  yields a very similar pattern, as shown in the right subpanel.

Table 1 provides the corresponding regression estimates across different fixed-effects specifications. Columns (1)–(3) examine the interaction between reinsurance cost changes and state-level reinsurance exposure, progressively adding year and property fixed effects. Columns (4)–(7) add interactions with local risk scores. The most demanding specification, Column (7), absorbs time-invariant property heterogeneity and allows the direct effects of reinsurance exposure and local risk to vary across years. The triple interaction therefore identifies whether similarly risky properties face larger insurance cost increases when national reinsurance costs rise in states with higher reinsurance exposure. Across all specifications, greater ex ante exposure to reinsurance markets amplifies the pass-through of rising reinsurance costs, especially in higher-risk areas.<sup>22</sup> Reinsurance shocks therefore do not raise insurance costs uniformly across exposed states. Once the interaction with local risk is introduced, the lower-order interaction between reinsurance cost changes and reinsurance exposure becomes small, while the triple interaction remains large and statistically significant, suggesting that reinsurance amplification is concentrated in riskier places.

As complementary evidence, Figure IA.14 uses a border-county-pair difference-in-differences design comparing properties on opposite sides of state borders. The pre-2018 estimates are close to zero, while the post-2018 estimates are generally positive, with the largest effects appearing when reinsurance prices are highest. This pattern is consistent with properties on the high-reinsurance-exposure side of a state border experiencing larger insurance cost increases after reinsurance markets harden. Together with the full-sample regression, this complementary evidence supports the interpretation that reinsurance exposure amplifies post-2018 commercial insurance cost growth, especially in higher-risk areas.

### 4.3 Regulatory Spillovers Between Commercial and Homeowners Insurance

We next test whether the relative-pricing wedge between homeowners and commercial property insurance documented in Subsection 3.3 is larger in states with greater homeowners insurance frictions. Following Oh, Sen, and Tenekedjjeva (2025), we use their state-level friction measure and estimate whether the ratio of commercial to homeowners insurance costs rises more steeply with local risk in high-friction states.<sup>23</sup> Specifically, we define

<sup>22</sup> Figure 5, Panel B is based on the regression specification shown in Column (7). Table IA.1 replicates Columns (4)–(7) of Table 1 using expected annual losses and finds similar results.

<sup>23</sup> This ratio should be interpreted as a reduced-form relative-pricing wedge across sectors rather than a matched-contract premium ratio. Our commercial measure is realized insurance expense per unit for Agency CMBS properties, where lender requirements impose broad and relatively standardized coverage, while the homeowners measure is the average premium per policy from Treasury data. Note that our cross-product-subsidization result below does not rely on homeowners premium data; it is identified using only commercial insurance costs in a border-county-pair design.

$$CHRatio_{i,z,t} = \frac{\text{Commercial Insurance/Unit}_{i,t}}{\text{Average Homeowners Insurance Premium}_{z,t}}, \quad (3)$$

and estimate

$$CHRatio_{i,z,t} = \beta \times LocalRisk_c \times \mathbb{1}(HighFriction)_s + \delta \times LocalRisk_c + \gamma_{s,t} + \varepsilon_{i,z,t}, \quad (4)$$

where property  $i$  is located in census tract  $c$ , ZIP code  $z$ , and state  $s$ .  $LocalRisk_c$  denotes either the tract-level risk score or expected annual building losses scaled by building value for census tract  $c$ , both from FEMA’s NRI, and  $\mathbb{1}(HighFriction)_s$  indicates whether state  $s$  is in the top tercile of the homeowners-friction measure. The regression includes state-by-year fixed effects, and standard errors are clustered at the state level.

Figure 3, Panel B shows that in high-friction states, the relative-pricing wedge between commercial and homeowners insurance costs rises sharply with local risk. In low- and medium-friction states, by contrast, the wedge is roughly flat. The divergence is economically meaningful: moving from the lowest to the highest risk scores raises the commercial-homeowners ratio by roughly six ppt in high-friction states, while the corresponding relationship in lower-friction states is near zero or negative. Because the regression includes state-by-year fixed effects, this pattern is not driven by statewide pricing cycles, aggregate regulatory changes, or other shocks common to a state during a given year. The identifying variation comes from whether, within the same state-year, higher-risk local areas exhibit a steeper commercial-homeowners wedge in high-friction states. This divergence is consistent with regulatory constraints preventing homeowners premiums from fully adjusting to geographic risk while commercial premiums remain better able to do so. We find a similar result with realized losses. Table IA.2 shows that areas experiencing greater recent losses exhibit a widening commercial-homeowners wedge, again driven primarily by high-friction states. When losses are interacted with local risk, the wedge expands most strongly in high-risk areas within high-friction states.<sup>24</sup> In other words, the divergence between commercial and homeowners insurance pricing is largest precisely where underlying disaster risk is greatest, even after netting out common state-year shocks.

These results suggest that homeowners-market frictions shape relative pricing across insurance lines. We now test the sharper implication that these frictions also generate spillovers into commercial premiums through cross-product subsidization. The mechanism operates through multi-line insurers: as of 2017, among insurers writing commercial insurance in a given state, 44% also wrote homeowners policies there on a premium-weighted basis.<sup>25</sup> This overlap creates the potential for insurers facing tighter constraints on homeowners rates to respond to large natural disasters by adjusting commercial premiums more aggressively to rebuild capital.<sup>26</sup>

To test this mechanism, we adopt a stacked border-county-pair difference-in-differences design using a property-year panel. We form county pairs by matching adjacent counties that straddle a state border, where properties on either side are likely to share similar economic fundamentals and exposure to regional shocks. Using the homeowners-friction measure from Oh, Sen, and Tenekedjieva (2025), we compare the high-friction side of each border pair with the lower-friction side. We also require both states in the pair to have low friction in commercial property insurance rates, so that the identifying difference comes from homeowners insurance-market regulation rather than direct regulation of commercial lines. Specifically, we estimate the following regression:

<sup>24</sup> Table IA.3 shows similar results when the percentage of homeowners policies with claims is used instead of loss ratios.

<sup>25</sup> This percentage is stable over time; as of 2022, it was 42%. These figures are calculated using insurer-by-state-by-line data from the “Exhibit of Premiums and Losses (Statutory Page 14).”

<sup>26</sup> Similar cross-product subsidization behavior has been documented in other insurance contexts. For example, Ge (2022) finds evidence that insurance groups engage in cross-subsidization between life and property-casualty insurance divisions following financial shocks, and Powell, Sommer, and Eckles (2008) find evidence that insurer groups use internal capital markets to reallocate funds across affiliates and business lines after shocks. Commercial-only insurers may not fully compete away this behavior because commercial property insurance is segmented by state-specific carrier participation, broker relationships, underwriting specialization, and capacity constraints tied to insurer and reinsurer capital.

$$PctChangeInsurance_{ipstc} = \beta \times \mathbb{1}(HighFriction)_s \times \mathbb{1}(Post)_{tc} \times \mathbb{1}(Treat)_{pc} + \mu_i + \gamma_{stc} + \delta_{psc} + \zeta_{ptc} + \varepsilon_{ipstc}, \quad (5)$$

where  $PctChangeInsurance_{ipstc}$  is the percentage change in insurance costs for property  $i$  located in county pair  $p$  in state  $s$  during event year  $t$  within cohort  $c$ .  $\mathbb{1}(HighFriction)_s$  equals one if state  $s$  is classified as having high homeowners insurance market frictions. For each county pair  $p$ , we identify major disasters using historical property damage data and define the peak-damage year as the event year.<sup>27</sup> We define cohorts  $c$  at the event level: in each disaster year, the county pairs experiencing a shock are the treated units, and the corresponding not-yet-treated and never-treated county pairs serve as controls. Therefore,  $\mathbb{1}(Treat)_{pc}$  is an indicator equal to one for county pairs  $p$  in cohort  $c$  that experience a major disaster shock, and  $\mathbb{1}(Post)_{tc}$  is an indicator equal to one for all county pairs in cohort  $c$  in the disaster year and all subsequent years. The sample window covers the two years before each disaster, the disaster year itself, and the year after.

A key concern is endogeneity from unobserved differences in local economic conditions, insurance markets, or state-level policies that may simultaneously affect disaster exposure and property outcomes. To address this concern, the specification includes property fixed effects ( $\mu_i$ ), cohort-by-state-by-event-year fixed effects ( $\gamma_{stc}$ ) to absorb state-level shocks specific to each cohort and event year, cohort-by-state-by-county-pair fixed effects ( $\delta_{psc}$ ) to absorb time-invariant differences across county pairs within states and cohorts, and cohort-by-event-year-by-county-pair fixed effects ( $\zeta_{ptc}$ ) to control for county-pair-specific dynamics around each disaster. Together, these fixed effects ensure that  $\beta$  is identified from within-border-pair comparisons, isolating differential post-disaster commercial insurance repricing attributable to the state's homeowners regulatory environment.

Table 2 reports a positive and statistically significant coefficient on  $HighFriction \times Post \times Treat$  in both specifications, with the estimate increasing slightly when property fixed effects are added. The estimated magnitudes imply that after a major disaster, commercial insurance costs rise by roughly 19–22 ppt more in counties on the high-friction side of the border than in their paired low-friction neighbors. This result aligns with a cross-product subsidization mechanism: when multi-line insurers cannot fully reprice homeowners coverage after large losses, commercial policies exhibit larger post-disaster repricing.

Together with the earlier commercial-homeowners comparison in Subsection 3.3, the evidence shows that homeowners-market frictions matter for commercial insurance in two ways. First, they widen the relative-pricing wedge between commercial and homeowners premiums by suppressing observed repricing in residential lines. Second, they are associated with spillovers into commercial pricing through cross-product subsidization after disasters. This second result points to a cross-line version of insurance-market subsidization: constraints in homeowners insurance are associated not only with redistribution across locations, but also with repricing in commercial policies. Together, the two results help explain why commercial insurance costs have risen much faster than homeowners insurance costs and imply that homeowners insurance-market regulation can affect renters even though renters are not the regulated policyholders. To the extent that higher commercial insurance costs are reflected in rents, this mechanism would amount to an indirect subsidy from renters to homeowners. We next consider whether simpler geographic, property-level, or market-structure characteristics account for the cross-sectional variation in the recent rise in insurance costs.

#### 4.4 Other Potential Factors

As additional checks, we examine whether distance to the coast, elevation, property features, or insurance market concentration can capture the cross-sectional differences in the recent rise in insurance costs. None of these factors tracks the core patterns as closely as local risk repricing, reinsurance exposure, and spillovers from homeowners-market frictions, as shown in Figures IA.15, IA.16, and IA.17. Simple geographic proxies such as distance to the coast and elevation bear little relation to the broad national increase in insurance costs: the distance-to-coast relationship is weak and negative, while the relationship with elevation is flat.

<sup>27</sup> Using SHELDUS data, we construct annual property damage per capita for each county and take the average across the two counties in a pair. We classify a county pair as experiencing a major disaster if its within-sample peak damage year (i) falls in the top decile of the county-pair damage distribution across all pairs and years and (ii) is at least 10 times the previous year's damage. This restriction ensures that the identified event reflects an unexpected shock rather than a gradual trend. We define the disaster year as the peak-damage year.

Property characteristics show mixed patterns—larger properties face somewhat larger increases, while older properties, if anything, face smaller increases—suggesting that observable property age and size do not by themselves capture the main patterns. Insurance market concentration also does not fit a market-power interpretation. State-level commercial multi-peril HHI declines over the sample, and the cross-sectional relationship between lagged HHI and insurance cost growth is weak and, at the state level, negative. The results point away from conventional concentration or observable property characteristics and back toward the supply-side mechanisms emphasized above.

The evidence in this section shows that the post-2018 surge is largest in high-disaster-risk locations, in states more exposed to reinsurance markets, and in states with high homeowners-market frictions. Together, these patterns characterize which locations bear larger commercial insurance-cost increases.<sup>28</sup> The next section turns to how these higher costs are divided between tenants and property owners through rents, NOI, property values, and required yields.

## 5 Burden Between Tenants and Property Owners

The previous section shows which locations bear larger commercial insurance-cost increases than others. We now turn to the second margin of incidence: how those higher costs are divided between tenants and property owners. Because Agency CMBS borrowers face comprehensive insurance requirements, they have limited scope to respond to premium increases by reducing coverage. The key question is whether higher insurance costs are reflected in rents or instead associated with lower NOI for property owners. When rents do not fully adjust, these shocks may also be capitalized into lower property valuations and higher cap rates.

### 5.1 Average Incidence on Rents and NOI

We first estimate the average relationship between insurance costs, rents, and NOI for multifamily properties. Specifically, we estimate

$$\log(y)_{imt} = \beta \times \log(\text{Insurance}/\text{Unit})_{imt} + \gamma_i + \eta_{mt} + \epsilon_{imt}, \quad (6)$$

where  $\log(y)$  represents the outcome variable—either  $\log(\text{Rents}/\text{Unit})$  or  $\log(\text{NOI}/\text{Unit})$ —for property  $i$  in CBSA  $m$  in year  $t$ ,  $\gamma_i$  denotes property fixed effects, and  $\eta_{mt}$  denotes CBSA-by-year fixed effects. Because both the dependent variable and insurance costs are in logs,  $\beta$  measures the elasticity of rents or NOI with respect to insurance costs within a property over time. We interpret these estimates as reduced-form incidence relationships rather than causal pass-through elasticities. Property fixed effects absorb time-invariant property heterogeneity and CBSA-by-year fixed effects absorb common local market-year shocks, but time-varying property-level confounders may remain. To address this concern, we also estimate specifications that control for occupancy, non-insurance operating expenses, capital expenses, renovation indicators, and measures of property age and effective age.<sup>29</sup>

Table 3, Panel A presents the results, with Columns (1)–(4) reporting the relationship with rents and Columns (5)–(8) reporting the relationship with NOI. All specifications include property fixed effects. Columns (1) and (5) include year fixed effects, while Columns (2) and (6) add CBSA-by-year fixed effects to absorb time-varying local shocks. Columns (3) and (7) replace these controls with CBSA-by-class-by-year fixed effects, where class is defined by terciles of rent per unit within each CBSA-year, allowing local shocks to vary flexibly across property-market segments.<sup>30</sup> Columns (4) and (8) additionally add the property-level

<sup>28</sup> These results focus on realized insurance expenses and therefore capture the cost burden faced by properties that maintain coverage. They do not measure non-price supply responses such as insurer exit, coverage restrictions, or rationing, which may also affect the availability and terms of commercial property insurance.

<sup>29</sup> We normalize both the dependent and independent variables by the number of units so that the CBSA-by-year fixed effects capture average rent and NOI trends within each local market.

<sup>30</sup> Griffin and Priest (2023) use rents, building age, and vacancy to proxy for property class. Following them, we use rent per unit as the main proxy because rents map most directly to property class, and Table IA.4 shows that the same conclusion holds when class is based on property age, occupancy, or all three class measures jointly.

controls described above in the subset of properties for which those variables are observed.<sup>31</sup> Standard errors are clustered at the CBSA level throughout. In the baseline specification with CBSA-by-year fixed effects, a 10% increase in insurance costs is associated with a 0.16% increase in rents and a 0.46% decrease in NOI. The rent coefficient declines modestly in the more demanding CBSA-by-class-by-year specifications, while the NOI coefficient remains large and negative: with CBSA-by-class-by-year fixed effects and property-level controls, a 10% increase in insurance costs is associated with a 0.12% increase in rents and a 0.46% decrease in NOI.<sup>32</sup> The estimates are therefore consistent with insurance cost shocks being shared between tenants and owners on average, but with a rent response that is far from complete.

To quantify the economic magnitude of the rent response, consider a 25% rise in insurance costs. Based on the baseline estimate in Column (2) of Table 3, this implies a 0.41% rent increase ( $25\% \times 0.0164$ ). Because insurance costs account for approximately 3.3% of rent on average, fully offsetting a 25% rise in insurance costs through rents would require a 0.83% rent increase ( $3.3\% \times 25\%$ ). This calculation implies that roughly 49% of the increase in insurance costs is reflected in rents ( $0.41/0.83$ ). The more demanding CBSA-by-class-by-year specifications imply smaller rent-response shares of roughly 37–39%.<sup>33</sup> Thus, across specifications, only part of the average increase in insurance costs is reflected in rents, while the remainder is associated with lower NOI for owners. The next subsection examines whether this average incidence differs systematically across market, owner, and tenant characteristics.

## 5.2 Where Is the Rent Response Stronger?

The incidence of insurance cost increases should depend on housing supply elasticity, local market power, and tenant and owner characteristics (Glaeser, Gyourko, and Saks, 2005; Weyl and Fabinger, 2013; Diamond, McQuade, and Qian, 2019). To examine these margins, Figure 6 re-estimates the baseline rent specification after interacting log insurance costs per unit with decile indicators for each heterogeneity variable. The dependent variable is log rent per unit, and all specifications include property fixed effects and CBSA-by-year fixed effects. The rent response is stronger in markets with more inelastic housing supply, among owners with greater local market share, in areas with greater moving frictions, and in areas with fewer tenant outside options.

Panel A uses the tract-level housing-supply-elasticity measure developed by Baum-Snow and Han (2024).<sup>34</sup> The rent response is largest in markets with more inelastic housing supply and generally declines as supply elasticity rises, consistent with a stronger rent response where new supply is more constrained. Panel B shows that the rent response increases with the property owner’s market share within the CBSA, suggesting that owners with a larger local presence are better able to respond to higher insurance costs by raising rents. Panel C uses three proxies for moving frictions: the share of residents living in the same home as one year earlier, the share of families with children, and the share of households that are married-couple families. The rent response rises with each of these measures, consistent with greater tenant mobility frictions strengthening the link between higher insurance costs and rents. Panel D uses three proxies for tenant outside options: the share of housing units in apartment buildings, the vacancy rate among apartment units, and the overcrowding rate. The rent response is stronger when tenant outside options are weaker: it declines as apartment shares and vacancy rates rise, and it increases as overcrowding rises.<sup>35</sup>

Figure IA.19 repeats the exercise using log NOI per unit as the outcome and shows the same heterogeneity patterns in the opposite direction. NOI declines are larger in markets where the rent response is weaker. Panels B and C of Table 3 report coarser median-split versions of the same heterogeneity patterns for the incidence of insurance cost increases on rents and NOI, respectively.

<sup>31</sup> We observe renovations in the Freddie Mac data, but not in the Fannie Mae data. Specifications that include only year fixed effects, rather than CBSA-by-year fixed effects, imply a larger rent response and a smaller negative relationship with NOI.

<sup>32</sup> Table IA.5 further shows that higher insurance costs are associated with lower operating margins and lower debt-service coverage ratios.

<sup>33</sup> Since the model estimates elasticities, these implied rent-response shares do not depend on the magnitude of the insurance cost shock.

<sup>34</sup> We control for the time-varying effects of the fraction of the tract that is developed, also based on data from Baum-Snow and Han (2024).

<sup>35</sup> The proxies for moving frictions and tenant outside options are based on American Community Survey (ACS) 5-year estimates at the census-tract level. We measure the share of residents living in the same home as one year earlier as of 2013 to avoid contaminating the measure with endogenous renter moves. Apartment buildings are defined as buildings with at least five units. The overcrowding rate is defined as the percentage of rental units with more than one person per room.

### 5.3 Nonlinearity and Time-Series Variation in Incidence

Although the preceding results reveal important cross-sectional heterogeneity, the average incidence still masks another form of variation: the relationship between insurance costs and rents is nonlinear and has weakened over time as repricing has intensified. Figure 7, Panel A plots log insurance costs per unit against log rents per unit (left subpanel) and log NOI per unit (right subpanel), with property and CBSA-by-year fixed effects residualized out and third-degree polynomial fits overlaid. Higher insurance costs are associated with higher rents on average, but the relationship is concave: the rent response diminishes as insurance costs rise and flattens at the upper end of the distribution, consistent with property owners facing increasing difficulty offsetting higher costs through rents. The nonlinearity is even sharper for NOI: NOI is roughly flat through the middle of the insurance-cost distribution but declines steeply once insurance costs become high. This pattern suggests a practical limit to rent pass-through: at moderate levels, owners can offset part of the shock, but at high levels, the marginal dollar of insurance cost is increasingly associated with lower profitability.

Figure 7, Panel B traces how the rent and NOI responses to insurance costs have evolved over time, using the baseline specification with log insurance costs per unit interacted with year indicators. The left subpanel shows a decline in the rent response over time, with a particularly sharp decrease between 2019 and 2020. In 2014, a 10% increase in insurance costs is associated with a rent increase of approximately 0.35%; by 2024, the same shock is associated with an increase of only 0.02%. Conversely, the relationship with NOI has become more negative. Before 2018, changes in insurance costs have no economically or statistically significant association with NOI. By 2024, however, a 10% increase in insurance costs is associated with a decline in NOI of more than 0.95%. The nonlinearity in Panel A and the time-series pattern in Panel B are consistent with the same underlying shift in incidence. As insurance costs have risen and large shocks have become more common, owners appear increasingly constrained in their ability to offset those costs through rents.

### 5.4 Implied Cumulative Effects on Rents and NOI

Figure 7, Panel C translates these reduced-form associations into implied cumulative effects on rents and NOI over the full 2014–2024 period by combining the time-varying response estimates from Panel B with the distribution of insurance cost growth.<sup>36</sup>

On average, the implied cumulative effects are modest: roughly a 0.9% increase in rents and a 5.1% decline in NOI. The upper tail tells a sharply different story. At the 95th percentile of insurance cost growth, the same calculation implies an approximately 11% increase in rents and a 26% decline in NOI over the decade.<sup>37</sup> Tail effects of this magnitude are large enough to be economically relevant for property valuations, which we examine next.

### 5.5 Capitalization into Prices and Cap Rates

If local climate risk and the associated rise in insurance costs are increasingly viewed as persistent rather than transitory, and these costs cannot be fully offset through rents, the same repricing should appear in transaction markets through lower valuations and higher required yields. Table 4 is consistent with this view: the pricing of local climate risk in transaction markets shifts materially after 2018.<sup>38</sup> In specifications without property fixed effects, local climate risk is positively associated with transaction prices and negatively associated with cap rates, consistent with riskier properties often being located in otherwise attractive markets where valuations are high and required yields are compressed. The interaction terms show that this relationship reverses materially after 2018: riskier properties transact at lower prices per unit and higher

<sup>36</sup> We use the annual percentage increase in the ratio of insurance costs to total operating expenses to account for general inflation in operating expenses. Internet Appendix Figure IA.18 replicates the analysis using percentiles of the percentage change in insurance costs per unit and yields similar results.

<sup>37</sup> This exercise assumes that areas remain at a given percentile of the annual insurance-shock distribution over time. To the extent that shocks mean-revert, the cumulative effects in the tails may be overstated.

<sup>38</sup> These results are based on the full sample of completed multifamily property sales in the RCA data from 2010 to 2024, excluding refinancing and construction transactions.

cap rates relative to the pre-2018 period. The within-property specifications, which add property fixed effects on top of CBSA-by-year fixed effects, sharpen this pattern by isolating how the pricing of climate risk changes within the same property over time. A one-log-point increase in expected annual building losses is associated with a 6.5% lower transaction price per unit and an 11.8-basis-point higher transaction cap rate in the post-2018 period, a 2.1% increase relative to an average cap rate of 5.6%. The joint movement in prices and cap rates is consistent with investors pricing rising insurance costs and climate risk as a persistent drag on expected net cash flows and requiring additional compensation for bearing climate risk.

Overall, this section shows that rising insurance costs are only partially reflected in rents. The share of rising insurance costs borne by tenants varies systematically with local market characteristics: the rent response is stronger where housing supply is more inelastic, owners have greater local market share, moving frictions are higher, and tenant outside options are fewer. In addition, owners' ability to offset these costs through rents has deteriorated sharply in recent years. The findings are therefore consistent with owners increasingly bearing the burden of climate-risk repricing through lower NOI, especially when shocks are large. The transaction-market evidence complements these results by showing that the same repricing is associated with lower property values and higher cap rates. This shift in incidence is especially important in the upper tail, where rent adjustment is weakest and implied NOI losses are largest, and it motivates the next section, which examines how the burden varies across property owners.

## 6 Burden Across Property Owners and Reallocation

As the rent response to rising insurance costs has weakened sharply over time, especially in the upper tail of the shock distribution, climate-risk repricing appears increasingly associated with lower owner NOI. This section turns to the third margin: how the burden varies across property owners. We document three main results. First, insurance pricing varies substantially across owners: larger owners and owners with lower-risk portfolios obtain lower insurance costs, especially for high-risk properties. Second, these advantages are not solely cross-sectional. They appear within continuing ownership relationships, where insurance costs change as incumbent owners' scale and portfolio risk evolve, and they emerge discretely when the same property is absorbed into a larger owner's portfolio through M&A events. Third, the advantages have intensified over time and increasingly coincide with a reallocation of high-risk properties toward larger owners. This reallocation operates on two margins: high-risk properties are more likely to transact when held by smaller owners, and conditional on sale, they are increasingly acquired by larger buyers. The tests below document these pricing patterns and their relation to reallocation, but they do not fully separate the underlying mechanisms, which may include scale in procurement, bargaining power, insurer relationships, risk-management technology, claims behavior, or portfolio diversification.

### 6.1 Owner Characteristics and Insurance Pricing

We begin by examining whether insurance costs vary systematically with owner characteristics. We first examine owner size, measured as the total number of multifamily units held nationally by the property's owner. Figure 8, Panel A plots insurance costs against owner size after absorbing CBSA-by-year fixed effects and shows a clear scale gradient: larger owners pay lower insurance costs per unit and as a share of rent, consistent with economies of scale, greater bargaining power, stronger insurer relationships, or differences in risk management. The relationship is approximately monotonic, with insurance costs declining from very small owners to mid-sized owners and continuing to fall for the largest portfolios.

To quantify this pattern, we estimate

$$Insurance/Rent_{i,o,c,t} = \beta \times RiskScore_i \times \log(OwnerSize)_{o,t} + \delta \times \log(OwnerSize)_{o,t} + \gamma_i + \eta_{c,t} + \varepsilon_{i,o,c,t}, \quad (7)$$

where  $RiskScore_i$  is the risk score of the census tract containing property  $i$ ,  $\log(OwnerSize)_{o,t}$  is the log of the number of multifamily units owned nationally by owner  $o$  in year  $t$ ,  $\gamma_i$  denotes property fixed effects, and  $\eta_{c,t}$  denotes CBSA-by-year fixed effects. Identification comes from within-property variation in insurance costs

as owner size changes over time, either through ownership turnover or through expansion or contraction of the incumbent owner’s portfolio.

Figure 8, Panel B shows that the owner-size advantage is small in low-risk areas but becomes large and statistically significant in high-risk areas. For the riskiest properties, a one-standard-deviation increase in owner size is associated with a reduction in the share of rental income spent on insurance costs of more than 0.34 ppt, or almost 10% of the average insurance-to-rent ratio. Table 5, Panel A confirms this pattern in regression form.<sup>39</sup> Because the specification includes property fixed effects and CBSA-by-year fixed effects, the estimates are not driven simply by larger owners holding systematically different properties or operating in cheaper markets. Instead, they reflect changes in insurance-to-rent ratios for the same property as owner size shifts, net of common local market-year conditions. Owner size therefore matters most where insurance repricing is most severe.

The next question is whether the composition of an owner’s broader portfolio also matters for insurance pricing at individual properties. We define owner portfolio risk as the unit-weighted average risk score of the owner’s multifamily holdings:

$$OwnerPortfolioRisk_{o,t} = \frac{\sum_{i \in Portfolio_o} Units_i \times RiskScore_i}{\sum_{i \in Portfolio_o} Units_i}. \quad (8)$$

We first estimate

$$Insurance/Rent_{i,o,c,t} = \beta \times OwnerPortfolioRisk_{o,t} + \delta \times \log(OwnerSize)_{o,t} + \gamma_i + \eta_{c,t} + \varepsilon_{i,o,c,t}, \quad (9)$$

where the specification includes property fixed effects, CBSA-by-year fixed effects, and a control for owner size. These controls reduce the concern that the relationship between portfolio risk and insurance costs simply reflects owner scale, persistent property differences, or common pricing conditions in a given local market and year. Figure 9, Panel A shows that properties in lower-risk owner portfolios tend to face lower insurance costs even after netting out those factors. This pattern suggests insurance pricing reflects portfolio composition in addition to the focal property’s own risk.<sup>40</sup>

We then ask whether this portfolio-risk channel is stronger for properties where insurance risk is most salient. To do so, we allow a property’s own risk to interact with the owner’s portfolio risk:

$$Insurance/Rent_{i,o,c,t} = \beta \times OwnerPortfolioRisk_{o,t} \times RiskScore_i + \delta \times OwnerPortfolioRisk_{o,t} + \gamma_i + \eta_{c,t} + \varepsilon_{i,o,c,t}. \quad (10)$$

Figure 9, Panel B shows that a decrease in owner portfolio risk is associated with lower insurance costs primarily for properties with higher local disaster risk. For low-risk properties, the estimated effect is close to zero; as property risk increases, the effect becomes increasingly negative. Column (2) of Table 5, Panel B confirms this pattern: the interaction between owner portfolio risk and property risk is positive and statistically significant, implying that higher-risk properties face higher insurance-cost-to-rent ratios when held by owners with riskier portfolios.

Finally, we examine whether the value of a lower-risk portfolio depends on owner scale by estimating

$$Insurance/Rent_{i,o,c,t} = \beta \times OwnerPortfolioRisk_{o,t} \times \log(OwnerSize)_{o,t} + \delta \times OwnerPortfolioRisk_{o,t} + \gamma_i + \eta_{c,t} + \varepsilon_{i,o,c,t}. \quad (11)$$

Figure 9, Panel C shows that the insurance-cost advantage associated with lower portfolio risk is concentrated among larger owners. The estimated effect of a one-standard-deviation decrease in owner portfolio risk is close to zero for small owners but becomes increasingly negative as owner size rises. Column (3) of Table 5, Panel B confirms this pattern: the interaction between portfolio risk and log owner size is positive and

<sup>39</sup> Figure IA.20 and Table IA.6 show similar patterns when local disaster risk is measured using expected annual losses rather than risk scores.

<sup>40</sup> The effect of portfolio risk is distinct from the owner-size effect discussed earlier; both remain economically and statistically significant when considered jointly. Figure IA.21 shows a similar relationship when portfolio risk is measured using unit-weighted expected annual losses.

statistically significant, indicating that riskier portfolios are associated with higher insurance-cost-to-rent ratios especially among larger owners. Thus, portfolio composition appears to matter most when combined with scale: lower portfolio risk is associated with substantially lower insurance costs for large owners but offers little apparent advantage for smaller owners.

## 6.2 Evidence Within Continuing Ownership Relationships

The preceding subsection shows that larger owners and owners with lower-risk portfolios pay less for insurance, after absorbing property and local-market-year differences. A remaining concern is transition-based selection: cheaper-to-insure properties may be the ones that move into larger or lower-risk portfolios. We address this concern by restricting the sample to property-year observations whose owner is unchanged from three years earlier. This rules out selection operating through changes in the focal owner-property match and instead examines whether owner-side insurance advantages appear within stable relationships as the incumbent owner’s total scale and portfolio risk change.<sup>41</sup>

Table 6 shows that the results mirror the cross-sectional patterns documented in the previous subsection. Increases in owner size are associated with declines in the insurance-cost-to-rent ratio, with steeper declines for higher-risk properties; increases in the owner’s average portfolio risk are associated with a higher insurance-cost-to-rent ratio, again concentrated among riskier properties. Because the sample excludes any ownership change over the three-year window, these estimates cannot be driven by selection into acquisitions or dispositions. Year fixed effects and controls for time-varying local risk further absorb broad repricing trends. The remaining variation comes from changes in incumbent owners’ portfolio characteristics within stable owner-property relationships. In line with the broader owner-heterogeneity evidence, properties whose owners become larger or whose portfolios become lower-risk experience lower insurance costs without any ownership transition. The next subsection asks whether insurance costs also shift when ownership itself changes, examining properties that move into larger portfolios through M&A events.

## 6.3 Evidence from Insurance Costs Around M&A Events

The preceding results indicate that larger owners and those with lower-risk portfolios obtain lower insurance costs, both cross-sectionally and within continuing ownership relationships. Whereas the continuing-ownership analysis holds the focal owner-property match fixed and asks whether insurance costs move as incumbent owners’ portfolios evolve, the portfolio-level M&A analysis uses the ownership transition itself as the source of variation. The design does not require acquisitions to be randomly assigned. Instead, it examines whether, relative to never-treated control properties in the same market-year and cohort, insurance costs decline discretely for acquired properties after they are absorbed into a larger owner’s portfolio. A post-acquisition decline under this comparison is consistent with portable owner-side advantages, especially if the decline is larger when the acquirer–target owner-size gap is larger, when the acquired property is riskier, and when the portfolio-risk reduction is larger.

Using the RCA property transaction data, we identify M&A events as concentrated portfolio-level ownership transfers. For each seller-year, we track the properties that exit the seller’s portfolio and classify the event as an M&A transaction if at least 70% of those properties are acquired by a single buyer, distinguishing portfolio-level consolidations from individual asset sales. We exclude transactions in which the acquirer is a bank, loan servicer, Fannie Mae, Freddie Mac, or a mortgage trust company, as these typically reflect foreclosure or loan-resolution activity rather than voluntary portfolio transfers. We require the acquirer’s pre-deal portfolio to exceed the target’s, restricting the sample to transactions in which properties genuinely move into larger ownership structures. Applying these filters yields 142 M&A events involving 1,023 target properties and 102 unique acquiring owners from 2011 through 2024.<sup>42</sup>

To estimate the insurance-cost response to an acquisition, we use a stacked difference-in-differences design. For each acquisition cohort year  $g$ , we construct a stack that combines treated properties acquired

<sup>41</sup> We examine changes in insurance costs over the same three-year period over which changes in the incumbent owner’s scale and portfolio risk are measured.

<sup>42</sup> We additionally exclude targets with fewer than five properties at  $t - 1$  to remove single-property sales and very small investors. We validate the M&A classification by manually comparing a random 10% sample of identified events to publicly reported M&A transactions.

in year  $g$  with control properties drawn from the never-treated pool. The never-treated pool consists of properties whose owners never appear as either an acquirer or a target in our M&A registry. Treated and control properties are observed over an event-time window spanning three years before and three years after the transaction. We estimate the following specification:

$$\text{Insurance/Rent}_{i,t,g} = \beta \times \text{Post}_{t,g} \times \text{Treated}_{i,g} + \gamma_{i,g} + \eta_{c,t,g} + \varepsilon_{i,t,g}, \quad (12)$$

where  $\text{Post}_{t,g} = \mathbb{1}\{t \geq g\}$ . The coefficient  $\beta$  provides an average estimate of the insurance-cost-to-rent response after acquisition, capturing whether the ratio of insurance costs to rent changes when properties are absorbed into acquirers' portfolios. We also estimate a dynamic specification:

$$\text{Insurance/Rent}_{i,t,g} = \sum_{\tau \neq -1} \beta_{\tau} \times \mathbb{1}\{t - g = \tau\} \times \text{Treated}_{i,g} + \gamma_{i,g} + \eta_{c,t,g} + \varepsilon_{i,t,g}, \quad (13)$$

which traces the year-by-year path of the insurance-cost-to-rent ratio around the acquisition. This dynamic specification allows us to assess whether treated properties are already on differential insurance-cost trends before the transaction and to examine how quickly the post-acquisition response emerges. In both specifications,  $i$  denotes property,  $t$  year,  $g$  cohort, and  $c$  CBSA;  $\gamma_{i,g}$  and  $\eta_{c,t,g}$  denote property-by-cohort fixed effects and CBSA-by-year-by-cohort fixed effects. Standard errors are clustered at the owner level.<sup>43</sup> The property-by-cohort fixed effects absorb all time-invariant differences across properties, while the CBSA-by-year-by-cohort fixed effects absorb common shocks to insurance pricing within a local market and year. The remaining variation therefore comes from whether the ratio of insurance costs to rent for the same property changes discretely around the ownership transition relative to other properties in the same market-year and cohort.

Table 7, Panel A reports estimates from Equation (12). The insurance-cost-to-rent ratio declines by 1.02 ppt after acquisition—an economically meaningful reduction that is consistent with acquired properties gaining access to the new owner's scale, bargaining leverage, and insurer relationships. Columns (2) and (3) show that the pattern is not specific to the rent-based measure: the insurance-cost-to-operating-expenses ratio falls by 1.63 ppt, and insurance costs per unit decline by 13.7%.

Figure 10 plots the event-time coefficients from the dynamic specification in Equation (13). The pre-acquisition coefficients are small and statistically indistinguishable from zero, consistent with the parallel-trends assumption. After acquisition, insurance costs decline sharply relative to rent: the insurance-cost-to-rent ratio falls by approximately 0.6 ppt in the transaction year, and the point estimates remain negative over the entire three-year post-event window. This persistence is consistent with acquired properties gaining durable access to the new owner's insurer relationships and portfolio-level bargaining leverage, rather than only a transitory repricing around the ownership transfer. Panels B and C show that the post-event decline is also visible for the insurance-cost-to-operating-expenses ratio and log insurance cost per unit.<sup>44</sup>

We next examine heterogeneity in the M&A effect along three dimensions: the acquirer-target owner-size gap, the acquired property's own disaster exposure, and the portfolio-risk reduction implied by the acquisition. We begin with the acquirer-target owner-size gap, which speaks directly to the owner-size channel. If the post-M&A decline reflects gains from scale, bargaining leverage, and insurer relationships, those gains should be more pronounced when the acquiring owner is substantially larger than the target. We define the owner-size gap at  $t - 1$  as the difference between the acquirer's and target's total portfolio units and split treated properties at the median.<sup>45</sup> Figure 11, Panel A shows that the post-M&A decline in insurance costs is

<sup>43</sup> Specifically, we cluster by acquiring owner for treated observations. For control observations, ownership remains unchanged throughout the event window.

<sup>44</sup> A natural concern is that M&A events may be accompanied by renovation activity at newly acquired properties. To address this concern, we estimate the dynamic M&A specification using an indicator for whether the property is renovated as the outcome and find that renovation activity does not change discontinuously around these acquisitions (see Figure IA.22). Building-permit records from Builtly provide a similar check: neither the probability of any building permit nor the probability of an insurance-cost-relevant permit changes discontinuously around acquisition (see Figure IA.23).

<sup>45</sup> Because the owner-size gap is observed only for acquired properties, this split affects only how treated properties are grouped and holds the never-treated control pool fixed. Each series in these heterogeneity figures is estimated separately using the relevant treated group and its associated control properties. For example, the blue and pink series in Figure 11, Panel A use high- and

stronger for high-owner-size-gap deals, with the gap between high- and low-owner-size-gap point estimates widening through the post-event window. This pattern is consistent with the interpretation that the magnitude of the owner-size gap, rather than the ownership transfer alone, is an important component of the insurance savings.

Second, we ask whether the M&A effect varies with the acquired property’s own disaster exposure, motivated by the earlier finding in Figure 8, Panel B and Table 5, Panel A that the insurance-cost advantage of larger owners is concentrated in high-risk locations.<sup>46</sup> Columns (1) and (2) of Table 7, Panel B show that post-M&A insurance savings are substantially larger for high-risk properties: the insurance-cost-to-rent ratio falls by 1.44 ppt for properties with above-median risk scores, compared with 0.49 ppt for those with below-median risk scores, a statistically significant difference with a  $p$ -value of 0.022. Columns (3) and (4) repeat the same property-risk split within the subsample of deals with an above-median owner-size gap, isolating how property risk interacts with a large owner-size gap. The high-risk effect strengthens to 1.99 ppt, while the low-risk effect remains smaller at 0.58 ppt, a statistically significant difference with a  $p$ -value of less than 0.01. By contrast, Columns (5) and (6) show that for deals with a below-median owner-size gap, both the high- and low-risk effects are smaller and cannot be statistically distinguished from one another ( $p$ -value = 0.44). Figure 11, Panel B shows the corresponding dynamic stacked-DiD results. This heterogeneity by owner-size gap indicates that acquisition into a larger portfolio is most valuable precisely where climate risk is greatest and insurance pricing is most responsive to ownership structure.

Finally, we examine whether the M&A effect varies with the portfolio-risk reduction, motivated by the earlier finding in Figure 9, Panel A and Table 5, Panel B that properties held in lower-risk portfolios face lower insurance costs, and by Figure 9, Panel C, which shows that this portfolio-risk channel is concentrated among large owners.<sup>47</sup> Columns (1) and (2) of Table 7, Panel C show that the post-M&A decline in the insurance-to-rent ratio is more than twice as large when the portfolio-risk reduction is high: 1.38 ppt for above-median deals, compared with 0.61 ppt for below-median deals, a statistically significant difference with a  $p$ -value of 0.079. Columns (3) and (4) repeat the split within the subsample of deals with an above-median owner-size gap and show that the effect of above-median portfolio-risk reductions strengthens to 1.72 ppt, while the below-median effect remains close to its unconditional value, a statistically significant difference with a  $p$ -value of less than 0.01. By contrast, Columns (5) and (6) show that for deals with a below-median owner-size gap, both the above- and below-median effects are smaller and cannot be statistically distinguished from one another ( $p$ -value = 0.62). Figure 11, Panel C shows the corresponding dynamic stacked-DiD results. The right subpanel shows that the most substantial decline in insurance costs post-acquisition occurs for deals that combine a large owner-size gap with a large portfolio-risk reduction.

Taken together, the continuing-ownership and M&A results indicate that owner-side insurance advantages are more than static correlations across properties or owners. They appear within incumbent relationships, emerge discretely when properties change hands through acquisition, and are largest where they are most consequential—for the highest-risk properties, when the owner-size gap is largest, and when the portfolio-risk reduction is largest. The results reinforce the broader interpretation that owner scale, risk management, portfolio composition, and bargaining power matter for insurance pricing. The next subsection examines whether these advantages have become more important as climate-risk repricing has intensified and whether they are associated with transaction behavior and the reallocation of high-risk properties toward larger owners.

## 6.4 Dynamics of Pricing Advantages and Ownership Reallocation

Figure 12 documents how the insurance-pricing advantages associated with owner size and owner portfolio risk have evolved over time. Panel A shows how the effect of a one-standard-deviation increase in owner

low-owner-size-gap treated properties, respectively, along with all control properties.

<sup>46</sup> Unlike the owner-size-gap test, property risk is observed for both treated and never-treated properties, so we partition the entire stacked panel at the global median risk score: high-risk treated properties are compared with high-risk controls, and low-risk treated properties are compared with low-risk controls. Tables IA.7 and IA.8 show similar heterogeneity when the insurance-cost-to-operating-expenses ratio or  $\log(\text{Insurance Cost Per Unit})$  is used as the dependent variable.

<sup>47</sup> We define the portfolio-risk reduction as the difference between the target’s and acquirer’s unit-weighted average portfolio risk score at  $t - 1$  and split treated properties at the median. “High Portfolio-Risk Reduction” deals are those in which the acquired property moves into a substantially less risky portfolio.

size differs over time between properties whose risk scores differ by 50 points. Before 2018, the differential owner-size advantage is similar to the 2017 benchmark. After 2020, the estimates become increasingly negative, indicating that the insurance-pricing advantage of larger owners becomes progressively stronger for higher-risk properties. By 2024, this differential effect is 0.18 ppt stronger, consistent with owner scale becoming more valuable precisely where local disaster risk is greater. Panel B shows a similar time-series pattern for owner portfolio risk. The effect of a one-standard-deviation decrease in owner portfolio risk is similar to the 2017 benchmark before 2020, increases sharply after 2020, and remains large in the most recent years, indicating that lower-risk owner portfolios are associated with larger insurance savings in the recent repricing period. Column (3) of Table 5, Panel A and Column (4) of Table 5, Panel B show this intensification in regression form.

These dynamics indicate that owner heterogeneity has become more consequential as climate-risk repricing has intensified.<sup>48</sup> When the rent response to rising insurance costs is larger, owner-side differences in insurance pricing matter less for profitability. As owners’ ability to offset rising costs through rents has weakened—especially in the upper tail, where rent adjustment is weakest and implied NOI losses are largest—differences in owner scale and portfolio risk have become increasingly important predictors of who can absorb insurance shocks.

We then examine whether these pricing advantages are reflected in ownership patterns and transaction behavior. Figure 13, Panel A compares the relationship between local risk and owner size in 2010 and 2024. In 2010, owner size is essentially unrelated to local risk. By 2024, this relationship has strengthened sharply: properties in riskier areas are significantly more likely to be held by larger owners. To quantify this shift, we estimate

$$\log(\text{OwnerSize})_{i,o,t} = \sum_{t \neq 2010} \beta_t \times \mathbb{1}(\text{Year} = t) \times \text{RiskScore}_i + \gamma_i + \tau_t + \varepsilon_{i,o,t}, \quad (14)$$

where the dependent variable is the log of the number of units owned nationally by property  $i$ ’s owner  $o$  in year  $t$ , and the independent variable is the risk score of the property’s location, interacted with year indicators. Because property fixed effects ( $\gamma_i$ ) are included, this specification isolates within-property changes in the size of the owner of a given property. Year fixed effects ( $\tau_t$ ) absorb aggregate changes in owner size common to all properties. Accordingly, the coefficients  $\beta_t$  trace how the relationship between local risk and owner size evolves over time relative to 2010.

Figure 13, Panel B shows that the positive relationship between local risk and owner size strengthens steadily over time, with the divergence concentrated after 2018. Table 8, Panel A shows this in regression form. The estimates with property fixed effects are particularly informative: after 2018, riskier properties experience larger within-property increases in owner size, ruling out an interpretation based solely on cross-sectional sorting.

Figure 14 provides complementary evidence on the sale margin, using regressions that include CBSA-by-year fixed effects so estimates are identified from within-market comparisons. Before 2018, high-risk properties are not systematically more likely to sell across the owner-size distribution. After 2018, a clear small-owner sale-margin response emerges: high-risk properties held by the smallest owners are the most likely to transact, with the largest estimates concentrated in the bottom two owner-size deciles and smaller estimates for mid-sized and larger owners.<sup>49</sup> The sale-margin evidence is consistent with an ownership response in which high-risk assets increasingly move out of smaller-owner portfolios during the period of rising insurance costs.

Table 8, Panel B shows that, conditional on a sale occurring, high-risk properties owned by smaller owners are transferred to significantly larger buyers after 2018. All columns include CBSA-by-year fixed effects, comparing transactions in the same local market and year. Columns (2) and (3) further absorb year-specific effects for small owners and for high-risk properties separately, so the triple-interaction coefficient captures whether being both high-risk and held by a small owner predicts being bought by a larger buyer after 2018,

<sup>48</sup> The timing differs from the initial post-2018 risk-pricing break: local-risk repricing begins after 2018, while owner-side pricing advantages become most visible after 2020, when insurance-cost growth accelerates and the rent response weakens.

<sup>49</sup> Figure IA.24 shows that this sale-margin effect strengthens over time, becomes statistically significant in 2021–2022, and remains positive thereafter.

net of general post-2018 shifts along either dimension alone. The key result is robust across all three specifications: after 2018, high-risk assets sold by smaller owners are acquired by buyers that are, on average, 16–18% larger. The pre-2018 triple interaction is close to zero and statistically insignificant, consistent with a post-2018 phenomenon. Together, these findings are consistent with an active sorting mechanism: as the insurance-pricing advantages of large owners have become more valuable in risky areas, high-risk assets are more likely to be sold when held by smaller owners and systematically reallocated toward larger buyers.

The evidence in this section shows that the owner-level burden of rising insurance costs is uneven: larger owners and those with lower-risk portfolios are better positioned to obtain favorable pricing, especially in high-risk locations. Owner-side pricing advantages—broadly uniform across risk tiers before 2018—have since become increasingly concentrated in the high-risk properties where the rent response has weakened most. Ownership patterns move in the same direction: after 2018, the same property is increasingly likely to be held by a larger owner when it is located in a riskier area, and when smaller owners of high-risk properties sell, they are bought by systematically larger buyers. Climate-risk repricing therefore goes beyond raising costs; it is increasingly associated with who holds risky assets.

The welfare implications of this reallocation depend on the source of the owner advantages. If larger and lower-risk-portfolio owners obtain lower insurance costs through better risk management, lower expected claims, or more efficient diversification, reallocation toward these owners would be consistent with improved risk bearing and could benefit tenants if lower insurance costs are reflected in rents. If instead the advantages primarily reflect bargaining power, the gains may reflect transfers from insurers to large owners and need not lower tenant costs. The current evidence documents the pricing advantages and reallocation patterns, while separating these mechanisms remains an important direction for future work.

## 7 Conclusion

We document a large and widespread rise in commercial property insurance costs in the United States over the last decade and study who bears these costs across locations, between tenants and property owners, and across property owners. Commercial pricing depends on more than local physical risk: it is shaped by the interaction of global reinsurance markets, regulatory spillovers from homeowners insurance, and owner scale and portfolio characteristics. These forces shape which locations face larger cost increases, how the burden is divided between tenants and owners, how it is capitalized into property values, and how it reshapes the ownership of exposed assets.

Across locations, we document three dimensions along which this repricing varies. First, insurers price local climate risk more aggressively after 2018, with insurance cost growth becoming substantially more sensitive to both expected and realized disaster risk. Second, rising reinsurance costs amplify local repricing, especially in states with greater ex ante exposure to reinsurance markets. Third, commercial premiums rise disproportionately in states with high homeowners-market frictions, which distort relative pricing across insurance lines and spill over into commercial policies through cross-product subsidization. In our border-county-pair design, after major disasters, commercial insurance costs rise 19–22 ppt more on the high-friction side of a state border.

Between tenants and property owners, there has been a material shift in who bears rising insurance costs and climate risk in multifamily housing. In the baseline specification, our estimates imply that 49% of the increase in insurance costs is reflected in rents on average, while more demanding CBSA-by-class-by-year specifications imply smaller shares of roughly 37–39%. Cross-sectionally, the rent response is stronger in markets with more inelastic housing supply, among owners with higher local market share, in areas with greater moving frictions, and in areas with fewer tenant outside options, while NOI declines are larger where the rent response is weaker. Rent adjustment also declines sharply over time. Early in the sample, the rent response to insurance cost increases is substantially larger; by 2024, the marginal rent response falls to nearly zero. The implied average cumulative effects over 2014–2024 are modest, but the upper tail is much more severe: for properties facing the largest insurance shocks, implied rent increases are meaningful and profitability declines sharply. The transaction evidence shows that this repricing is increasingly capitalized into property valuations, with riskier properties trading at lower prices and higher cap rates relative to the pre-2018 period. The effects of climate-risk repricing therefore go beyond increasing insurance expenses to also who ultimately bears the risk and how it is capitalized into property values.

Across property owners, the burden of this repricing is highly uneven. Larger owners obtain lower insurance costs than smaller owners, especially in high-risk areas, and owners with lower-risk portfolios pay less even for otherwise similar high-risk properties. These advantages are not solely cross-sectional: they also appear within continuing ownership relationships, where increases in owner size are associated with lower insurance costs for incumbent properties, while reductions in portfolio risk are associated with lower costs. Insurance costs also decline discretely following portfolio-level M&A events, with the largest post-acquisition savings appearing when the acquirer-target owner-size gap is largest, acquired properties are riskier, and the acquisition produces a larger reduction in portfolio risk. Since 2020, these pricing advantages have become increasingly concentrated in high-risk properties and have coincided with a reallocation of high-risk assets toward larger owners with scale advantages. After 2018, high-risk properties owned by smaller owners become more likely to change hands and, conditional on sale, more likely to be acquired by larger buyers.

Because insurance is required for multifamily finance, repricing in insurance markets converts climate exposure into a recurring operating-cost shock. That shock is allocated along three margins: across locations through local risk, reinsurance exposure, and homeowners-market frictions; between tenants and property owners through rents, NOI, and asset prices; and across property owners through insurance-pricing advantages and ownership reallocation. When homeowners-market frictions constrain repricing, part of the burden may be shifted into commercial policies; because commercial insurance costs are partly reflected in rents, these cross-line spillovers may imply that renters indirectly subsidize homeowners. More broadly, when coverage requirements limit adjustment margins and premiums cannot be fully offset by rent increases, climate risk is allocated not only through NOI compression, lower valuations, and higher required yields, but also through the reallocation of properties among owners.

## References

- Aunon-Nerin, Daniel, and Paul Ehling, 2008, Why firms purchase property insurance, *Journal of Financial Economics* 90, 298–312.
- Austin, Neroli, 2022, Keeping up with the blackstones: Institutional investors and gentrification, Working Paper.
- Bakkensen, Laura A, and Lint Barrage, 2021, Going Underwater? Flood Risk Belief Heterogeneity and Coastal Home Price Dynamics, *Review of Financial Studies* 35, 3666–3709.
- Baum-Snow, Nathaniel, and Lu Han, 2024, The Microgeography of Housing Supply, *Journal of Political Economy* 132, 1897–1946.
- Bernstein, Asaf, Matthew T. Gustafson, and Ryan Lewis, 2019, Disaster on the horizon: The price effect of sea level rise, *Journal of Financial Economics* 134, 253–272.
- Board of Governors of the Federal Reserve System, 2026, Financial stability report, Technical report, Board of Governors of the Federal Reserve System, May 2026. Accessed May 15, 2026.
- Boomhower, Judson, Meredith Fowlie, and Andrew J. Plantinga, 2023, Wildfire Insurance, Information, and Self-Protection, *AEA Papers and Proceedings* 113, 310–15.
- Born, Patricia H., and Barbara Klimaszewski-Blettner, 2013, Should I stay or should I go? the impact of natural disasters and regulation on u.s. property insurers’ supply decisions, *Journal of Risk and Insurance* 80, 1–36.
- Buschbom, Stephen, Evan Eastman, Chongyu Wang, and Tingyu Zhou, 2025, Climate risk and commercial property insurance, Working Paper.
- Carroll, Robert J, and John Yinger, 1994, Is the property tax a benefit tax? the case of rental housing, *National Tax Journal* 47, 295–316.
- Cookson, J Anthony, Emily Gallagher, and Philip Mulder, 2025, Coverage Neglect in Homeowner’s Insurance, Working Paper.
- Coven, Joshua, 2023, The impact of institutional investors on homeownership and neighborhood access, Working Paper.
- Diamond, Rebecca, Tim McQuade, and Franklin Qian, 2019, The effects of rent control expansion on tenants, landlords, and inequality: Evidence from san francisco, *American Economic Review* 109, 3365–94.
- Eastman, Evan M., and Kyeonghee Kim, 2024, Regulatory capital and catastrophe risk, Working Paper.
- Fang, Lu, Lingxiao Li, David Scofield, and Abdullah Yavas, 2024, Price impact of climate risk on commercial real estate, Working Paper.
- Foerster, Kai, Ellen Ryan, and Benedikt Alois Scheid, 2025, Pricing or panicking? commercial real estate markets and climate change, Working Paper Series 3059, European Central Bank.
- Froot, Kenneth A., 1997, The limited financing of catastrophe risk: An overview, NBER Working Paper 6025, National Bureau of Economic Research.
- Froot, Kenneth A., 2001, The market for catastrophe risk: a clinical examination, *Journal of Financial Economics* 60, 529–571.
- Froot, Kenneth A., and Paul G. J. O’Connell, 1999, The pricing of u.s. catastrophe reinsurance, in Kenneth A. Froot, ed., *The Financing of Catastrophe Risk*, chapter 5, 195–232 (University of Chicago Press, Chicago).
- Froot, Kenneth A., and Paul G. J. O’Connell, 2008, On the pricing of intermediated risks: Theory and application to catastrophe reinsurance, *Journal of Banking & Finance* 32, 69–85.

- Ge, Shan, 2022, How do financial constraints affect product pricing? Evidence from weather and life insurance premiums, *Journal of Finance* 77, 449–503.
- Ge, Shan, Stephanie Johnson, and Nitzan Tzur-Ilan, 2026, The Effect of Rising Insurance Premiums on Mortgage Delinquency and Household Relocation, Working Paper.
- Ge, Shan, Ammon Lam, and Ryan Lewis, 2024, The Effect of Insurance Premiums on the Housing Market and Climate Risk Pricing, Working Paper.
- Glaeser, Edward L., Joseph Gyourko, and Raven E. Saks, 2005, Why have housing prices gone up?, *American Economic Review* 95, 329–333.
- Gorback, Caitlin, Franklin Qian, and Zipei Zhu, 2024, Impact of institutional owners on housing markets, Working Paper.
- Griffin, John M., and Alex Priest, 2023, Is COVID revealing a virus in CMBS 2.0?, *Journal of Finance* 78, 2233–2276.
- Gron, Anne, 1994, Capacity constraints and cycles in property-casualty insurance markets, *RAND Journal of Economics* 25, 110–127.
- Heeb, Gina, 2024, Fannie, Freddie Are Poised to Tighten Real-Estate Lending Rules, <https://www.wsj.com/real-estate/fannie-mae-freddie-mac-commercial-property-lenders-brokers-rules-116907c2>, Wall Street Journal Article.
- Hino, Miyuki, and Marshall Burke, 2021, The effect of information about climate risk on property values, *Proceedings of the National Academy of Sciences* 118, e2003374118.
- Holtermans, Rogier, Matthew E. Kahn, and Nils Kok, 2024, Climate risk and commercial mortgage delinquency, *Journal of Regional Science* 64, 994–1037.
- Hoyt, Robert E., and Ho Khang, 2000, On the demand for corporate property insurance, *Journal of Risk and Insurance* 67, 91–107.
- Ibragimov, Rustam, Dwight Jaffee, and Johan Walden, 2009, Nondiversification Traps in Catastrophe Insurance Markets, *Review of Financial Studies* 22, 959–993.
- Jaffee, Dwight M., and Thomas Russell, 1997, Catastrophe insurance, capital markets, and uninsurable risks, *Journal of Risk and Insurance* 64, 205–230.
- Kalda, Ankit, Varun Sharma, Vikas Soni, and Derek Wenning, 2025, Beyond the storm: Climate risk and homeowners' insurance, Working Paper.
- Keys, Benjamin J, and Philip Mulder, 2025, Property Insurance and Disaster Risk: New Evidence from Mortgage Escrow Data, Working Paper.
- Kim, Kyeonghee, J. Tyler Leverty, and Junhao Liu, 2025, Compliance costs of contract regulation, Working Paper.
- Koijen, Ralph S. J., Neel Shah, and Stijn Van Nieuwerburgh, 2026, The Commercial Real Estate Ecosystem, Working Paper.
- Koijen, Ralph S. J., and Motohiro Yogo, 2015, The cost of financial frictions for life insurers, *American Economic Review* 105, 445–75.
- Lee, Jaeyeon, 2024, Asymmetric pass-through of interest rates to rental prices: Evidence from rental listings for multi-unit housing, Working Paper.
- Mayers, David, and Jr. Smith, Clifford W., 1990, On the corporate demand for insurance: Evidence from the reinsurance market, *Journal of Business* 63, 19–40.

- Mills, James, Raven Molloy, and Rebecca Zarutskie, 2019, Large-scale buy-to-rent investors in the single-family housing market: The emergence of a new asset class, *Real Estate Economics* 47, 399–430.
- Murfin, Justin, and Matthew Spiegel, 2020, Is the risk of sea level rise capitalized in residential real estate?, *Review of Financial Studies* 33, 1217–1255.
- Oh, Sangmin, Ishita Sen, and Ana-Maria Tenekedjieva, 2025, Pricing of Climate Risk Insurance: Regulation and Cross-Subsidies, *Journal of Finance* Forthcoming.
- Powell, Lawrence S., David W. Sommer, and David L. Eckles, 2008, The role of internal capital markets in financial intermediaries: Evidence from insurer groups, *Journal of Risk and Insurance* 75, 439–461.
- Sastry, Parinitha, 2026, Who Bears Flood Risk? Evidence from Mortgage Markets in Florida, *Review of Financial Studies* Forthcoming.
- Sastry, Parinitha, Tess Scharlemann, Ishita Sen, and Ana-Maria Tenekedjieva, 2025, The Insurance Protection Gap, Working Paper.
- Sastry, Parinitha, and Ishita Sen, 2025, Perspectives on insurance and climate risk, *Journal of Finance: Insights and Perspectives* Forthcoming.
- Sastry, Parinitha, Ishita Sen, and Ana-Maria Tenekedjieva, 2026, When insurers exit: Climate losses, fragile insurers, and mortgage markets, Working Paper.
- Seltzer, Lee H, Laura Starks, and Qifei Zhu, 2026, Climate Regulatory Risks and Corporate Bonds, *Journal of Financial Economics* Forthcoming.
- Sen, Ishita, 2023, Regulatory Limits to Risk Management, *Review of Financial Studies* 36, 2175–2223.
- Sen, Ishita, and David Humphry, 2020, Capital Regulation and Product Market Outcomes, Working Paper.
- U.S. Department of the Treasury, 2025, Analyses of U.S. Homeowners Insurance Markets, 2018–2022: Climate-Related Risks and Other Factors, Technical report, U.S. Department of the Treasury.
- Wagner, Katherine R. H., 2022, Adaptation and adverse selection in markets for natural disaster insurance, *American Economic Journal: Economic Policy* 14, 380–421.
- Weyl, E. Glen, and Michal Fabinger, 2013, Pass-through as an economic tool: Principles of incidence under imperfect competition, *Journal of Political Economy* 121, 528–583.
- Winter, Ralph A., 1994, The dynamics of competitive insurance markets, *Journal of Financial Intermediation* 3, 379–415.

**Figure 1: Time-Series Changes in Commercial Property Insurance Costs**

This figure documents the rise in commercial property insurance costs over time. Panel A plots insurance costs for multifamily properties as a share of rent and total operating expenses from 2010 to 2024, along with 25th–75th percentile bands. Panels B and C plot annual percentage changes in insurance costs, with Panel B focusing on multifamily properties and Panel C on other commercial property types using Bloomberg data.

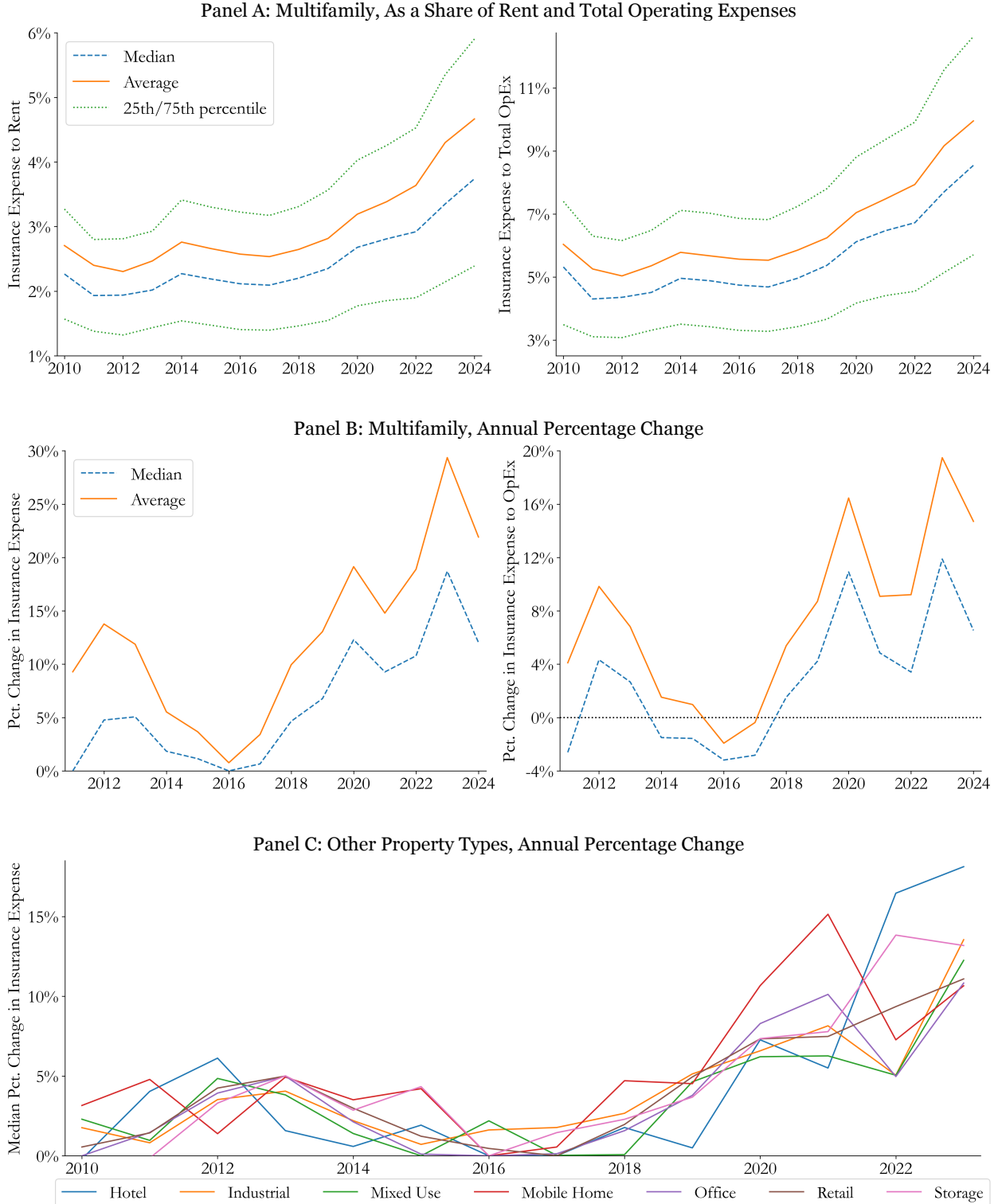
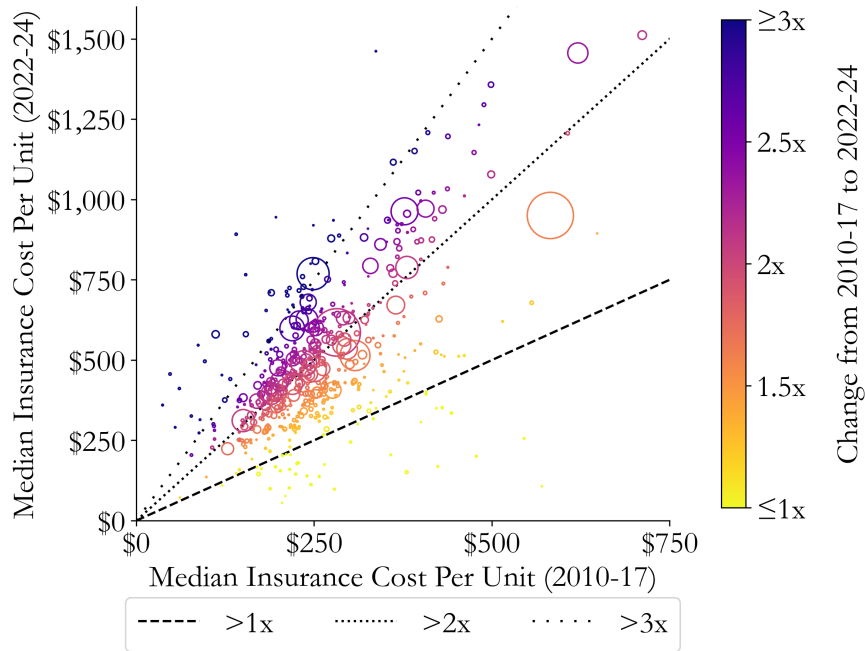


**Figure 2: Cross-Sectional Variation in Insurance Cost Changes**

This figure shows cross-sectional variation in the rise in insurance costs for multifamily properties across Core-Based Statistical Areas (CBSAs). Panel A compares median insurance cost per unit in 2010–2017 with median insurance cost per unit in 2022–2024 for each CBSA. Each circle represents a CBSA, with circle size proportional to the number of sample properties; dashed lines indicate one-, two-, and three-fold increases. Panel B maps the percentage change in insurance costs between 2022 and 2023 across CBSAs. Colors indicate the magnitude of the change, as shown in the respective color bars. Both panels restrict to CBSAs with at least five observations in the relevant periods (2010–2017 and 2022–2024 for Panel A; 2022 and 2023 for Panel B).

Panel A: Median Insurance Cost Per Unit by CBSA, 2010–2017 vs. 2022–2024



Panel B: CBSA-Level Insurance Cost Increase, 2022–2023



### Figure 3: Commercial vs. Homeowners Insurance Costs

This figure compares commercial property insurance costs with homeowners insurance costs. The commercial-homeowners ratio should be interpreted as a reduced-form relative-pricing wedge across sectors, not as a literal matched-premium ratio for comparable contracts. Panel A presents county-level scatterplots of annual average percentage changes in commercial and homeowners insurance costs for 2019–2020, 2020–2021, and 2021–2022. Each bubble represents a county and is sized by population. Dashed reference lines indicate equal growth, twice as much growth in commercial costs, and five times as much growth in commercial costs relative to homeowners costs. Region labels report the share of the U.S. population living in counties with the corresponding relative cost changes. Homeowners insurance data are from [U.S. Department of the Treasury \(2025\)](#). Panel B examines how the commercial-homeowners wedge varies with local risk and state-level homeowners insurance frictions. The specification includes state-by-year fixed effects, and standard errors are clustered at the state level. The state-level friction measure is from [Oh, Sen, and Tenekedjieva \(2025\)](#). Risk scores and expected annual losses are measured at the census tract level using FEMA’s National Risk Index.

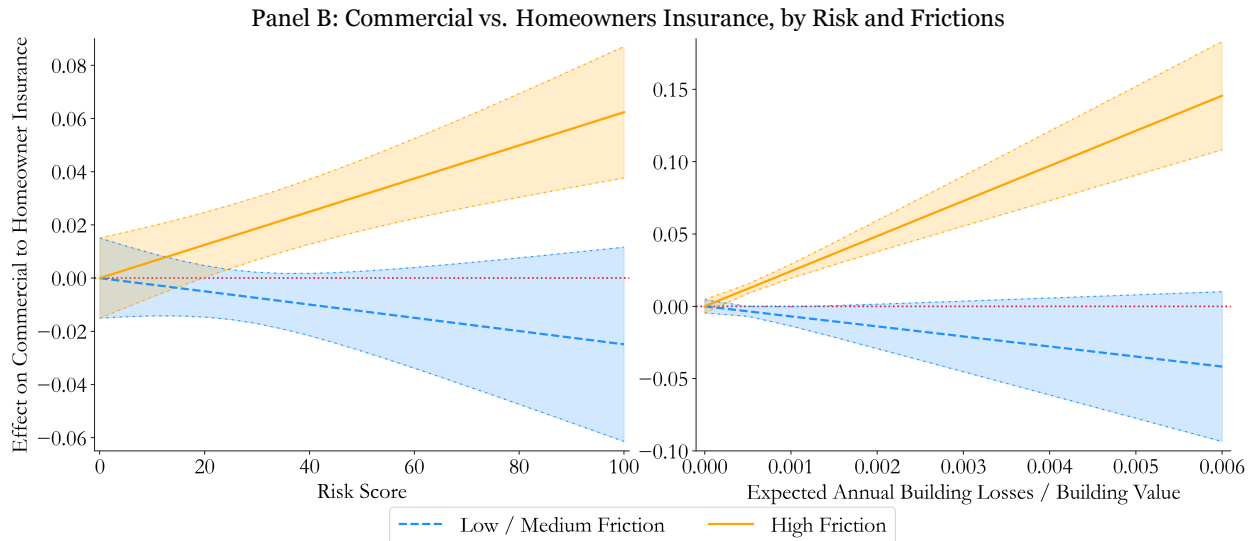
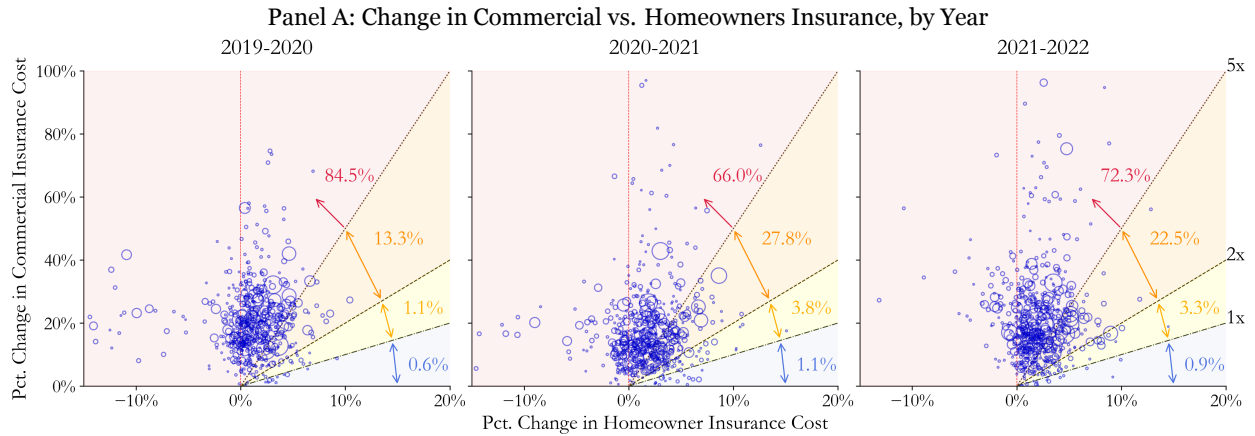


### Figure 4: Expected Risk, Realized Risk, and Insurance Cost Growth

This figure examines how local expected disaster risk and realized disaster damages relate to insurance cost growth. Panel A shows how the relationship between insurance costs and local risk measures evolves over time. The left subpanel plots annual coefficients on the tract-level risk score, and the right subpanel plots annual coefficients on expected annual building losses per capita; the dependent variable is insurance cost per unit. Panel B examines realized disaster damages using county-level property damage data from Arizona State University’s Spatial Hazard Events and Losses Database. The left subpanel reports coefficients from regressions of percentage changes in insurance costs on average property damages per capita over one- to five-year horizons. The right subpanel estimates the same coefficients separately for early years (2017 and earlier) and later years (2018 and later). All specifications include year fixed effects. Error bars represent 95% confidence intervals.

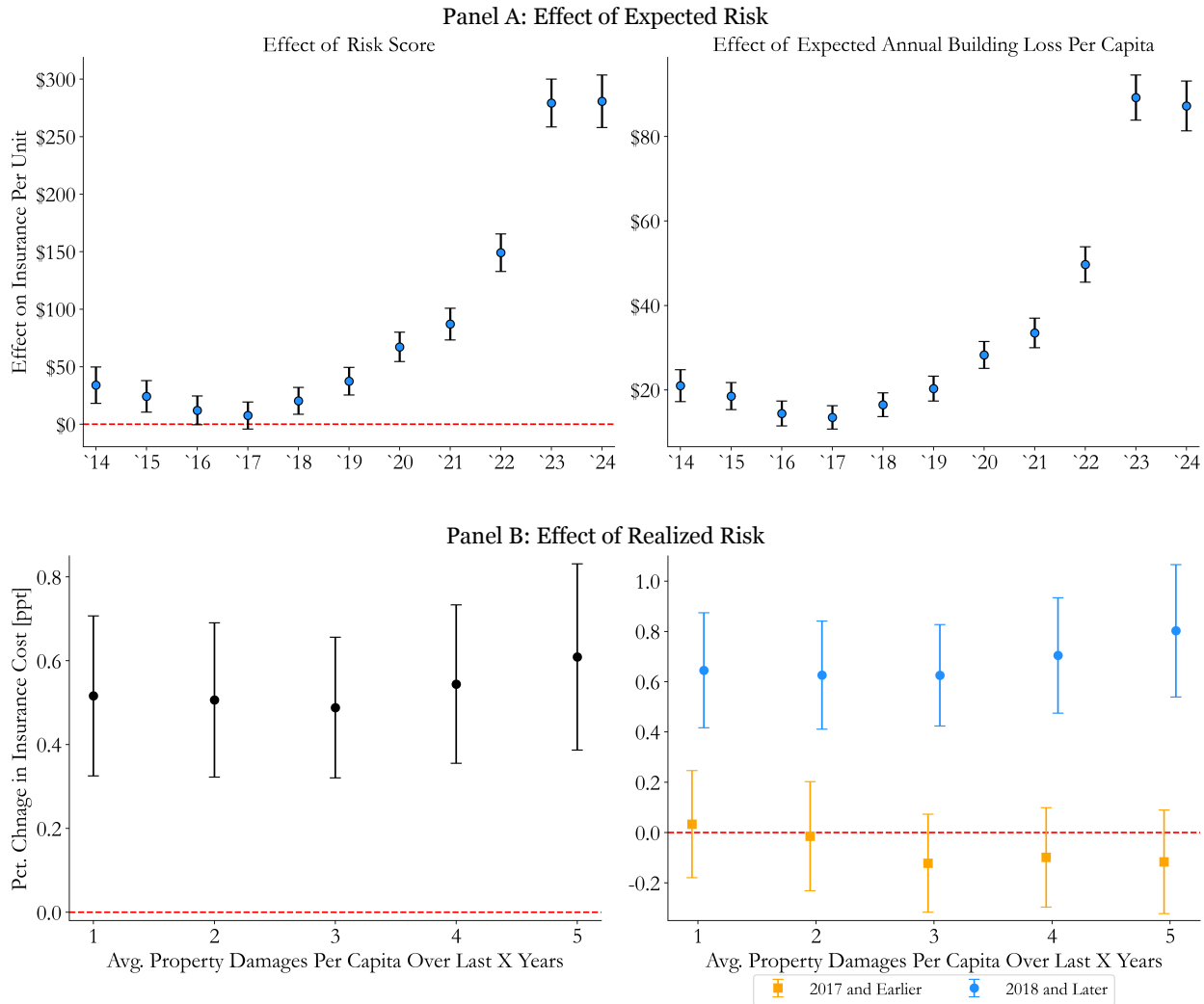
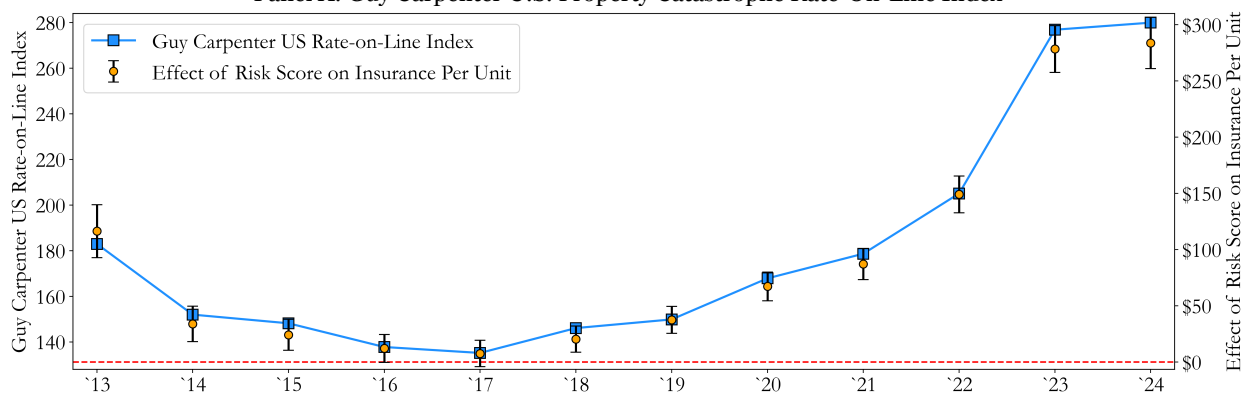


**Figure 5: Reinsurance Costs and Amplification**

This figure examines the role of rising reinsurance costs. Panel A plots the Guy Carpenter U.S. Property Catastrophe Rate-On-Line Index, a benchmark for national reinsurance pricing (blue, squares, left axis), and the year-specific estimated relationship between local disaster risk and insurance-cost growth (orange, dots, right axis), with 95% confidence intervals based on standard errors clustered by census tract. Panel B plots marginal effects from the triple-interaction regression in Equation (2), showing the implied change in insurance cost per unit from a 10-index-point increase in reinsurance costs across levels of local risk (horizontal axis) and state-level reinsurance exposure (colored lines). The lines in Panel B are implied by the single triple-interaction specification rather than estimated separately. Reinsurance exposure is defined at the state level following [Keys and Mulder \(2025\)](#) and is based on the percentage of each insurer’s risk ceded to unaffiliated reinsurers and premiums written in each state in 2017. Specifically,  $ReinsuranceExposure_s = \frac{\sum_{i \in I} DirectPremiumsWritten_{i,s} \times PctCeded_i}{\sum_{i \in I} DirectPremiumsWritten_{i,s}}$ .

Panel A: Guy Carpenter U.S. Property Catastrophe Rate-On-Line Index



Panel B: Differential Effects of Reinsurance Cost Changes by Reinsurance Exposure  
Effect of 10 Index Point Increase in Reinsurance Cost

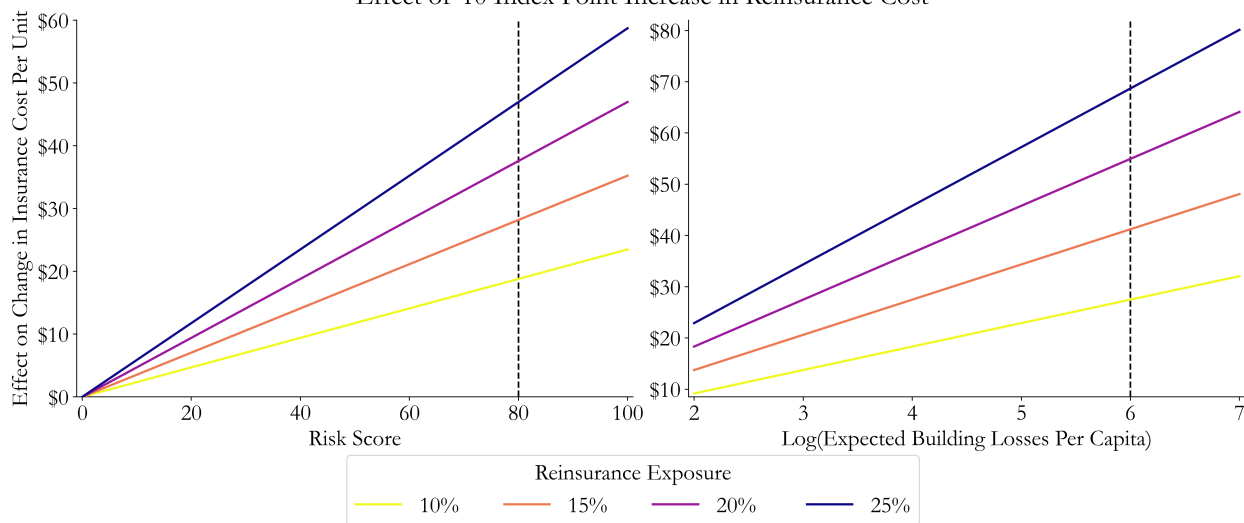


**Figure 6: Incidence of Insurance Cost Increases on Rents, Heterogeneity**

This figure examines heterogeneity in the incidence of insurance cost increases on rents across levels of local housing-supply elasticity, local owner market share, moving frictions, and tenant outside options. The dependent variable is log rent per unit, and the plotted coefficients come from regressions of log rent per unit on log insurance cost per unit interacted with indicators for deciles of the relevant heterogeneity variable; the coefficients can therefore be interpreted as decile-specific rent-insurance elasticities. Panel A splits properties by housing supply elasticity bins and controls for the time-varying effects of the fraction of the tract developed, with bins formed nationally; both the housing supply elasticity and the fraction of the tract developed are from [Baum-Snow and Han \(2024\)](#). Panel B splits properties by owner-market-share bins, where owner market share is measured by the percentage of multifamily units within the CBSA owned by the property's owner, with bins formed within CBSA-year. Panel C splits properties by proxies for moving-frictions: the share of residents living in the same home as one year earlier, the share of families with children, and the share of households that are married-couple families. Panel D splits properties by proxies for tenant outside options: the share of housing units in apartment buildings, the vacancy rate among apartment units, and the overcrowding rate. The variables in Panels C and D are from ACS 5-year estimates, matched to properties at the tract-by-year level, and binned within CBSA-year. The exception is the same-home-as-one-year-earlier measure, which uses the 2013 ACS estimate snapshot to avoid contaminating the variable with endogenous moving responses by renters. Log rent per unit and log insurance cost per unit are winsorized within year at the 1st and 99th percentiles. All panels include property fixed effects and CBSA-by-year fixed effects, and standard errors are clustered at the CBSA level. Error bars represent 95% confidence intervals; the red dashed horizontal line denotes zero.

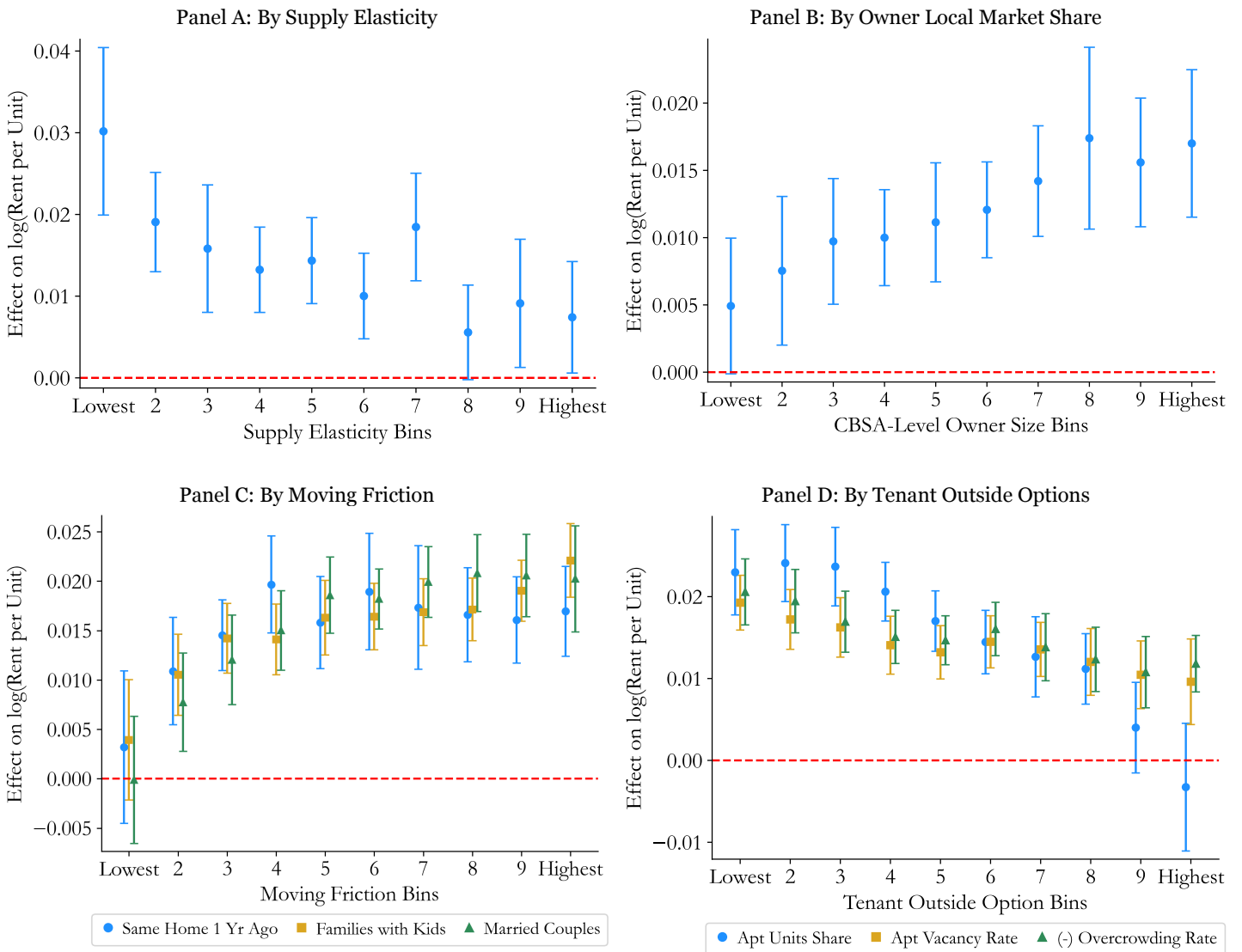


### Figure 7: Incidence of Insurance Cost Increases on Rents & NOI, Nonlinearity & Time-Series

This figure examines nonlinearity and the time-series of the incidence relationships between insurance costs, rents, and net operating income (NOI). Panel A presents residualized binscatters relating log insurance cost per unit to log rents per unit (left subpanel) and log NOI per unit (right subpanel). The black curves are third-degree polynomial fits based on data residualized using property fixed effects and CBSA-by-year fixed effects; gray regions represent 95% confidence intervals based on standard errors clustered by CBSA. Panel B plots annual coefficients from regressions that interact log insurance cost per unit with year indicators, including property fixed effects and CBSA-by-year fixed effects, to show how rent and NOI responses evolve from 2011 to 2024. Error bars represent 95% confidence intervals based on standard errors clustered by CBSA. Panel C reports implied cumulative effects on rents and NOI over 2014–2024 by combining the time-varying estimates from Panel B with the distribution of annual insurance cost growth, measured relative to operating expenses to account for broader expense inflation.

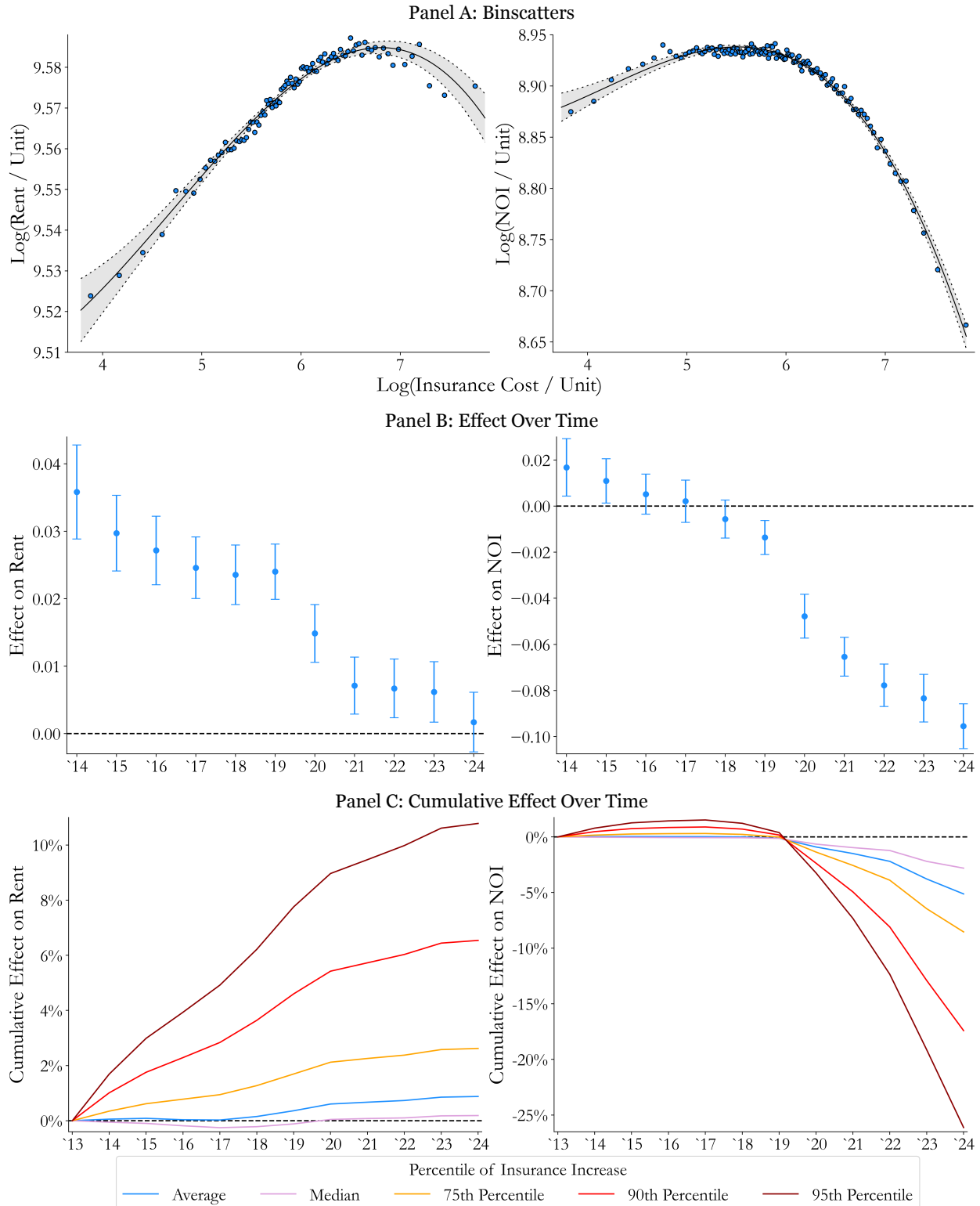


### Figure 8: Owner Size and Insurance Costs

This figure examines how owner size is related to insurance costs and how that relationship varies with property risk. Panel A plots insurance costs against owner size, measured as the number of multifamily units owned nationally. The left subpanel uses insurance cost as a percentage of rent, while the right subpanel uses insurance cost per unit. Fitted lines are based on the underlying data. Panel B examines how the relationship with owner size varies across risk scores for the same two cost measures. Error bands represent 95% confidence intervals based on standard errors clustered by owner. Panel A includes CBSA-by-year fixed effects, and Panel B includes property fixed effects and CBSA-by-year fixed effects. Risk scores are from FEMA’s National Risk Index (see Figure IA.9). Property ownership is based on transaction and holdings data from Real Capital Analytics.

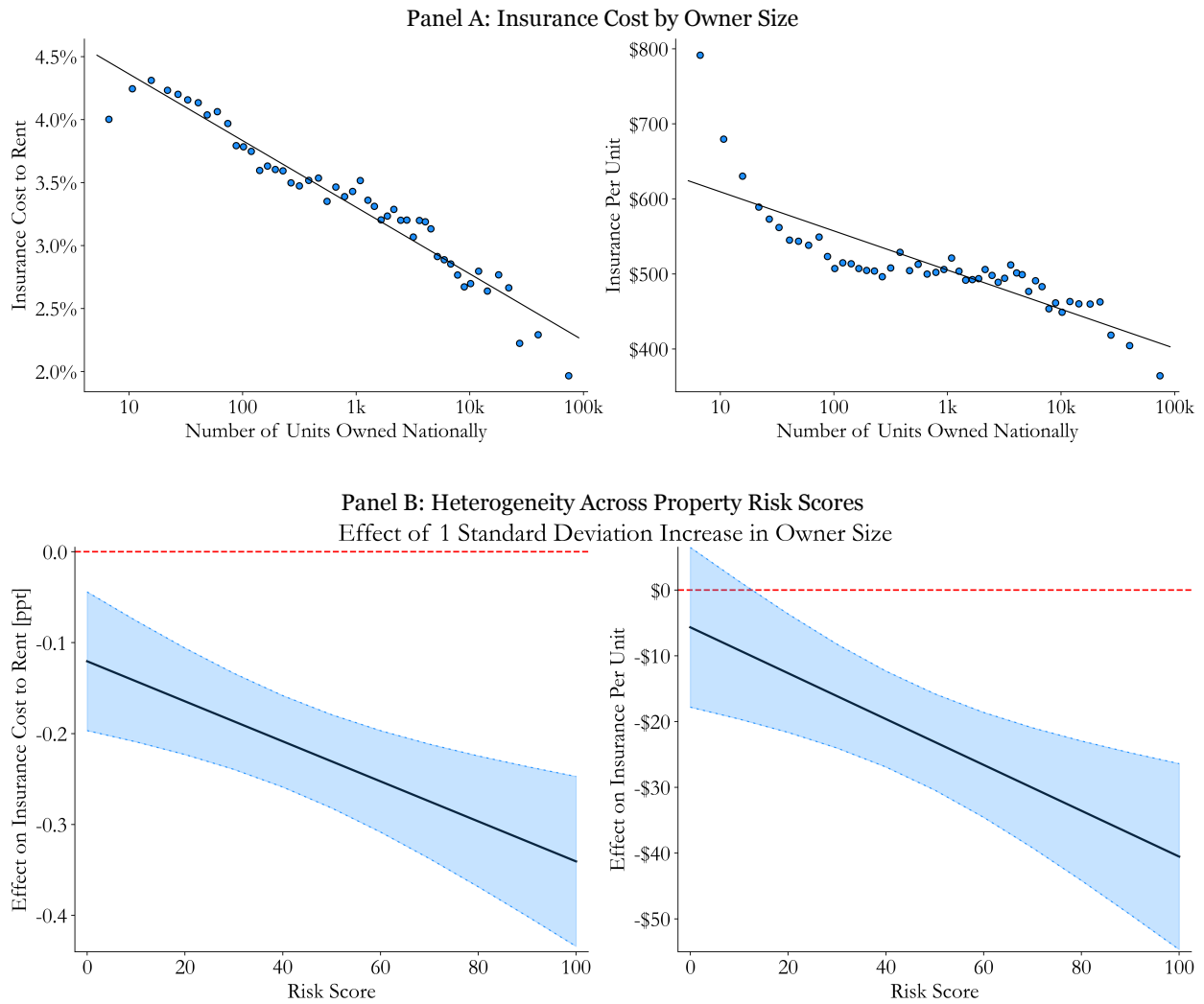


### Figure 9: Owner Portfolio Risk and Insurance Costs

This figure examines how the average risk of an owner’s portfolio relates to insurance costs. We define  $OwnerPortfolioRisk_{o,t} = \frac{\sum_{i \in Portfolio_o} Units_i \times RiskScore_i}{\sum_{i \in Portfolio_o} Units_i}$ . Panel A shows the binscatter relationship between insurance costs and  $OwnerPortfolioRisk_{o,t}$ , controlling for owner size, property fixed effects, and CBSA-by-year fixed effects. Panels B and C show how the relationship between a one-standard-deviation decrease in owner portfolio risk and insurance costs varies across levels of the focal property’s risk and owner portfolio size, respectively. Panels B and C both include property fixed effects and CBSA-by-year fixed effects. Error bands represent 95% confidence intervals based on standard errors clustered by owner. Property ownership is based on transaction and holdings data from Real Capital Analytics.

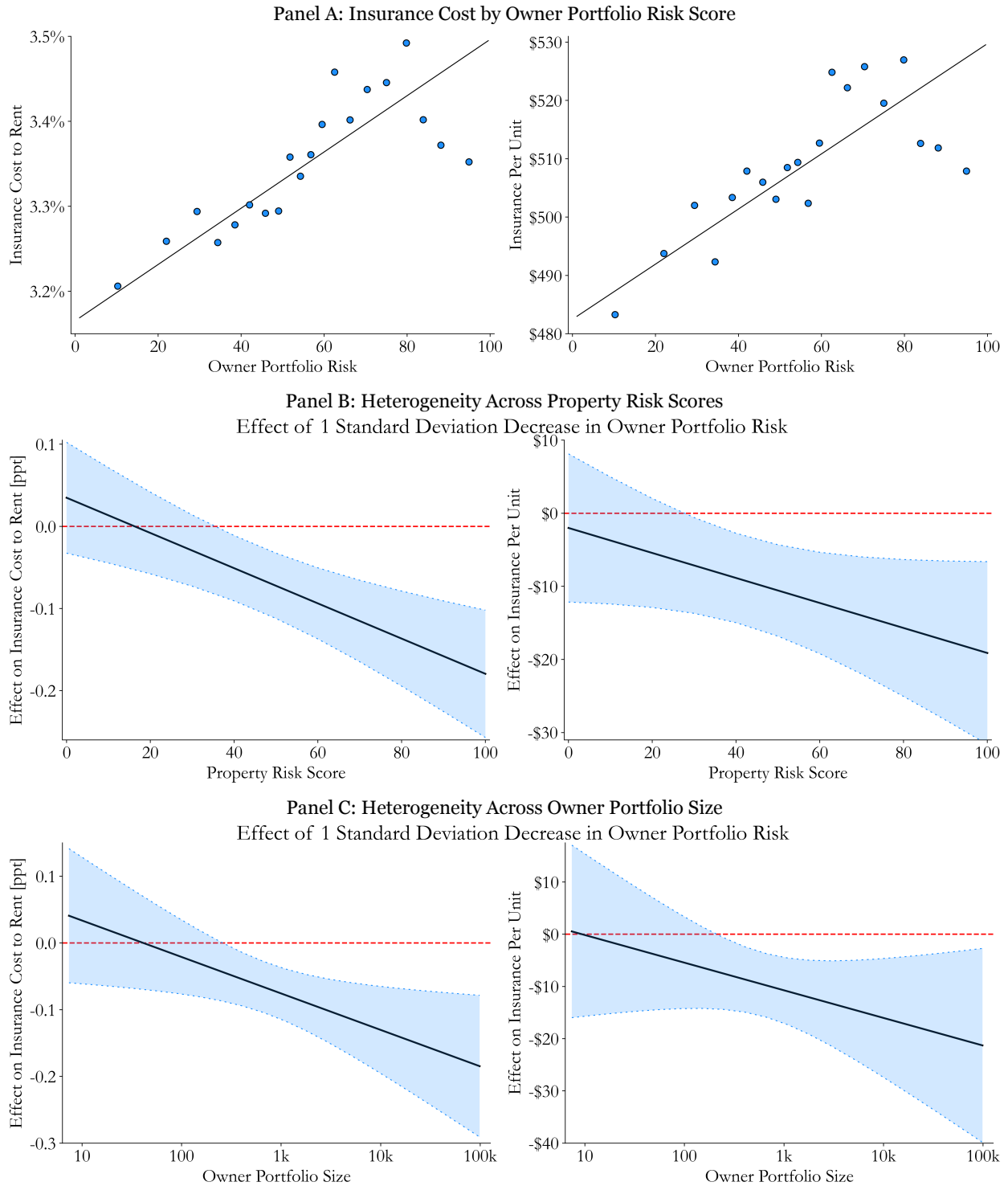


**Figure 10: Insurance Costs Around M&A Events**

This figure examines how insurance costs evolve around portfolio-level mergers and acquisitions (M&A) events using a stacked difference-in-differences framework. Event time is measured in years relative to the M&A transaction, with the year immediately before the event ( $t = -1$ ) omitted as the reference period. Panel A plots estimates for the insurance-cost-to-rent ratio, Panel B for the insurance-cost-to-operating-expenses ratio, and Panel C for the  $\log(\text{Insurance Cost Per Unit})$ . All panels are based on regressions with property-by-cohort fixed effects and CBSA-by-year-by-cohort fixed effects. Error bars denote 95% confidence intervals based on standard errors clustered by owner.

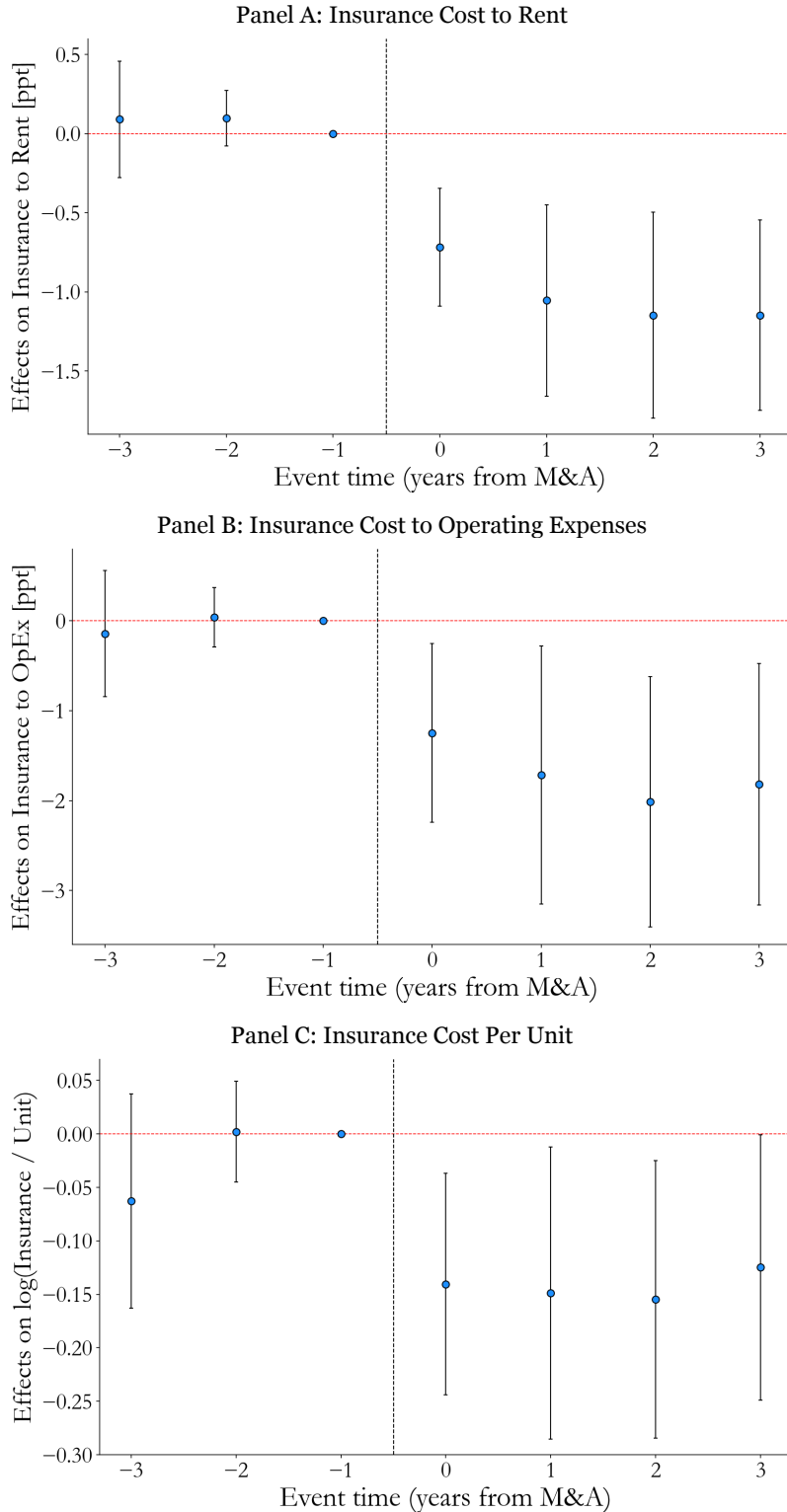


**Figure 11: Insurance Costs Around M&A Events, Heterogeneity**

This figure examines heterogeneity in the insurance-cost response around portfolio-level mergers and acquisitions (M&A) events using the stacked difference-in-differences design. The dependent variable in all panels is the insurance-cost-to-rent ratio. Panel A splits treated properties by whether the acquirer-target owner-size gap is above or below the median. Panel B examines heterogeneity by the acquired property's local disaster risk. The left subpanel splits the full sample into high- and low-risk properties, while the right subpanel further interacts property risk with the owner-size gap. The control properties are split by property risk but not by the owner-size gap, since the owner-size gap is not defined for control properties. Panel C examines heterogeneity by the portfolio-risk reduction. The left subpanel splits treated properties by whether the portfolio-risk reduction is above or below the median, while the right subpanel further interacts the portfolio-risk reduction with the owner-size gap. The control properties are not split by either portfolio-risk reduction or owner-size gap, since neither is defined for these properties. All specifications include property-by-cohort fixed effects and CBSA-by-year-by-cohort fixed effects, and each series is estimated separately using the relevant set of treated properties and their associated control properties (e.g., high-owner-size-gap [low-owner-size-gap] treated properties and all control properties for the blue [pink] series in Panel A). Error bars denote 95% confidence intervals based on standard errors clustered by owner. Risk scores are measured using FEMA's NRI, and property ownership is based on transaction and holdings data from RCA.

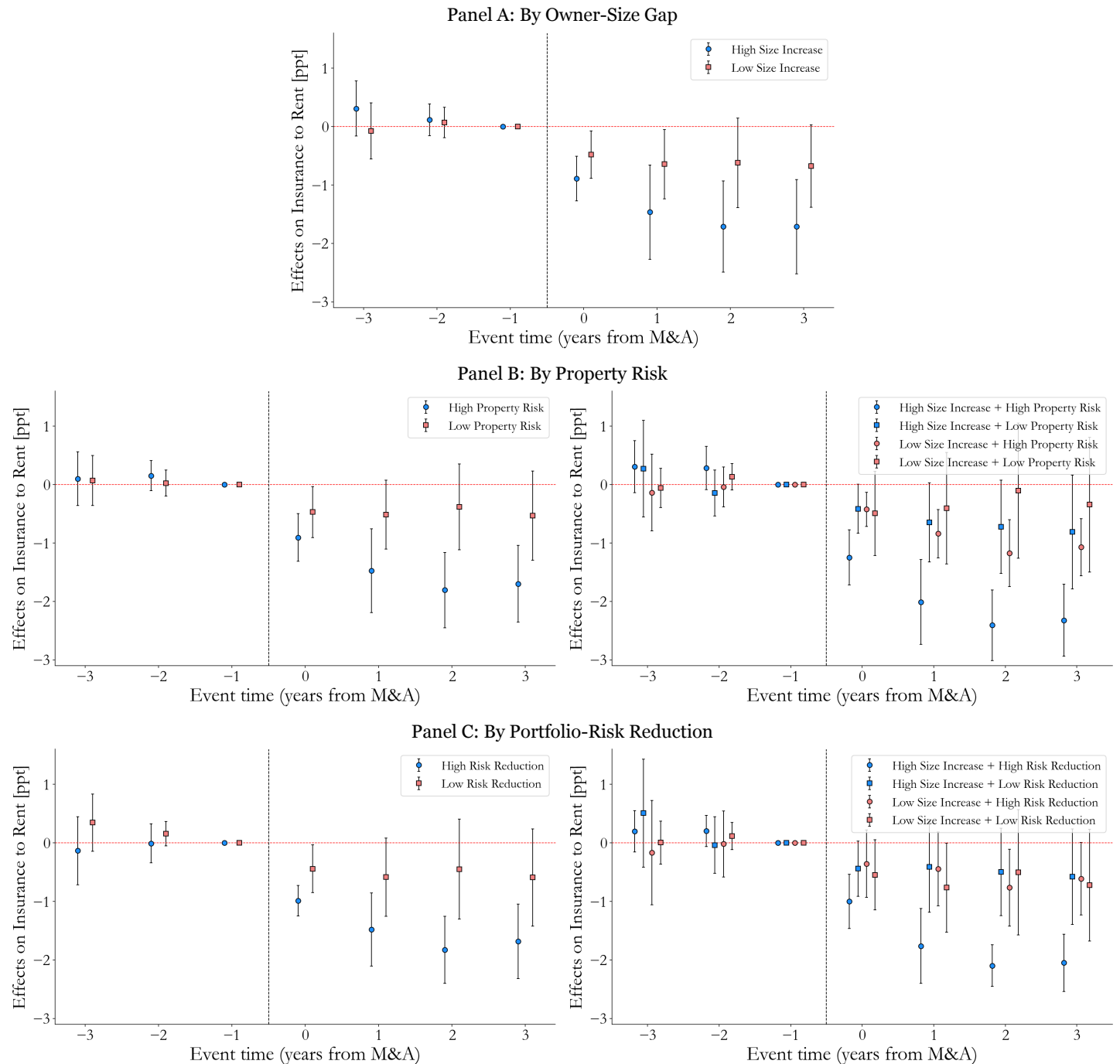


### Figure 12: Owner Pricing Advantages Over Time

This figure examines how the relationship between owner characteristics and the insurance-cost-to-rent ratio varies over time. Panel A shows how the effect of a one-standard-deviation increase in owner size differs over time between properties whose risk scores differ by 50 points. Panel B shows the effect of a one-standard-deviation decrease in owner portfolio risk over time. Both panels include property fixed effects and CBSA-by-year fixed effects and use 2017 as the omitted year. Error bars denote 95% confidence intervals based on standard errors clustered by owner. Property ownership is based on transaction and holdings data from Real Capital Analytics.

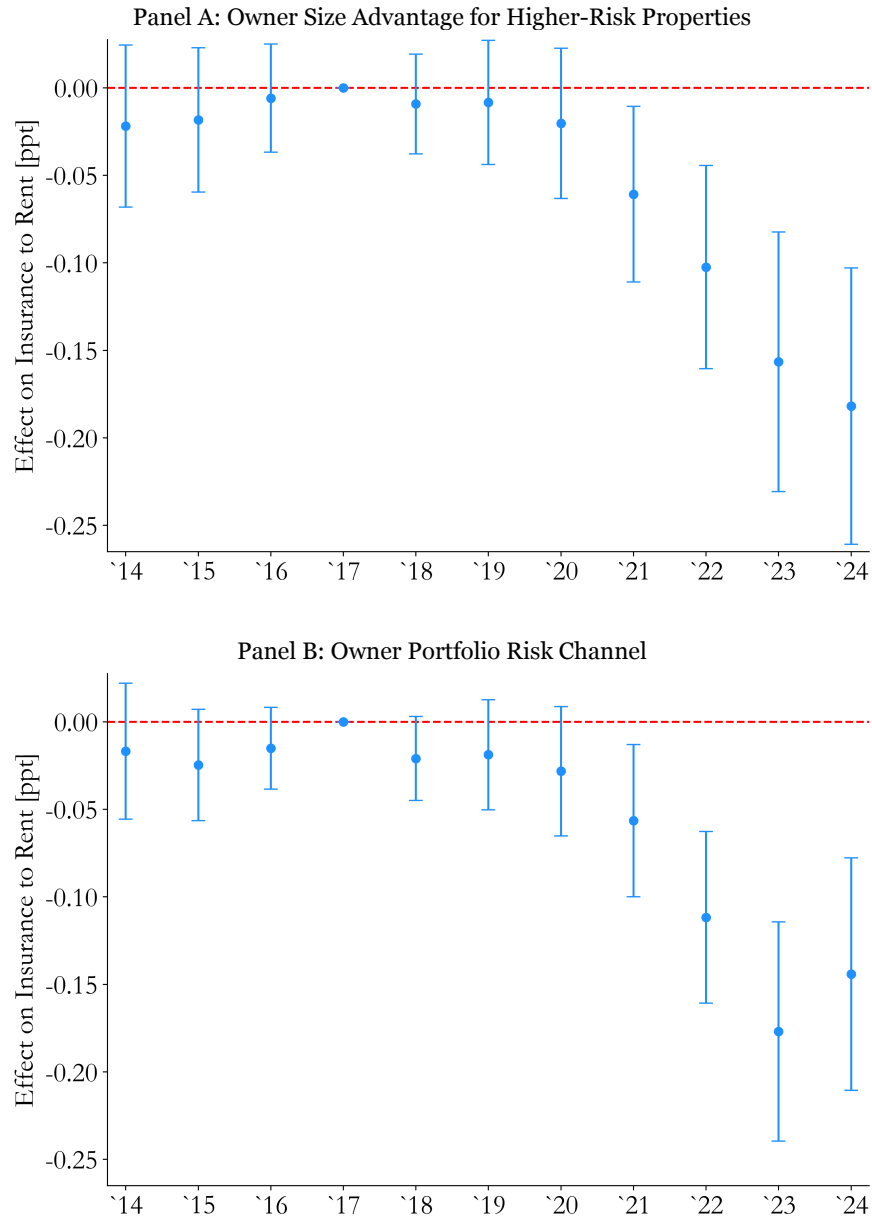


### Figure 13: Property Risk and Owner Size

This figure examines how property risk relates to owner size. Panel A shows binscatter plots of the logarithm of expected annual building losses per capita (x-axis) against the logarithm of owner size, measured as the number of units owned nationally (y-axis), separately for 2010 and 2024. Each binscatter includes a fitted regression line controlling for CBSA fixed effects; slopes and corresponding  $t$ -statistics based on standard errors clustered by owner are reported. Panel B plots year-by-year estimates of the relationship between property risk and owner size over 2010–2024. Specifically, the following regression is estimated for each risk measure:

$$\log(\text{OwnerSize})_{o,t} = \sum_{t \neq 2010} \beta_t \times \mathbb{1}(\text{Year} = t) \times \text{RiskScore}_i + \gamma_i + \eta_t + \varepsilon_{i,o,t}$$

The plotted coefficients ( $\beta_t$ ) capture the relationship between owner size and a one-unit increase in log(expected annual building losses per capita) (left subpanel) or a 25-point increase in risk score (right subpanel). The regression includes property ( $\gamma_i$ ) and year ( $\eta_t$ ) fixed effects. Error bars denote 95% confidence intervals based on standard errors clustered by owner. Risk scores and expected annual losses are measured at the census tract level using FEMA’s National Risk Index. Property ownership is based on transaction and holdings data from Real Capital Analytics.

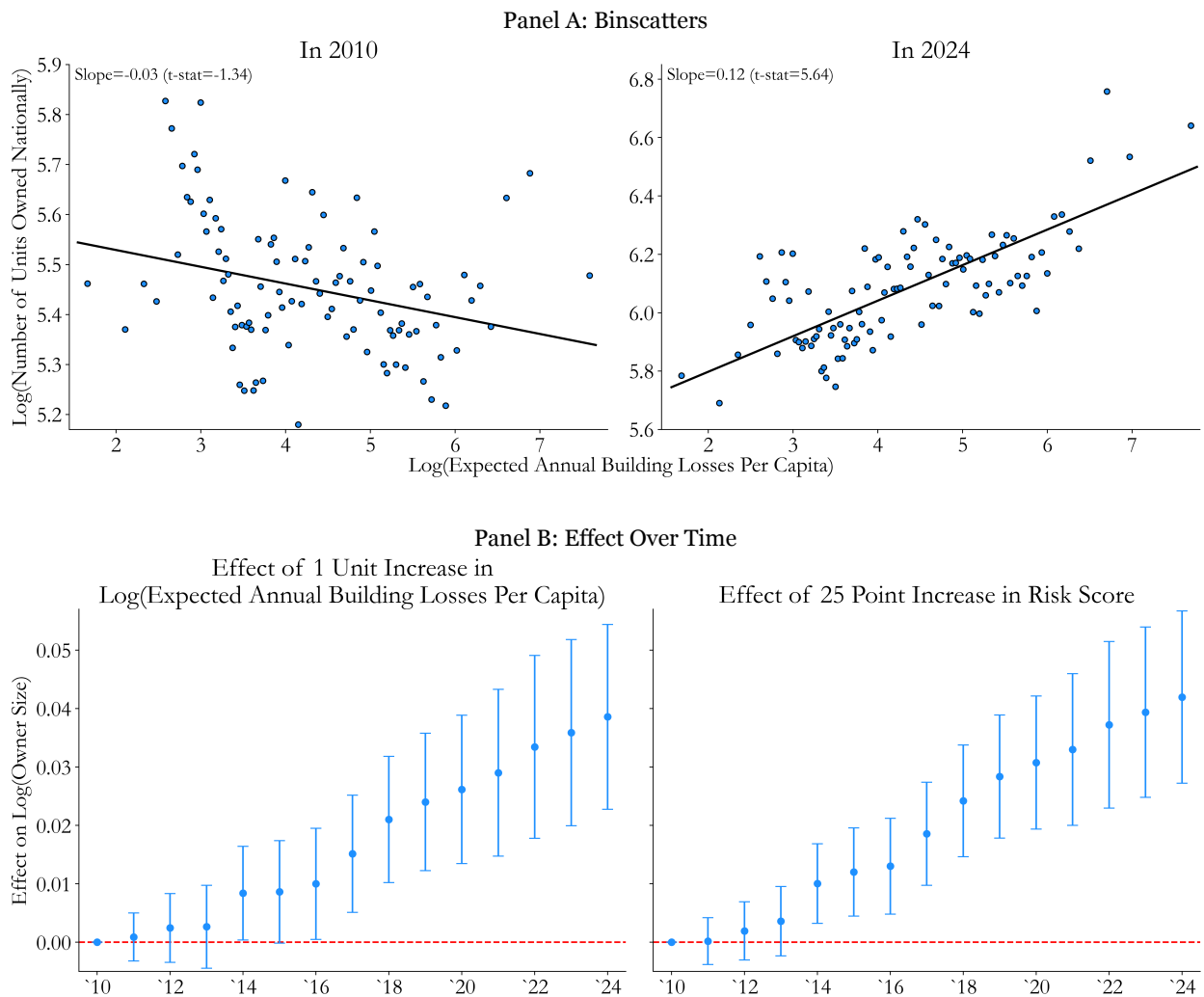


**Figure 14: Property Risk, Owner Size, and Property Sales**

This figure examines how the relationship between high-risk locations and the probability that a property is sold varies by owner size and period. For each subperiod, we estimate the following regression:

$$Sale_{i,o,m,t} = \sum_{d \neq 5} \beta_d \times HighRisk_i \times \mathbf{1}(OwnerSizeDecile_{o,t} = d) + \sum_{d \neq 5} \delta_d \times \mathbf{1}(OwnerSizeDecile_{o,t} = d) + \alpha \times HighRisk_i + \eta_{m,t} + \varepsilon_{i,o,m,t}.$$

The dependent variable is an indicator equal to one if property  $i$ , located in CBSA  $m$  and owned by owner  $o$ , is sold in year  $t$ .  $HighRisk$  is defined as above-median expected annual building losses. The specification includes CBSA-by-year fixed effects ( $\eta_{m,t}$ ) to absorb common local shocks to transaction activity in a given year. The omitted owner-size category is decile 5, and the plotted points ( $\beta_d$ ) report the estimated relationship between high risk and sale probability for each owner-size decile relative to decile 5. The orange (squares) series shows estimates for 2010–2017, while the blue (dots) series shows estimates for 2018–2024. Error bars denote 95% confidence intervals based on standard errors clustered by owner.

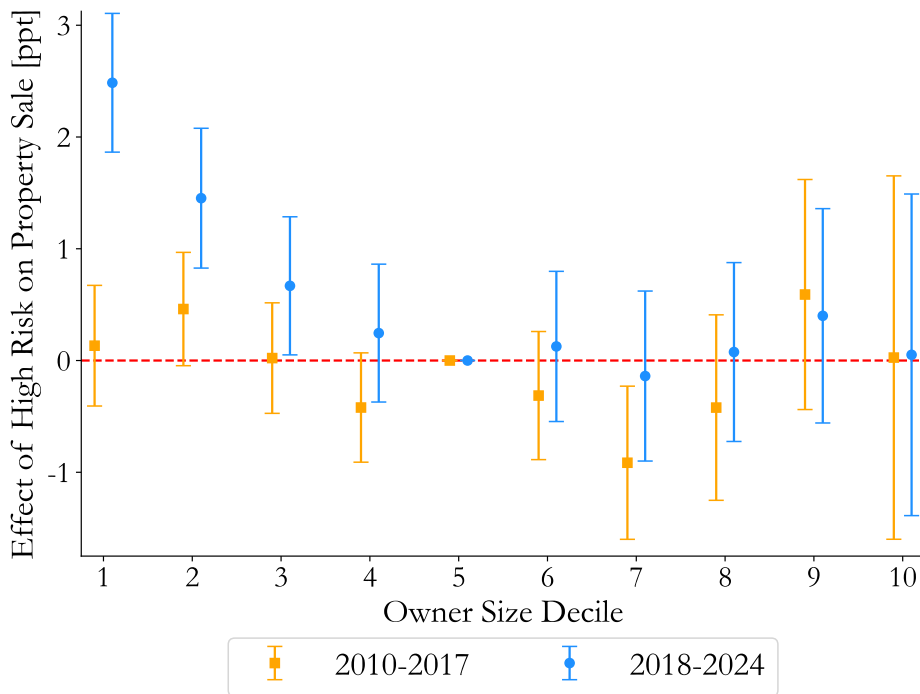


**Table 1: Reinsurance Exposure and Insurance Cost Increases**

This table examines whether state-level exposure to reinsurance markets amplifies the pass-through of rising national reinsurance costs to commercial property insurance costs. The dependent variable in all columns is the change in insurance cost per unit for property  $i$  in state  $s$  and year  $t$ . Reinsurance exposure is measured at the state level as the weighted average share of direct premiums ceded to unaffiliated reinsurers by insurers operating in the state, following [Keys and Mulder \(2025\)](#).  $\Delta$ Reins. Cost denotes the annual change in the Guy Carpenter Rate-On-Line Index. Columns (1)–(3) estimate the interaction between reinsurance cost changes and state reinsurance exposure. Columns (4)–(7) introduce a triple interaction with FEMA tract-level disaster risk scores to examine whether the pass-through of rising reinsurance costs is stronger for properties in higher-risk locations. Robust standard errors are double-clustered by state and year.

Dep. Variable:	$\Delta$ Insurance Cost Per Unit						
	(1)	(2)	(3)	(4)	(5)	(6)	(7)
Reins. Exposure	60.98*			111.5			
	(2.12)			(0.71)			
$\Delta$ Reins. Cost $\times$ Reins. Exposure	1924.3***	1919.1***	1802.4***	-44.06	-38.03	15.99	
	(6.56)	(4.67)	(4.74)	(-0.25)	(-0.09)	(0.04)	
Risk Score				10.89	28.66		
				(0.55)	(1.03)		
$\Delta$ Reins. Cost $\times$ Risk Score				-258.6***	-257.3***	-227.2***	
				(-6.05)	(-3.37)	(-3.09)	
Reins. Exposure $\times$ Risk Score				-84.19	-201.4		
				(-0.45)	(-0.98)		
$\Delta$ Reins. Cost $\times$ Reins. Exposure $\times$ Risk Score				2617.3***	2593.9***	2346.0***	2338.2***
				(10.54)	(4.63)	(4.66)	(4.52)
Year FE	✓	✓	✓	✓	✓	✓	✓
State FE		✓			✓		
Property FE			✓			✓	✓
Year $\times$ Risk Score							✓
Year $\times$ Reins. Exposure							✓
Observations	325,695	325,695	312,907	325,637	325,637	312,851	312,851
Adjusted $R^2$	0.0849	0.0915	0.0413	0.0871	0.0934	0.0427	0.0432

$t$ -statistics in parentheses.

\* $p < 0.10$ , \*\* $p < 0.05$ , \*\*\* $p < 0.01$

**Table 2: Homeowners Insurance Market Frictions and Commercial Insurance Costs**

This table implements a border-county-pair stacked difference-in-differences design to evaluate whether frictions in homeowners insurance markets spill over to commercial property insurance. County pairs are formed by matching adjacent counties that straddle a state border. Within each pair, one county is located in a state with high homeowners insurance frictions ( $HighFriction = 1$ ), while the neighboring county is located in a state with lower homeowners frictions; the friction measure is from [Oh, Sen, and Tenekedjieva \(2025\)](#). Both states in the pair are required to have low frictions in commercial property insurance rates, so the identifying difference comes from homeowners insurance-market regulation rather than direct regulation of commercial lines. *Treated* equals one for county pairs that experience a large natural-disaster shock during the sample period. The disaster year is the peak-damage year for the pair's average county property damage per capita, conditional on the peak being in the top decile across all county pairs and at least 10 times the previous year's damage. Cohorts are defined at the event level: in each disaster year, treated county pairs and the corresponding not-yet-treated and never-treated county pairs form a cohort. *Post* equals one in the disaster year and all subsequent years. The dependent variable is the annual percentage change in commercial insurance cost at the property-year level. Fixed effects are indicated at the bottom of each column. Robust standard errors are double-clustered by county pair and state.

Dep. Variable:	Percentage Change in Insurance Cost	
	(1)	(2)
$\mathbb{1}(\text{High Friction}) \times \mathbb{1}(\text{Post}) \times \mathbb{1}(\text{Treated})$	0.193** (2.79)	0.222*** (9.51)
Cohort $\times$ State $\times$ Event-year FE	✓	✓
Cohort $\times$ State $\times$ County-pair FE	✓	✓
Cohort $\times$ Event-year $\times$ County-pair FE	✓	✓
Property FE		✓
Observations	49,707	49,624
Adjusted $R^2$	0.0912	0.2342

*t*-statistics in parentheses

\*  $p < 0.10$ , \*\*  $p < 0.05$ , \*\*\*  $p < 0.01$

**Table 3: Incidence of Insurance Cost Increases on Rents and NOI**

This table reports estimates of the incidence of insurance costs on rents and net operating income (NOI). Panel A reports baseline estimates. Columns (3)–(4) and (7)–(8) include CBSA  $\times$  class  $\times$  year fixed effects, where class is determined by splitting properties in a given CBSA  $\times$  year into terciles based on rent per unit. Columns (4) and (8) additionally control for occupancy, log(Operating Expenses Excluding Insurance Cost Per Unit), log(Capital Expenses), an indicator for renovations in the previous year, an indicator for renovations in the previous five years, log(Property Age), and log(Effective Property Age). Panels B and C test for heterogeneity in the incidence of insurance cost increases on rents and NOI, respectively. In each panel, we split the sample at the median of the relevant heterogeneity variable and interact insurance costs with an indicator for the above-median group. Columns (1)–(2) split on housing supply elasticity (Baum-Snow and Han, 2024) and the owner’s market share within the CBSA, respectively; Columns (3)–(5) use proxies for moving frictions; and Columns (6)–(8) use proxies for tenant outside options. See Figure 6 for additional details regarding the proxies. Dependent and independent variables are winsorized at the 1% tails within each year. Fixed effects and controls are indicated at the bottom of each column. Robust standard errors are clustered by CBSA.

Panel A: Baseline

Dep. Variable:	log(Rent Per Unit)				log(NOI Per Unit)			
	(1)	(2)	(3)	(4)	(5)	(6)	(7)	(8)
log(Insurance Cost Per Unit)	0.0223*** (8.98)	0.0164*** (9.92)	0.0127*** (10.26)	0.0122*** (9.16)	-0.0412*** (-10.78)	-0.0461*** (-13.63)	-0.0511*** (-14.66)	-0.0462*** (-10.87)
Property FE	✓	✓	✓	✓	✓	✓	✓	✓
Year FE	✓				✓			
CBSA $\times$ Year FE		✓				✓		
CBSA $\times$ Class $\times$ Year FE			✓	✓			✓	✓
Additional Controls				✓				✓
Observations	411,951	411,951	407,134	170,246	411,951	411,951	407,134	170,246
Adjusted $R^2$	0.976	0.979	0.984	0.981	0.918	0.924	0.932	0.941

Panel B: Incidence on Rents, Heterogeneity

Dep. Variable:	log(Rent Per Unit)							
	Supply Elasticity	Owner Mkt Share	Same Home	Family w/ Children	Married Couple	Apartment Share	Apartment Vacancy	Overcrowding Rate
Split Variable:	(1)	(2)	(3)	(4)	(5)	(6)	(7)	(8)
log(Insurance/Unit)	0.0193*** (8.71)	0.00995*** (4.90)	0.0131*** (6.74)	0.0134*** (7.19)	0.0124*** (6.16)	0.0212*** (13.17)	0.0177*** (11.55)	0.0139*** (8.25)
$\mathbb{1}(\text{High}) \times \log(\text{Insurance/Unit})$	-0.0085*** (-3.66)	0.00562*** (3.17)	0.00513*** (2.62)	0.00471*** (4.14)	0.00694*** (3.91)	-0.0108*** (-5.12)	-0.00439*** (-4.88)	0.00391*** (3.63)
Property FE	✓	✓	✓	✓	✓	✓	✓	✓
CBSA $\times$ Year	✓	✓	✓	✓	✓	✓	✓	✓
Observations	390,290	294,632	395,780	405,433	405,496	405,498	400,747	405,469
Adjusted $R^2$	0.979	0.975	0.979	0.979	0.979	0.979	0.979	0.979

Panel C: Incidence on NOI, Heterogeneity

Dep. Variable:	log(NOI Per Unit)							
	Supply Elasticity	Owner Mkt Share	Same Home	Family w/ Children	Married Couple	Apartment Share	Apartment Vacancy	Overcrowding Rate
Split Variable:	(1)	(2)	(3)	(4)	(5)	(6)	(7)	(8)
log(Insurance/Unit)	-0.0396*** (-8.27)	-0.0667*** (-14.15)	-0.0510*** (-13.73)	-0.0505*** (-15.31)	-0.0579*** (-16.91)	-0.0394*** (-10.09)	-0.0441*** (-12.51)	-0.0497*** (-15.13)
$\mathbb{1}(\text{High}) \times \log(\text{Insurance/Unit})$	-0.0155*** (-3.11)	0.0213*** (5.50)	0.00626* (1.68)	0.00450** (2.44)	0.0201*** (6.40)	-0.0178*** (-4.92)	-0.00919*** (-4.52)	0.00306* (1.95)
Property FE	✓	✓	✓	✓	✓	✓	✓	✓
CBSA $\times$ Year	✓	✓	✓	✓	✓	✓	✓	✓
Observations	390,290	294,632	395,780	405,433	405,496	405,498	400,747	405,469
Adjusted $R^2$	0.923	0.934	0.922	0.923	0.923	0.923	0.923	0.923

$t$ -statistics in parentheses.

\*  $p < 0.10$ , \*\*  $p < 0.05$ , \*\*\*  $p < 0.01$

**Table 4: Transaction Prices and Cap Rates**

This table examines how local climate risk is reflected in multifamily transaction prices and cap rates, and whether that relationship changes after 2018. The dependent variable is either the log of transaction price per unit [Columns (1) and (2)] or the transaction cap rate [Columns (3) and (4)]. The key explanatory variable is  $\log(\text{Expected Annual Building Losses})$ , measured using FEMA's National Risk Index, and its interaction with an indicator for 2018 or later. All specifications include CBSA  $\times$  year fixed effects; Columns (2) and (4) additionally include property fixed effects. Robust standard errors are clustered by CBSA.

Dep. Variable:	log(Transaction Price Per Unit)		Transaction Cap Rate	
	(1)	(2)	(3)	(4)
$\mathbb{1}(\text{2018 or Later})$ $\times \log(\text{Expected Annual Building Losses})$	-0.0747*** (-3.41)	-0.0653*** (-7.00)	0.000872*** (3.15)	0.00118*** (3.58)
$\log(\text{Expected Annual Building Losses})$	0.230*** (5.43)		-0.00230*** (-6.19)	
CBSA $\times$ Year FE	✓	✓	✓	✓
Property FE		✓		✓
Observations	102,294	49,955	38,551	10,535
Adjusted $R^2$	0.564	0.902	0.452	0.650
Dep. Variable Mean	11.84	11.74	0.0555	0.0558

*t*-statistics in parentheses.

\*  $p < 0.10$ , \*\*  $p < 0.05$ , \*\*\*  $p < 0.01$

**Table 5: Owner Size, Owner Portfolio Risk, and Insurance Costs**

This table examines how owner size (Panel A) and average risk of a property owner’s national portfolio (Panel B) are related to insurance costs as a share of rent and how this relationship varies by property risk and over time. The dependent variable is the insurance-cost-to-rent ratio. Owner size is the log of the total number of multifamily units owned nationally by each owner in a given year and owner portfolio risk is defined as the unit-weighted average FEMA National Risk Index risk score across all properties owned nationally by that owner in a given year. All regressions include CBSA-by-year fixed effects and property fixed effects. Property risk scores are from FEMA’s National Risk Index. Property ownership is from Real Capital Analytics. Robust standard errors are clustered by owner.

Panel A: Owner Size			
Dep. Variable:	Insurance Cost to Rent		
	(1)	(2)	(3)
log(Owner Size)	-0.00108*** (-8.65)	-0.000406** (-2.36)	-0.000691*** (-3.68)
log(Owner Size) × Property Risk Score		-0.00122*** (-4.02)	-0.000882*** (-2.66)
1(2018 or Later) × log(Owner Size)			0.000366*** (3.24)
1(2018 or Later) × Property Risk Score			0.00307** (2.37)
1(2018 or Later) × log(Owner Size) × Property Risk Score			-0.000436*** (-2.65)
CBSA × Year FE	✓	✓	✓
Property FE	✓	✓	✓
Observations	301,853	301,853	301,853
Adjusted $R^2$	0.767	0.767	0.767
Mean of Dep. Variable	0.0335	0.0335	0.0335

Panel B: Owner Portfolio Risk				
Dep. Variable:	Insurance Cost to Rent			
	(1)	(2)	(3)	(4)
Owner Portfolio Risk	0.00364*** (3.87)	-0.00155 (-1.00)	-0.00400 (-1.25)	0.00196* (1.93)
Owner Portfolio Risk × Property Risk Score		0.00969*** (3.45)		
log(Owner Size)			-0.00166*** (-6.06)	
Owner Portfolio Risk × log(Owner Size)			0.00108** (2.30)	
1(2018 or Later) × Owner Portfolio Risk				0.00257*** (3.53)
CBSA × Year FE	✓	✓	✓	✓
Property FE	✓	✓	✓	✓
Observations	301,853	301,853	301,853	301,853
Adjusted $R^2$	0.767	0.767	0.767	0.767
Mean of Dep. Variable	0.0335	0.0335	0.0335	0.0335

*t*-statistics in parentheses.

\*  $p < 0.10$ , \*\*  $p < 0.05$ , \*\*\*  $p < 0.01$

**Table 6: Insurance Costs Within Continuing Ownership Relationships**

This table examines the role of owner size and owner portfolio risk while holding the focal owner-property match fixed. The dependent variable is the three-year change in the insurance-cost-to-rent ratio, and the key independent variables ( $\Delta\log(\text{Owner Size})$  and  $\Delta\text{Owner Portfolio Risk}$ ) are defined over the same three-year period. The sample includes only property-year observations in which the same owner holds the property across the previous three years. All regressions include year fixed effects and controls for time-varying effects of local risk. Robust standard errors are clustered by owner.

Dep. Variable:	Insurance Cost to Rent <sub>t</sub> – Insurance Cost to Rent <sub>t-3</sub>			
	(1)	(2)	(3)	(4)
$\Delta\log(\text{Owner Size})$	-0.00200*** (-6.71)	-0.000783* (-1.65)		
$\Delta\log(\text{Owner Size}) \times \text{Property Risk Score}$		-0.00218*** (-2.67)		
$\Delta\text{Owner Portfolio Risk}$			0.00364** (2.12)	-0.00453 (-1.63)
$\Delta\text{Owner Portfolio Risk} \times \text{Property Risk Score}$				0.0150*** (3.04)
Year FE	✓	✓	✓	✓
Year $\times$ Property Risk Score	✓	✓	✓	✓
Observations	132,958	132,958	132,958	132,958
Adjusted $R^2$	0.115	0.115	0.113	0.114
Mean of Dep. Variable	0.00735	0.00735	0.00735	0.00735

*t*-statistics in parentheses.

\*  $p < 0.10$ , \*\*  $p < 0.05$ , \*\*\*  $p < 0.01$

**Table 7: Insurance Costs Around M&A Events**

This table examines how insurance costs change around portfolio-level mergers and acquisitions (M&A) events using a stacked difference-in-differences design. The key independent variable is the interaction between an indicator for treated properties and an indicator for the post-M&A period. Panel A reports baseline estimates for three outcomes: the insurance-cost-to-rent ratio, the insurance-cost-to-operating-expenses ratio, and  $\log(\text{Insurance Cost Per Unit})$ . Panel B examines heterogeneity in the insurance-cost-to-rent response by property risk. Columns (1) and (2) split the full sample of properties according to whether property risk is above or below the median, while Columns (3) and (4) [(5) and (6)] apply the same split within the subsample where the owner-size gap is above [below] the median. The control properties included in each specification vary by property risk but not by the owner-size gap, since the owner-size gap is not defined for control properties. Panel C examines heterogeneity in the insurance-cost-to-rent response by the portfolio-risk reduction. Columns (1) and (2) split treated properties according to whether the portfolio-risk reduction is above or below the median, while Columns (3) and (4) [(5) and (6)] apply the same split within the subsample where the owner-size gap is above [below] the median. The full set of control properties is retained in all six specifications since neither the portfolio-risk reduction nor the owner-size gap is defined for these properties. Fixed effects and controls are indicated at the bottom of the table. Robust standard errors are clustered by owner. In Panels B and C, the Wald  $t$ -statistics and  $p$ -values reported at the bottom of each panel test whether the estimated treatment effects differ between the high and low groups, both unconditionally and within each owner-size-gap subsample.

Panel A: Baseline						
Dep. Variable:	Insurance Cost to Rent		Insurance Cost to OpEx		log(Insurance Cost Per Unit)	
	(1)	(2)	(3)	(4)	(5)	(6)
$1(\text{Treated}) \times 1(\text{Post})$	-0.0102*** (-3.84)	-0.0163*** (-2.59)	-0.0163*** (-2.59)	-0.0163*** (-2.59)	-0.1371** (-2.31)	-0.1371** (-2.31)
Property $\times$ Cohort FE	✓	✓	✓	✓	✓	✓
CBSA $\times$ Year $\times$ Cohort FE	✓	✓	✓	✓	✓	✓
Observations	550,872	550,872	550,872	550,872	550,797	550,797
Adjusted $R^2$	0.825	0.830	0.830	0.830	0.887	0.887

Panel B: Heterogeneity by Property Risk						
Dep. Variable:	Insurance Cost to Rent					
Owner-Size Gap:	Unconditional		High		Low	
Property Risk:	High	Low	High	Low	High	Low
$1(\text{Treated}) \times 1(\text{Post})$	-0.0144*** (-4.69)	-0.0049* (-1.77)	-0.0199*** (-8.15)	-0.0058** (-2.18)	-0.0080*** (-3.92)	-0.0039 (-0.81)
Property $\times$ Cohort FE	✓	✓	✓	✓	✓	✓
CBSA $\times$ Year $\times$ Cohort FE	✓	✓	✓	✓	✓	✓
Observations	279,249	266,648	266,928	277,050	282,406	262,053
Adjusted $R^2$	0.841	0.797	0.842	0.798	0.841	0.796
Wald $t$ -stat ( $p$ -value)	-2.29 (0.022)		-3.90 (0.000)		-0.78 (0.436)	

Panel C: Heterogeneity by Portfolio-Risk Reduction						
Dep. Variable:	Insurance Cost to Rent					
Owner-Size Gap:	Unconditional		High		Low	
Portfolio-Risk Reduction:	High	Low	High	Low	High	Low
$1(\text{Treated}) \times 1(\text{Post})$	-0.0138*** (-4.40)	-0.0061** (-1.96)	-0.0172*** (-7.55)	-0.0056*** (-1.99)	-0.0047** (-2.84)	-0.0067* (-1.77)
Property $\times$ Cohort FE	✓	✓	✓	✓	✓	✓
CBSA $\times$ Year $\times$ Cohort FE	✓	✓	✓	✓	✓	✓
Observations	549,311	549,104	548,373	548,132	548,476	548,517
Adjusted $R^2$	0.825	0.825	0.825	0.825	0.825	0.825
Wald $t$ -stat ( $p$ -value)	-1.76 (0.079)		-3.22 (0.001)		0.50 (0.618)	

$t$ -statistics in parentheses.  
 \*  $p < 0.10$ , \*\*  $p < 0.05$ , \*\*\*  $p < 0.01$

**Table 8: Local Risk, Owner Size, and Reallocation**

This table examines how local climate risk relates to owner size and how that relationship changes over time. Panel A studies the relationship between the riskiness of a property's location and the size of its current owner. The dependent variable is the log of the total number of multifamily units owned nationally by the property's owner in a given year. Each risk measure is interacted with an indicator for the post-2018 period to assess how the relationship between local risk and owner size changes. Panel B examines whether, conditional on sale, high-risk properties owned by smaller owners are sold to larger buyers after 2018. The dependent variable is the log of the buyer's national multifamily unit count at the time of sale, and the key variable is the triple interaction between indicators for the post-2018 period, high risk, and small-owner status. High risk is defined as above-median expected annual building losses, and small owner is defined as being in the bottom 20% of the owner-size distribution. The regressions in Panel B also include lower-order interaction terms, but only the coefficients of primary interest are reported for space. Fixed effects and controls are indicated at the bottom of the table. In Panel A, robust standard errors are clustered by owner; in Panel B, robust standard errors are clustered by CBSA.

Panel A: Local Risk and Owner Size

Dep. Variable:	log(Owner Size)			
	(1)	(2)	(3)	(4)
$\mathbb{1}(2018 \text{ or Later}) \times \text{Risk Score}$	0.107*** (2.58)	0.104*** (5.36)		
Risk Score	-0.592*** (-9.04)			
$\mathbb{1}(2018 \text{ or Later}) \times \log(\text{Expected Annual Building Losses})$			0.0241* (1.95)	0.0237*** (4.60)
$\log(\text{Expected Annual Building Losses})$			-0.189*** (-8.84)	
Year FE	✓	✓	✓	✓
Property FE		✓		✓
Observations	1,932,802	1,932,750	1,932,802	1,932,750
Adjusted $R^2$	0.009	0.890	0.013	0.890

Panel B: Reallocation of High-Risk Properties from Small Owners

Dep. Variable:	log(New Owner Size)		
	(1)	(2)	(3)
$\mathbb{1}(2018 \text{ or Later}) \times \mathbb{1}(\text{High Risk}) \times \mathbb{1}(\text{Small Owner})$	0.151** (2.39)	0.161*** (2.67)	0.162*** (2.70)
$\mathbb{1}(\text{High Risk}) \times \mathbb{1}(\text{Small Owner})$	0.0510 (0.20)	0.0469 (0.18)	0.0479 (0.19)
CBSA $\times$ Year FE	✓	✓	✓
Year $\times$ $\mathbb{1}(\text{Small Owner})$		✓	✓
Year $\times$ $\mathbb{1}(\text{High Risk})$			✓
Observations	100,583	100,583	100,583
Adjusted $R^2$	0.308	0.308	0.309

*t*-statistics in parentheses.

\*  $p < 0.10$ , \*\*  $p < 0.05$ , \*\*\*  $p < 0.01$

**For Online Publication**

**Internet Appendix For:  
“Who Bears Rising Commercial Property Insurance Costs?”**

**Figure IA.1: CMBS Data Coverage**

This figure evaluates the coverage of multifamily units in the CMBS operating statement data. The left panel plots the total number of units in the CMBS data from 2010 to 2024. The right panel compares 2024 multifamily units by Metropolitan Statistical Area (MSA) in the CMBS data with benchmark counts from the American Community Survey (ACS). The dashed red line is the 45-degree line, and the dotted black line is the fitted relationship.

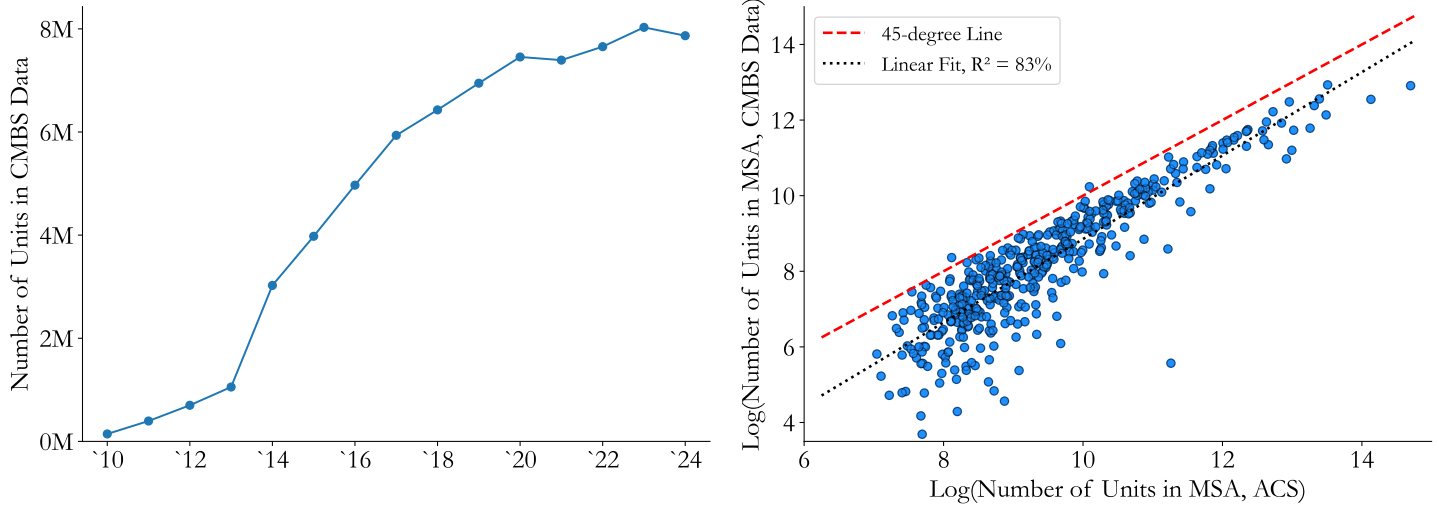


**Figure IA.2: RCA Data Coverage**

This figure compares multifamily unit coverage in the RCA data with benchmark estimates from the American Community Survey (ACS). The left panel plots total multifamily units in the RCA data and the ACS from 2010 to 2024. The right panel compares 2024 multifamily units by Metropolitan Statistical Area (MSA) in the RCA data and the ACS. The dashed red line is the 45-degree line, and the dotted black line is the fitted relationship.

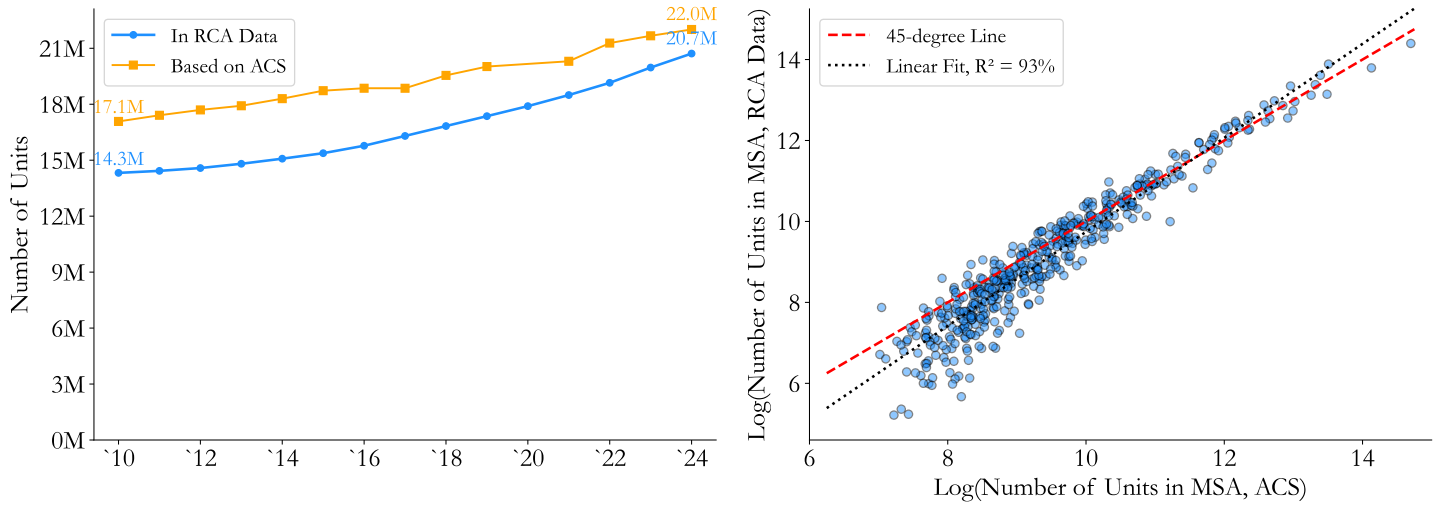
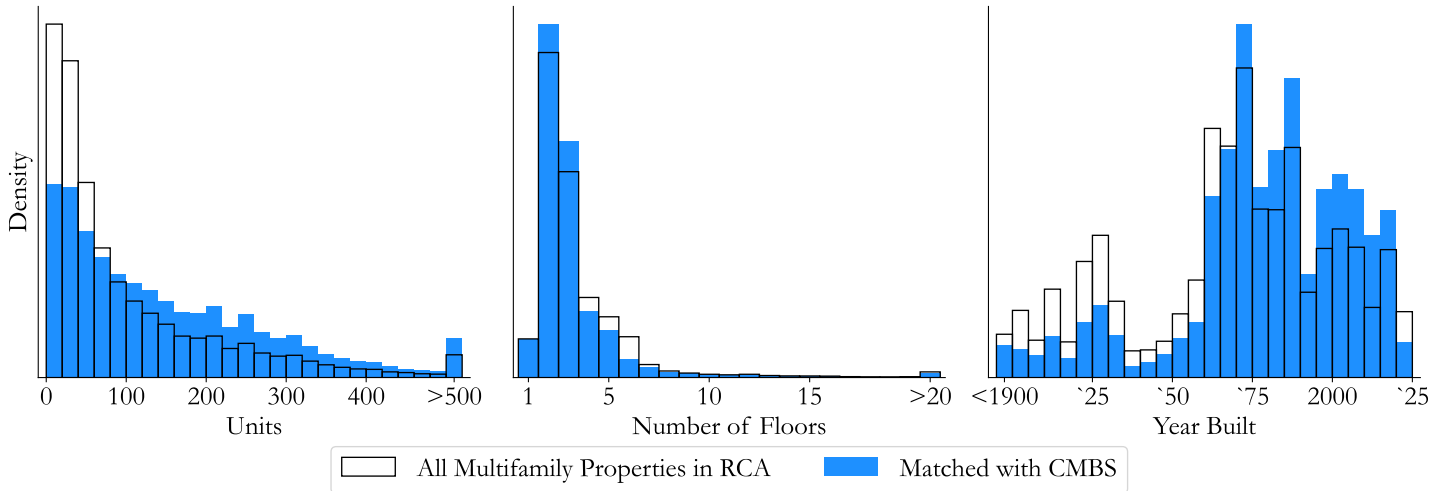


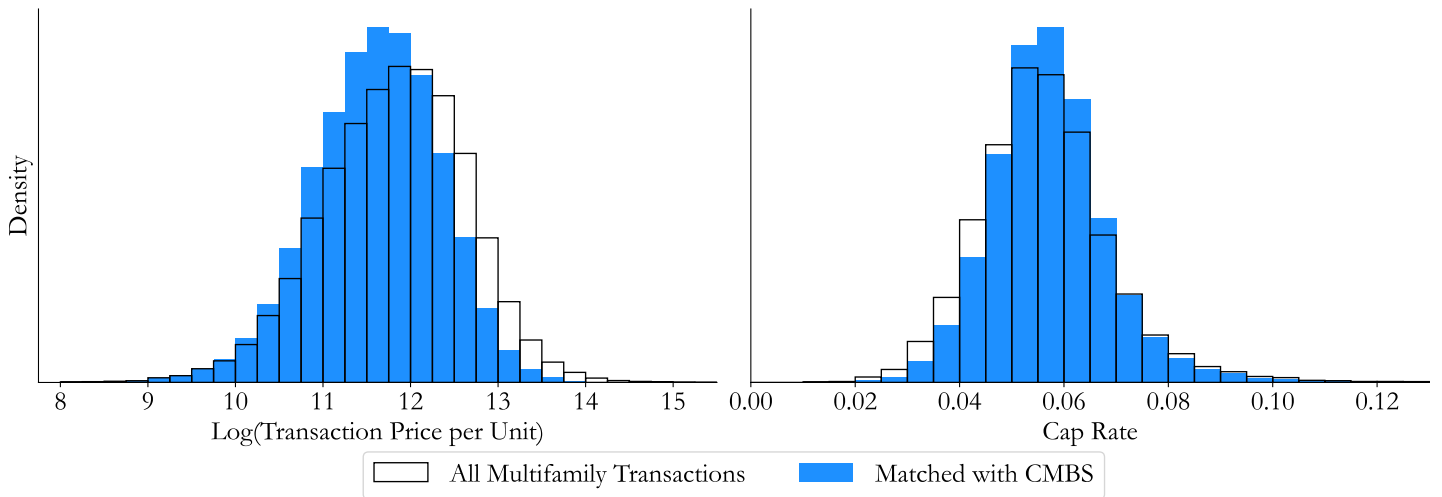
### Figure IA.3: RCA Population and CMBS-Matched Properties

This figure compares all properties in the RCA data with properties matched to the CMBS sample. Panel A compares property characteristics, with the left, middle, and right panels showing the distributions of unit counts, floor counts, and year built, respectively. Panel B compares transaction prices per unit and cap rates using RCA transaction data. Panel C compares each Metropolitan Statistical Area's (MSA's) share of all RCA multifamily units with its share of CMBS-matched units.

Panel A: Property Features



Panel B: Transaction Prices and Cap Rates



Panel C: Location

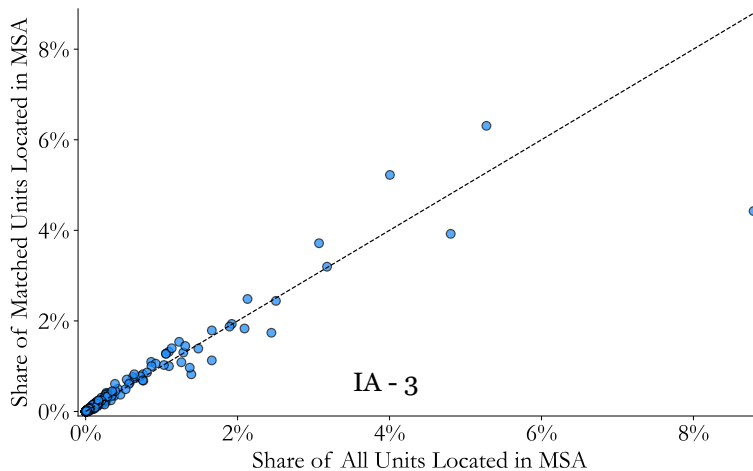


**Figure IA.4: Property Insurance Costs, As a Share of NOI and Debt Service**

This figure plots insurance costs for multifamily properties as a share of NOI and debt service from 2010 to 2024, along with 25th--75th percentile bands.

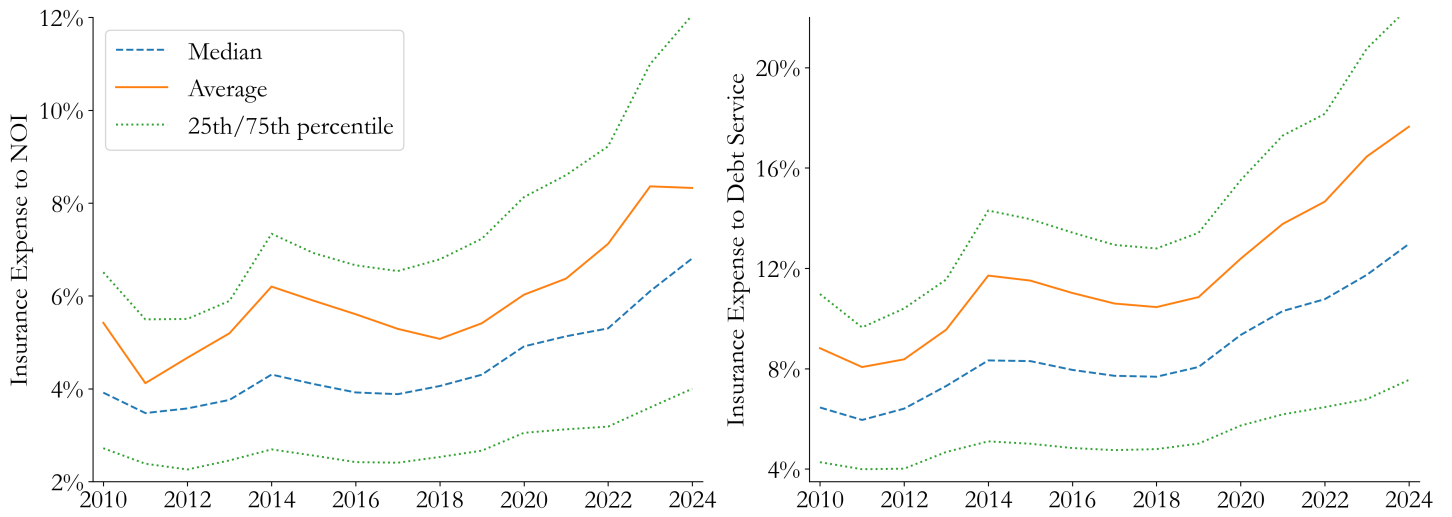


**Figure IA.5: Commercial vs. Homeowners Insurance Costs, Data from [Keys and Mulder \(2025\)](#)**

This figure compares commercial property insurance costs with homeowners insurance costs. It presents county-level scatterplots of average percentage changes in commercial and homeowners insurance costs for 2014–2019 and 2019–2024. Each bubble represents a county and is sized by population. Dashed reference lines indicate equal growth, twice as much growth in commercial costs, and five times as much growth in commercial costs relative to homeowners costs. Region labels report the share of the U.S. population living in counties with the corresponding relative cost changes. Homeowners insurance data are from [Keys and Mulder \(2025\)](#).

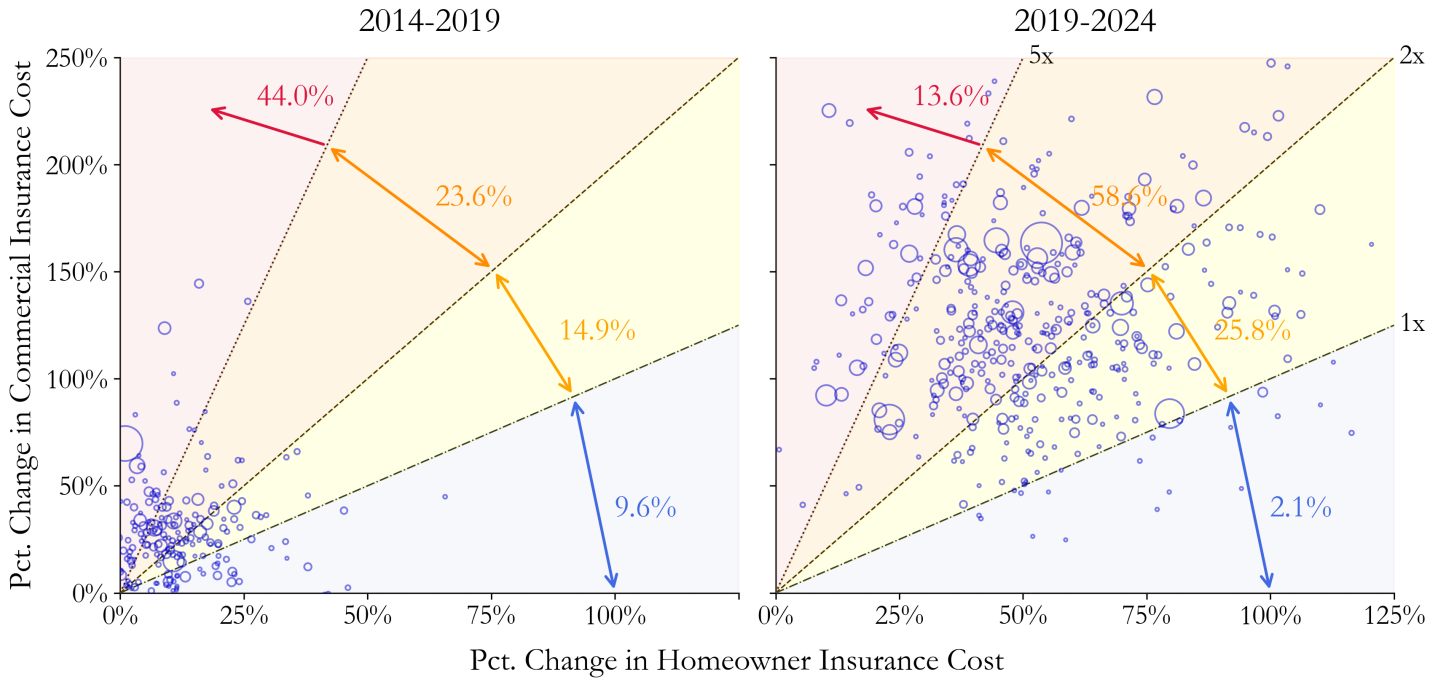


**Figure IA.6: County-Level Risk Scores**

This figure maps county-level risk scores. The main analyses use FEMA National Risk Index risk scores measured at the census tract level; for illustration, this figure aggregates those scores to the county level.

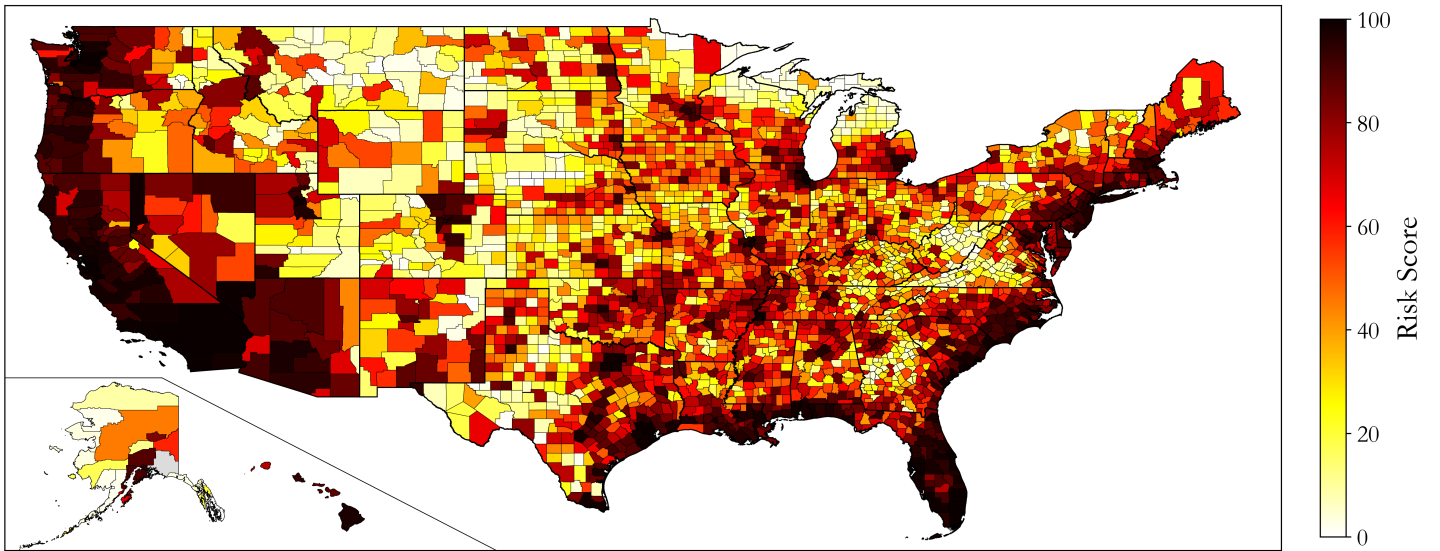
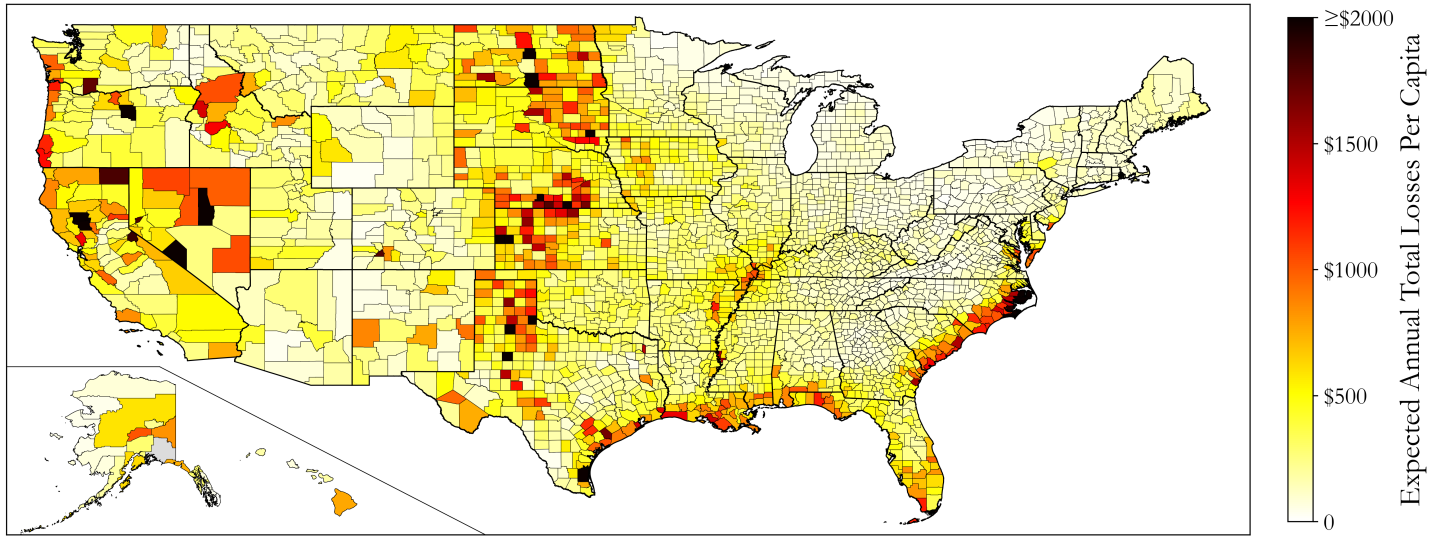


### Figure IA.7: County-Level Expected Annual Losses

This figure maps expected annual total losses per capita (Panel A) and expected annual building losses divided by building value (Panel B), aggregated to the county level.

Panel A: Expected Annual Total Losses Per Capita



Panel B: Expected Annual Building Losses / Building Value

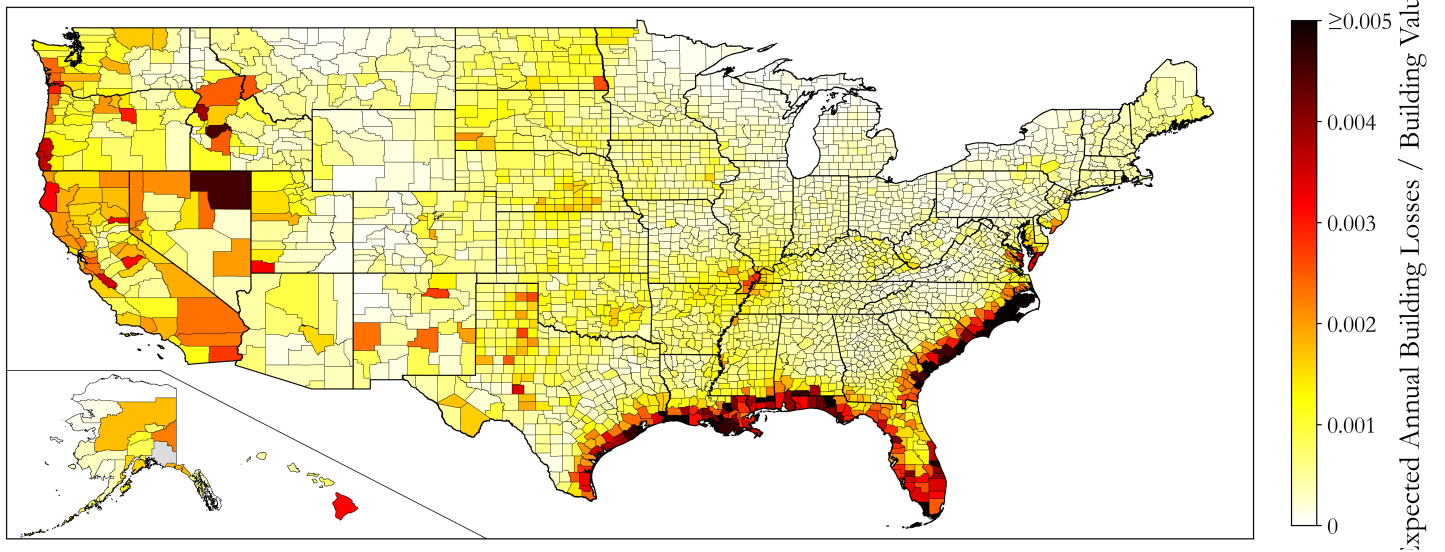


**Figure IA.8: Risk Measures and Insurance Cost Growth Over Time**

This figure shows how the relationship between the annual percentage changes in insurance costs and local risk measures changes over time. Both regressions include year fixed effects.

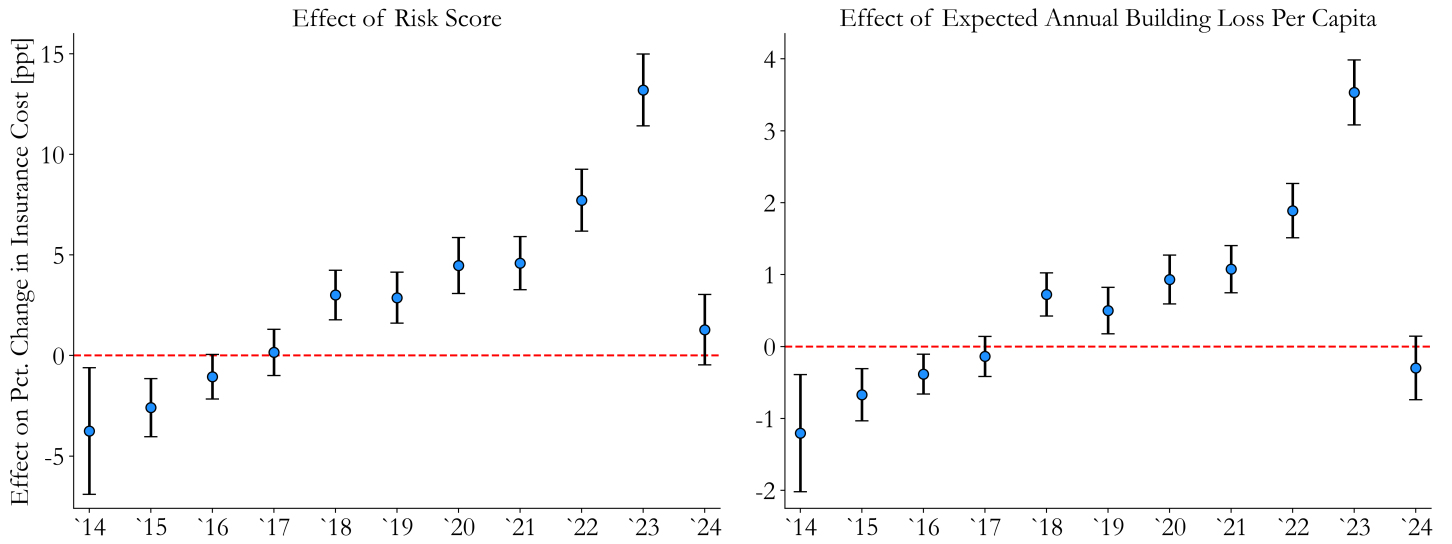
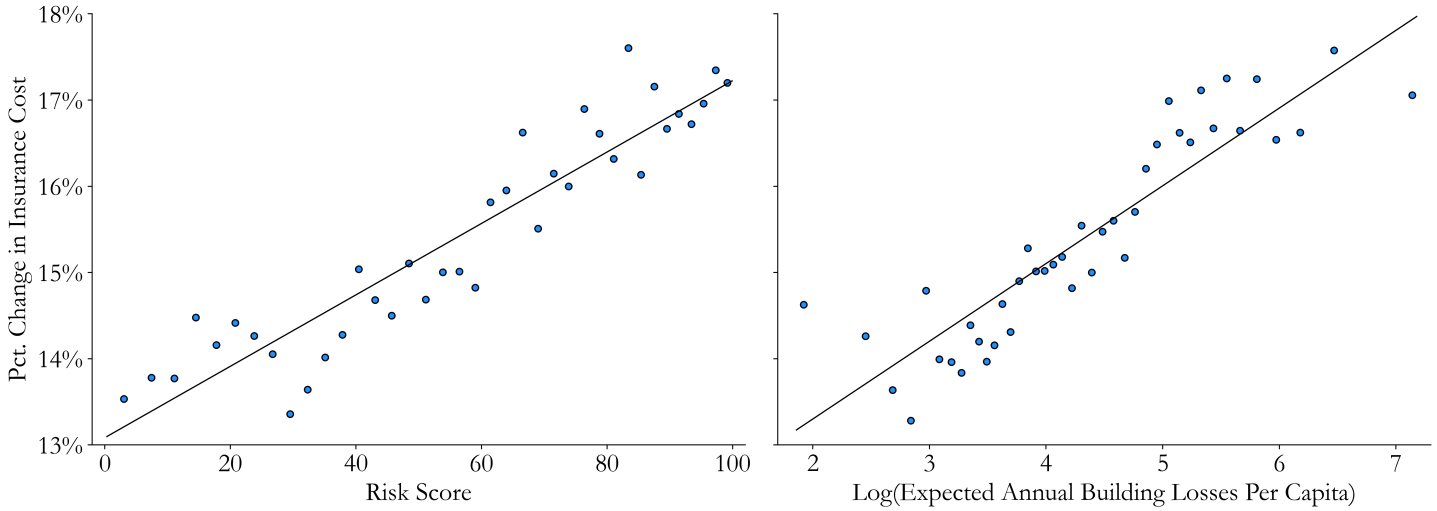


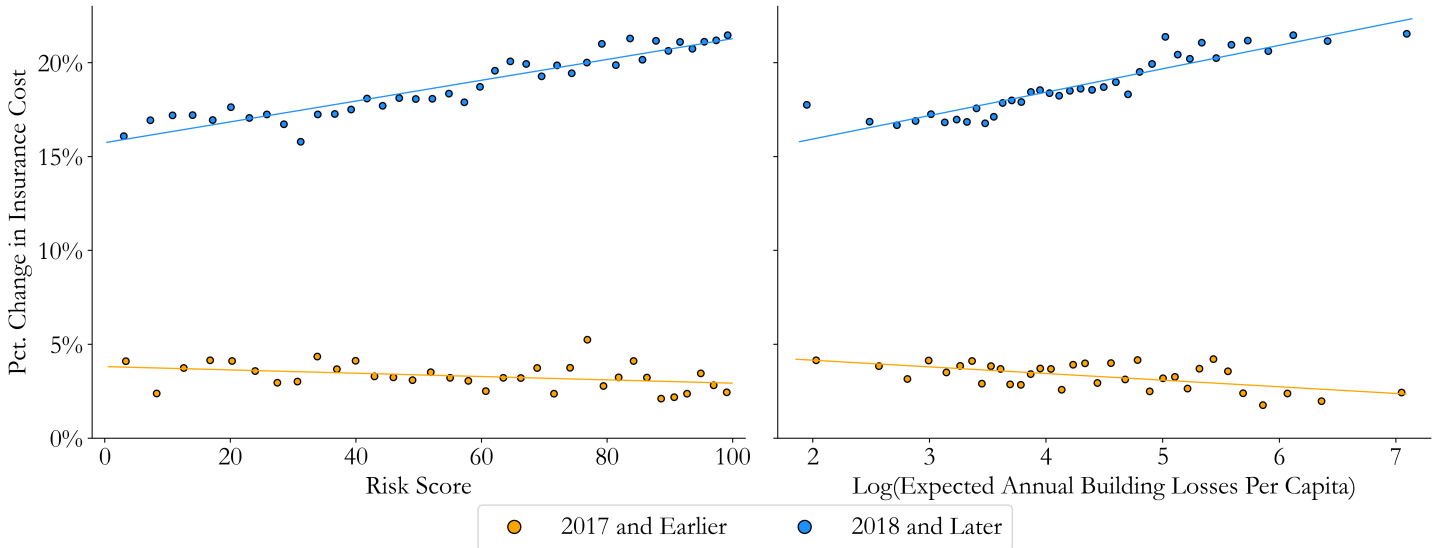
### Figure IA.9: Risk Scores, Expected Annual Losses, and Insurance Cost Growth

This figure examines how FEMA risk scores and expected annual building losses relate to changes in insurance costs. Panel A shows the relationships over the full sample period, 2010–2024. Panel B estimates the relationships separately for early years (2017 and earlier) and later years (2018 and later). In both panels, the left subpanels plot percentage changes in insurance costs against risk scores, while the right subpanels plot percentage changes in insurance costs against the logarithm of expected annual building losses per capita. All panels include year fixed effects, and fitted lines are based on the underlying data. Risk scores and expected annual losses are measured at the census tract level using FEMA’s National Risk Index.

Panel A: Risk Scores and Expected Annual Losses



Panel B: Split into Early and Late Years



● 2017 and Earlier      ● 2018 and Later

**Figure IA.10: Additional Risk Measures and Insurance Cost Growth**

This figure examines how alternative measures of FEMA National Risk Index risk scores and expected annual losses relate to insurance cost growth. All regressions include year fixed effects.

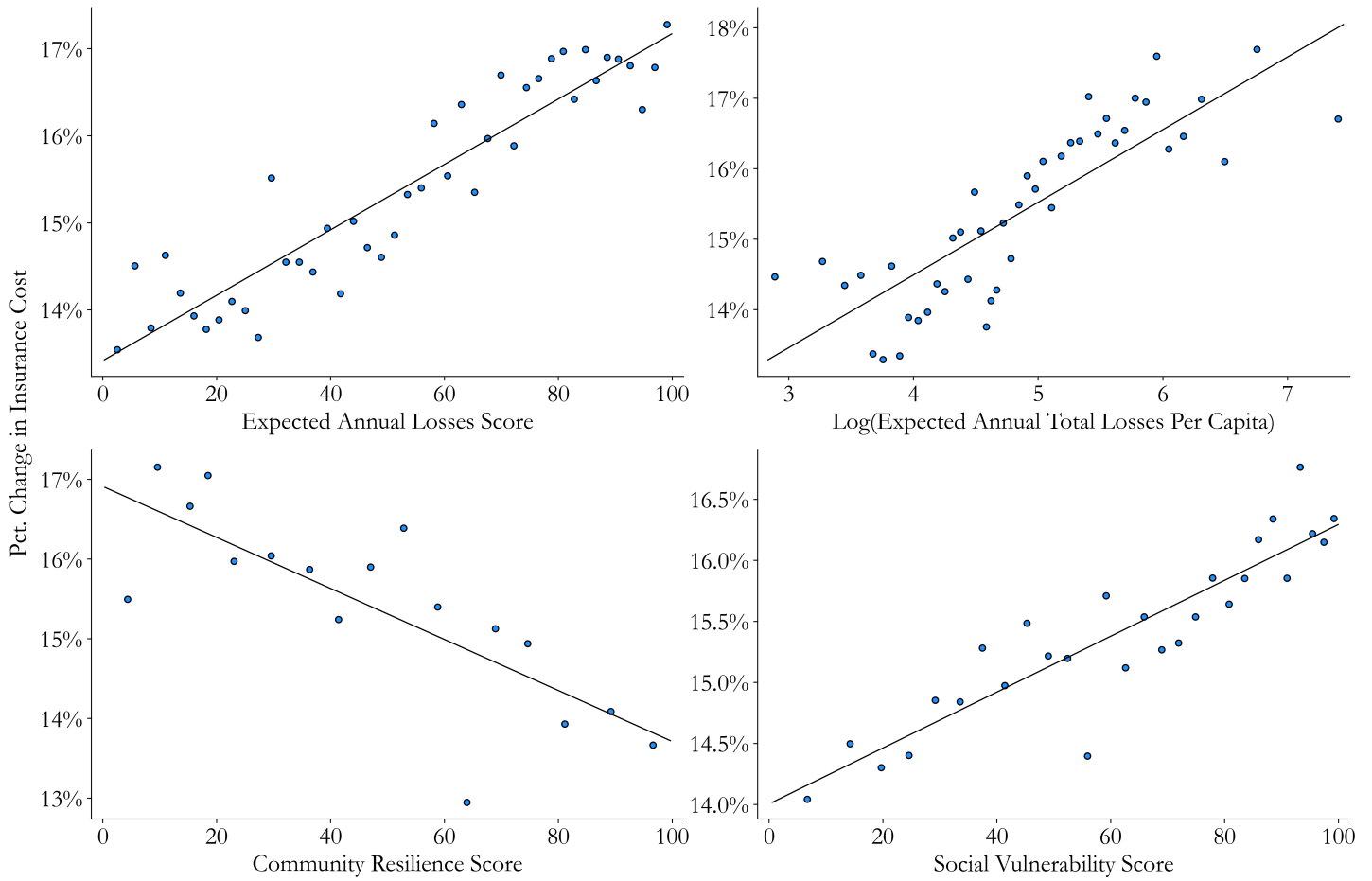
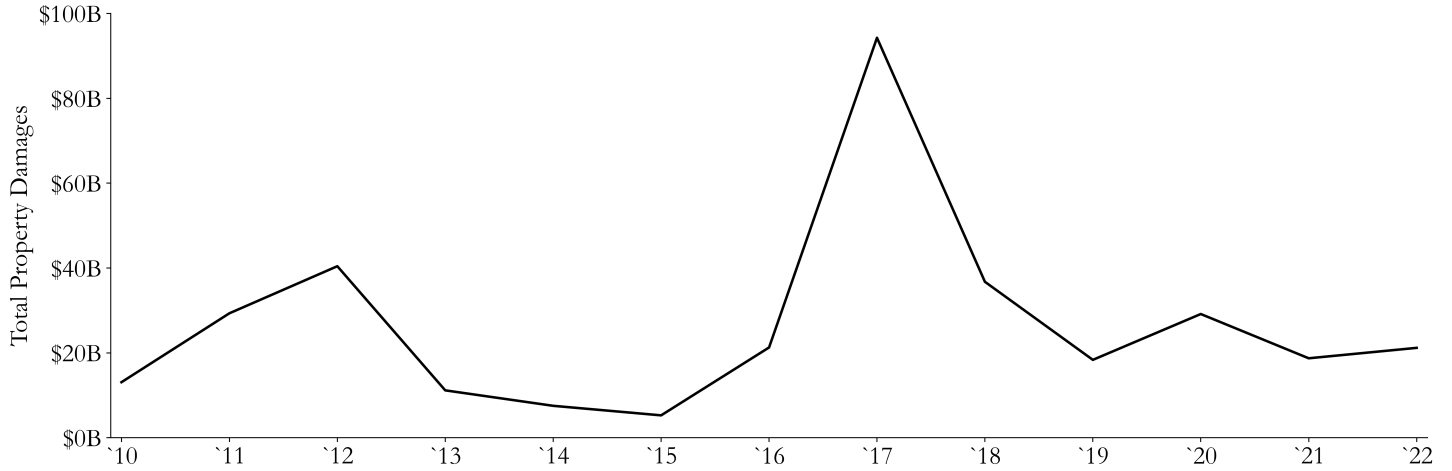


### Figure IA.11: Property Damages, 2010–2022

This figure shows annual national property damages (Panel A) and average annual property damages per capita by county (Panel B).

Panel A: Total Property Damages in Each Year



Panel B: Average Annual Property Damages Per Capita, County-level Map

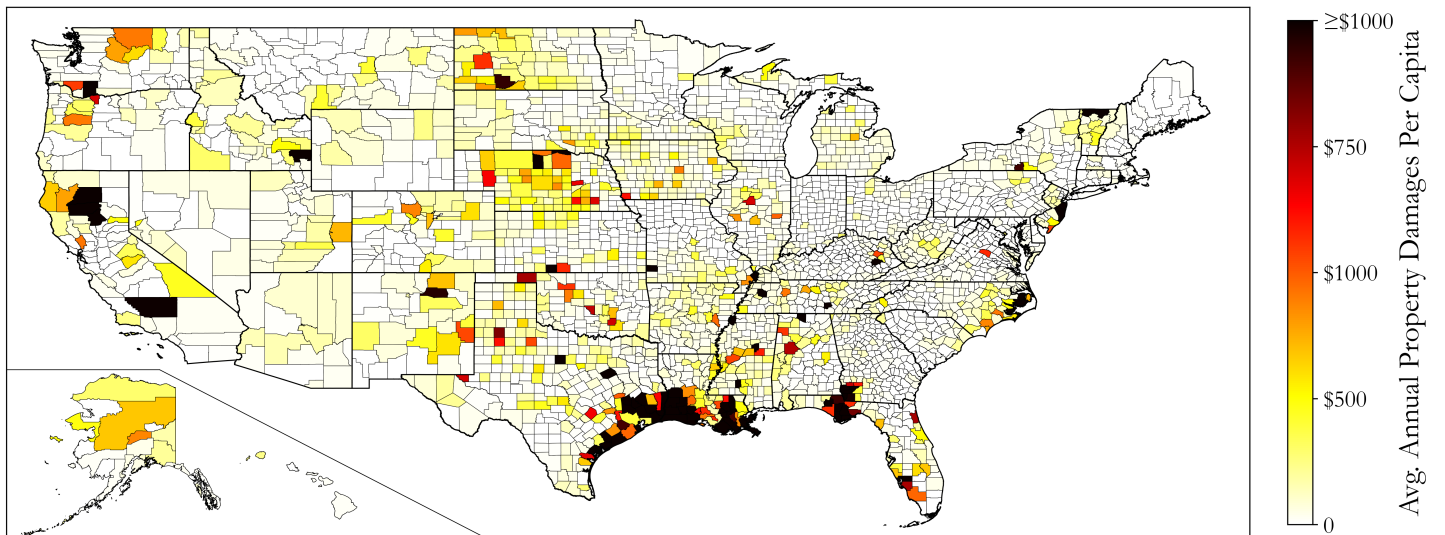


**Figure IA.12: Past Property Damages and the Rise in Insurance Costs**

This figure examines how past property damages relate to percentage changes in insurance costs. The figure shows a binscatter of percentage changes in insurance costs against the inverse hyperbolic sine (asinh) transformation of average property damages per capita over the previous five years. The fitted line is based on the underlying data. The specification includes year fixed effects. Property damage data are measured at the county level using Arizona State University's Spatial Hazard Events and Losses Database.

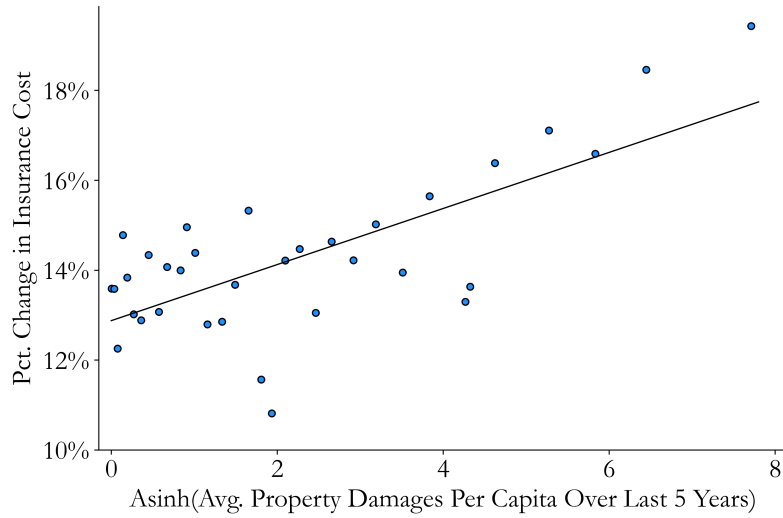
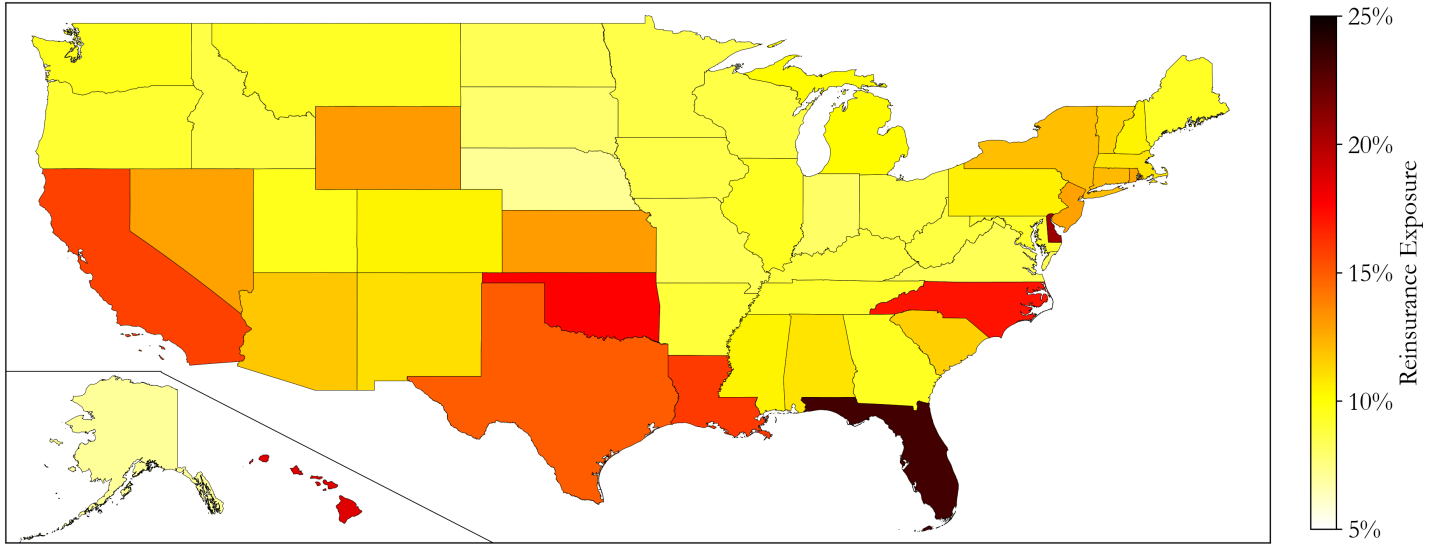


### Figure IA.13: Reinsurance Exposure

This figure documents state-level exposure to reinsurance markets (Panel A) and the stability of reinsurance exposure over time at the company level, measured by the share of risk ceded to unaffiliated reinsurers, and at the state level (Panel B).

Panel A: Reinsurance Exposure by State



Panel B: Stability of Reinsurance Exposure

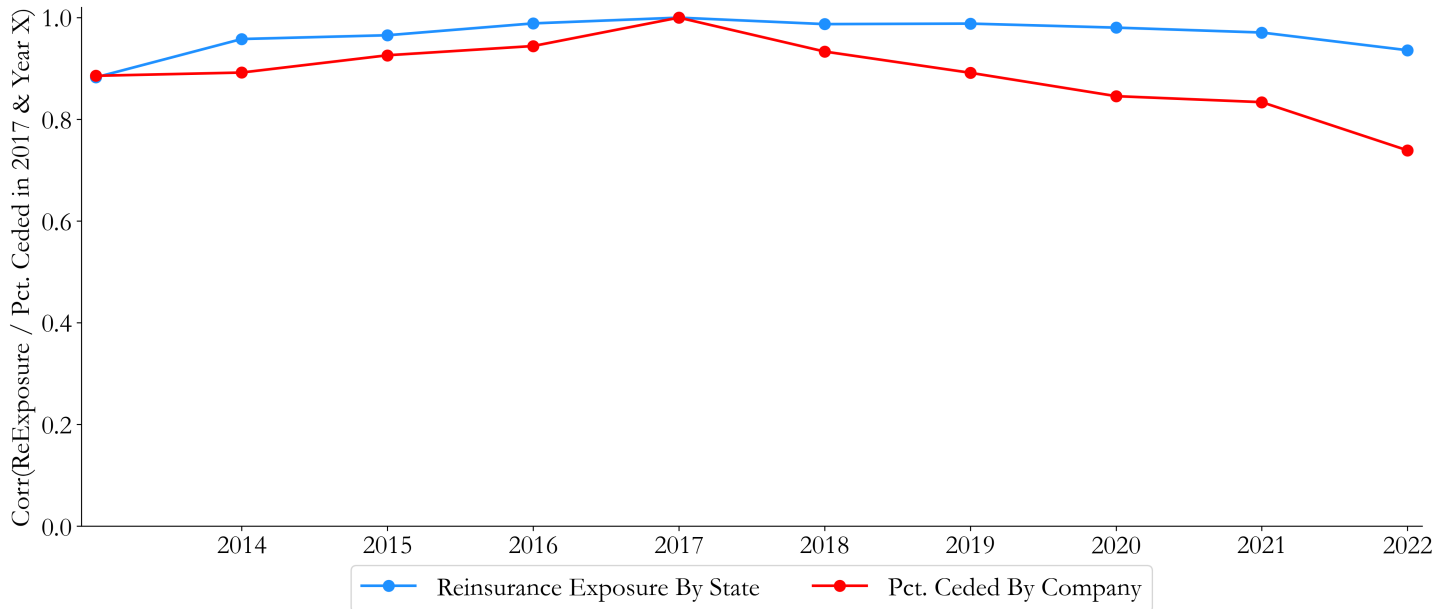


**Figure IA.14: Reinsurance Exposure: Border-County-Pair Evidence**

This figure provides complementary evidence on the role of reinsurance exposure using a border-county-pair difference-in-differences design. The sample is restricted to properties near state borders, and the plotted coefficients come from the dynamic specification

$$\Delta(\text{Insurance/Unit})_{i,p,s,t} = \sum_{t \neq 2017} \beta_t \times \mathbf{1}(\text{Year} = t) \times \text{HighReinsuranceExposure}_s + \gamma_i + \eta_{p,t} + \theta_p \times \text{RiskScore}_i + \varepsilon_{i,p,s,t},$$

where property  $i$  is located in state  $s$  and border county pair  $p$ , and  $\text{HighReinsuranceExposure}_s$  equals one if the state has above-median commercial reinsurance exposure. The specification includes property fixed effects, county-pair-by-year fixed effects, and county-pair-specific controls for local risk, allowing the pricing of local disaster risk to vary flexibly across border county pairs. Error bars denote 95% confidence intervals.

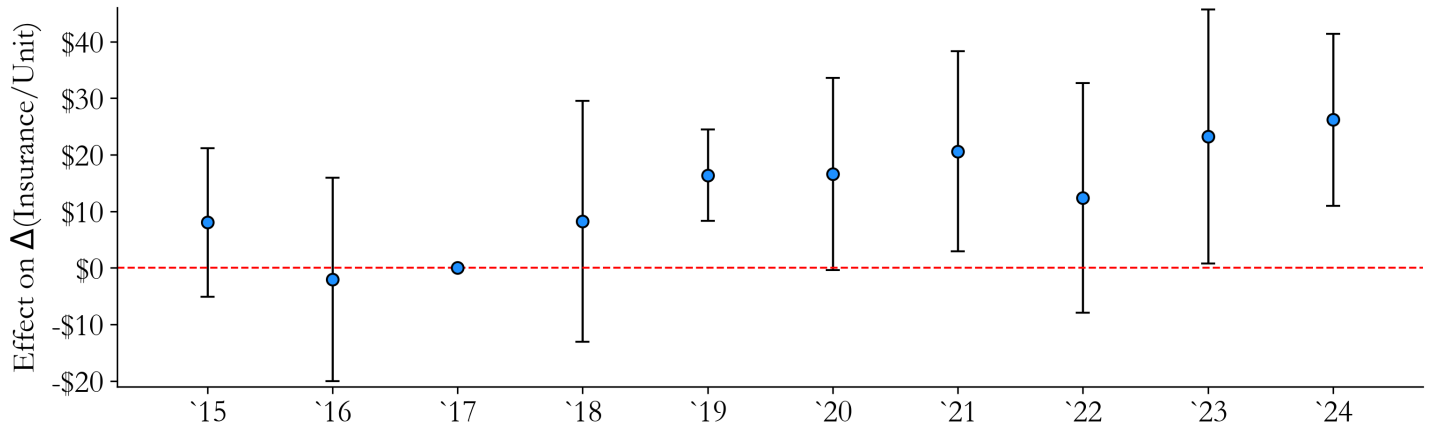


**Figure IA.15: Location Characteristics and Insurance Cost Growth**

This figure relates geographic location characteristics to changes in insurance costs. Panel A plots percentage changes in insurance costs against distance to the nearest coast, measured in 1,000 kilometers. Panel B plots percentage changes in insurance costs against elevation, measured in kilometers. Both panels include year fixed effects and fitted lines based on the underlying data. Distance to coast and elevation are calculated from geocoded property locations, U.S. Census Geocoder output, Natural Earth coastline data, and National Elevation Dataset topographic data.

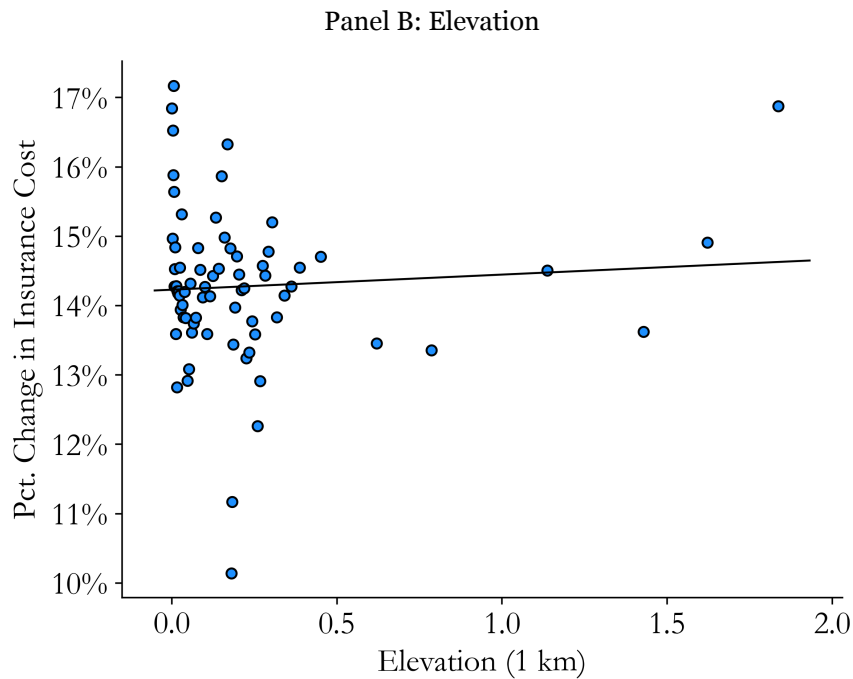
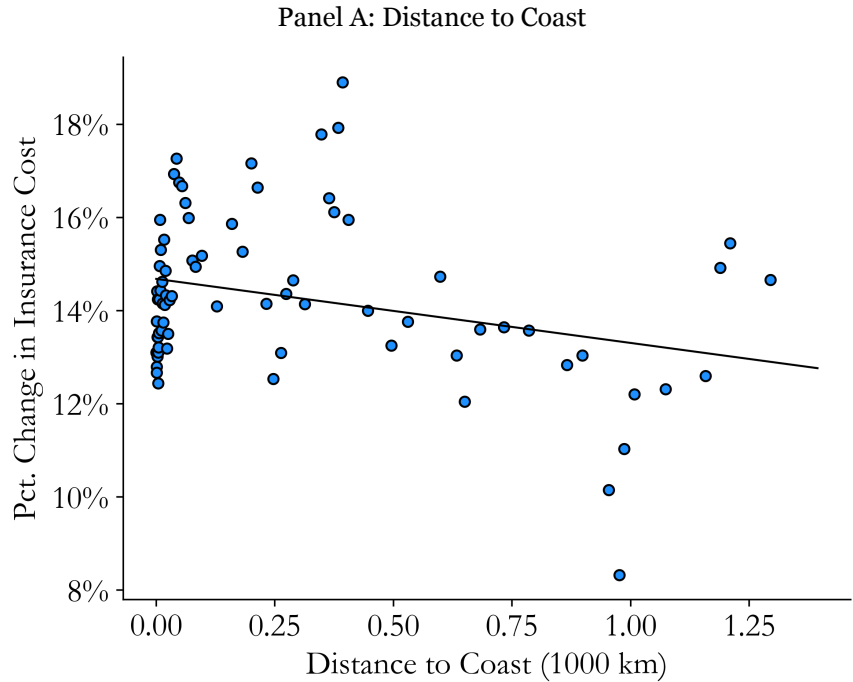
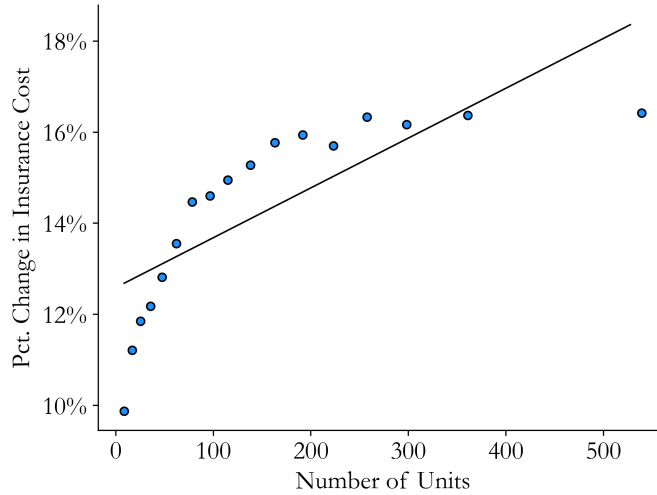


### Figure IA.16: Property Features and Insurance Cost Growth

This figure relates property-specific characteristics to changes in insurance costs. Panel A plots percentage changes in insurance costs against the number of units in a property. Panel B examines property age, with the left subpanel using actual age and the right subpanel using effective age. Effective age is the number of years since the last renovation; if no renovation has occurred, it equals building age. Renovation data are available only for properties in the Freddie Mac sample. Both panels include year fixed effects and fitted lines based on the underlying data.

Panel A: Units



Panel B: Age

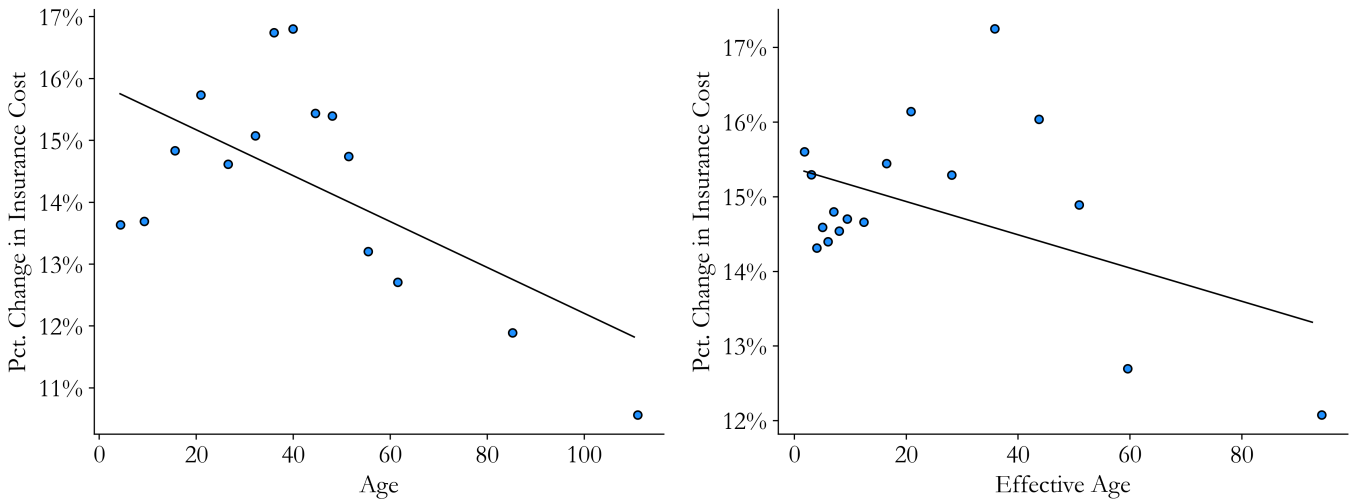


**Figure IA.17: Insurance Market Concentration and Insurance Cost Growth**

This figure examines whether insurance market concentration, measured by the Herfindahl-Hirschman Index (HHI), helps explain changes in insurance costs. Panel A and the left subpanel of Panel C use state-level HHI, while Panel B and the right subpanel of Panel C use county-level HHI for California. The left subpanels of Panels A and B plot average and median commercial multi-peril HHI from 2010 to 2022. The right subpanels compare HHI in 2010 and 2022, with circle sizes scaled by the number of sample properties in 2022. Panel C relates lagged HHI to changes in insurance costs, with year fixed effects and fitted lines based on the underlying data. State-level HHIs are from the National Association of Insurance Commissioners' annual Competition Database Report; California county-level HHIs are from the California Department of Insurance's Community Service Statement data.

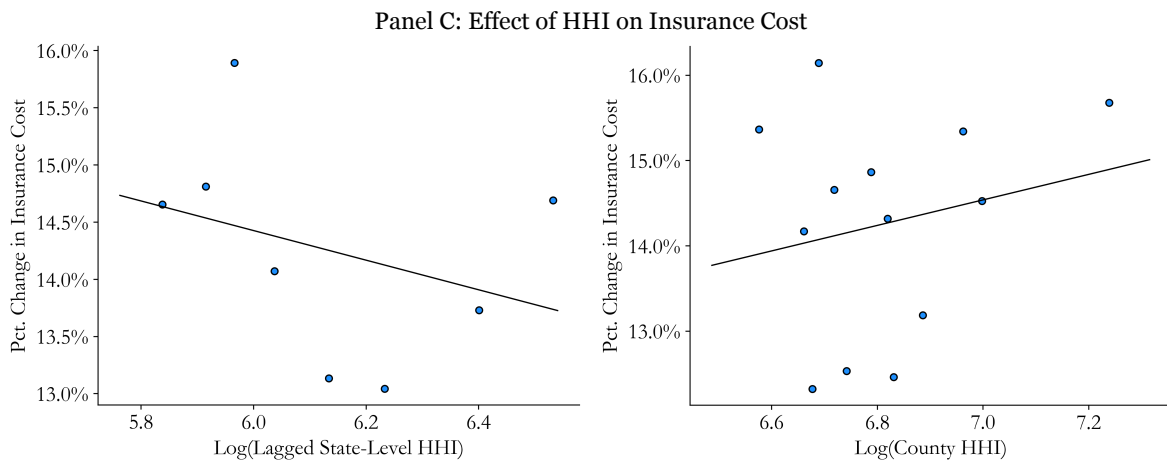
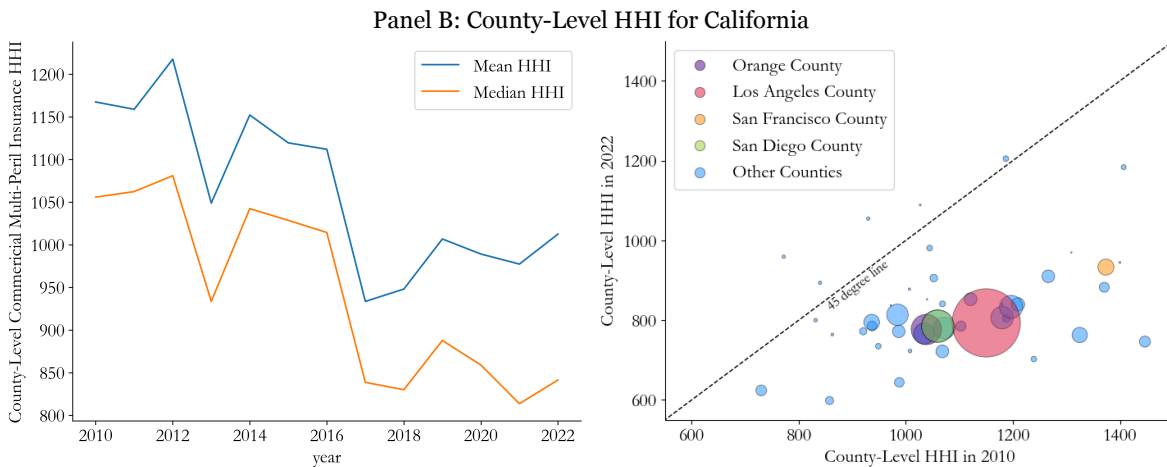
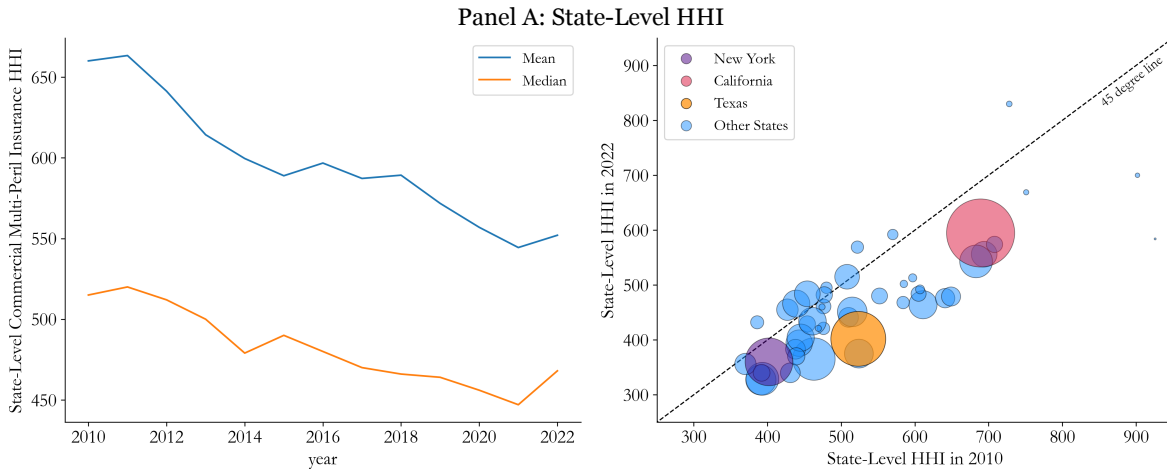


**Figure IA.18: Cumulative Effects Using Percentage Changes in Insurance Cost Per Unit**

This figure replicates Figure 7, Panel C using percentiles of the percentage change in insurance cost per unit rather than percentiles of the percentage change in the insurance-cost-to-operating-expenses ratio.

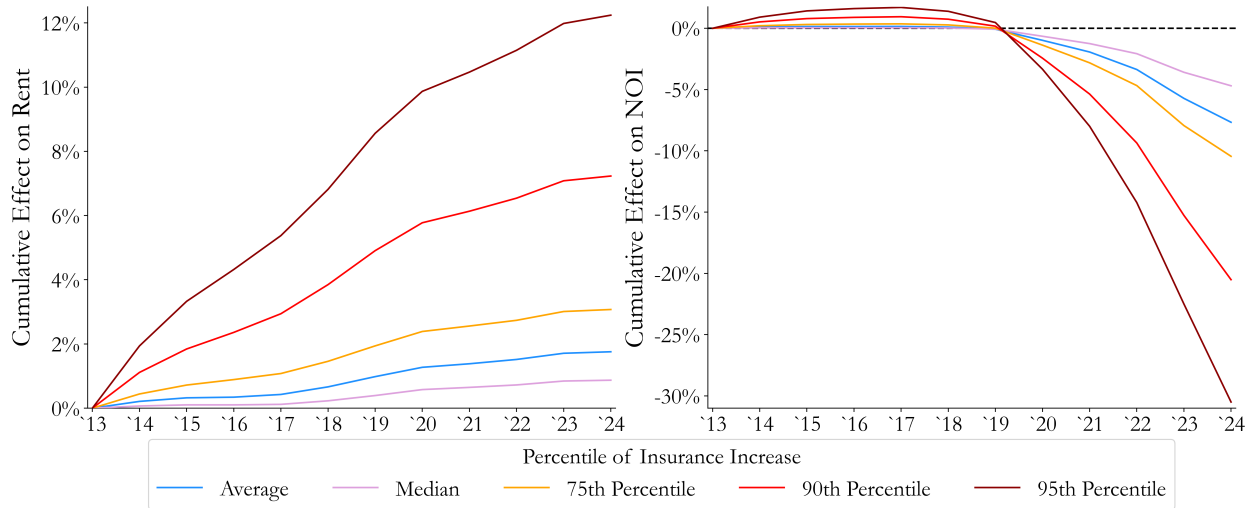


### Figure IA.19: Incidence of Insurance Cost Increases on NOI, Heterogeneity

This figure examines heterogeneity in the incidence of insurance cost increases on NOI across levels of local housing-supply elasticity, local owner market share, moving frictions, and tenant outside options. The dependent variable is log NOI per unit, and the plotted coefficients come from regressions of log NOI per unit on log insurance cost per unit interacted with indicators for deciles of the relevant heterogeneity variable; the coefficients can therefore be interpreted as decile-specific NOI-insurance elasticities. Panel A splits properties by housing supply elasticity bins and controls for the time-varying effects of the fraction of the tract developed, with bins formed nationally; both the housing supply elasticity and the fraction of the tract developed are from [Baum-Snow and Han \(2024\)](#). Panel B splits properties by owner-market-share bins, where owner market share is measured by the percentage of multifamily units within the CBSA owned by the property's owner, with bins formed within CBSA-year. Panel C splits properties by proxies for moving-frictions: the share of residents living in the same home as one year earlier, the share of families with children, and the share of households that are married-couple families. Panel D splits properties by proxies for tenant outside options: the share of housing units in apartment buildings, the vacancy rate among apartment units, and the overcrowding rate. The variables in Panels C and D are from ACS 5-year estimates, matched to properties at the tract-by-year level, and binned within CBSA-year. The exception is the same-home-as-one-year-earlier measure, which uses the 2013 ACS estimate snapshot to avoid contaminating the variable with endogenous moving responses by renters. Log NOI per unit and log insurance cost per unit are winsorized within year at the 1st and 99th percentiles. All panels include property fixed effects and CBSA-by-year fixed effects, and standard errors are clustered at the CBSA level. Error bars represent 95% confidence intervals; the red dashed horizontal line denotes zero.

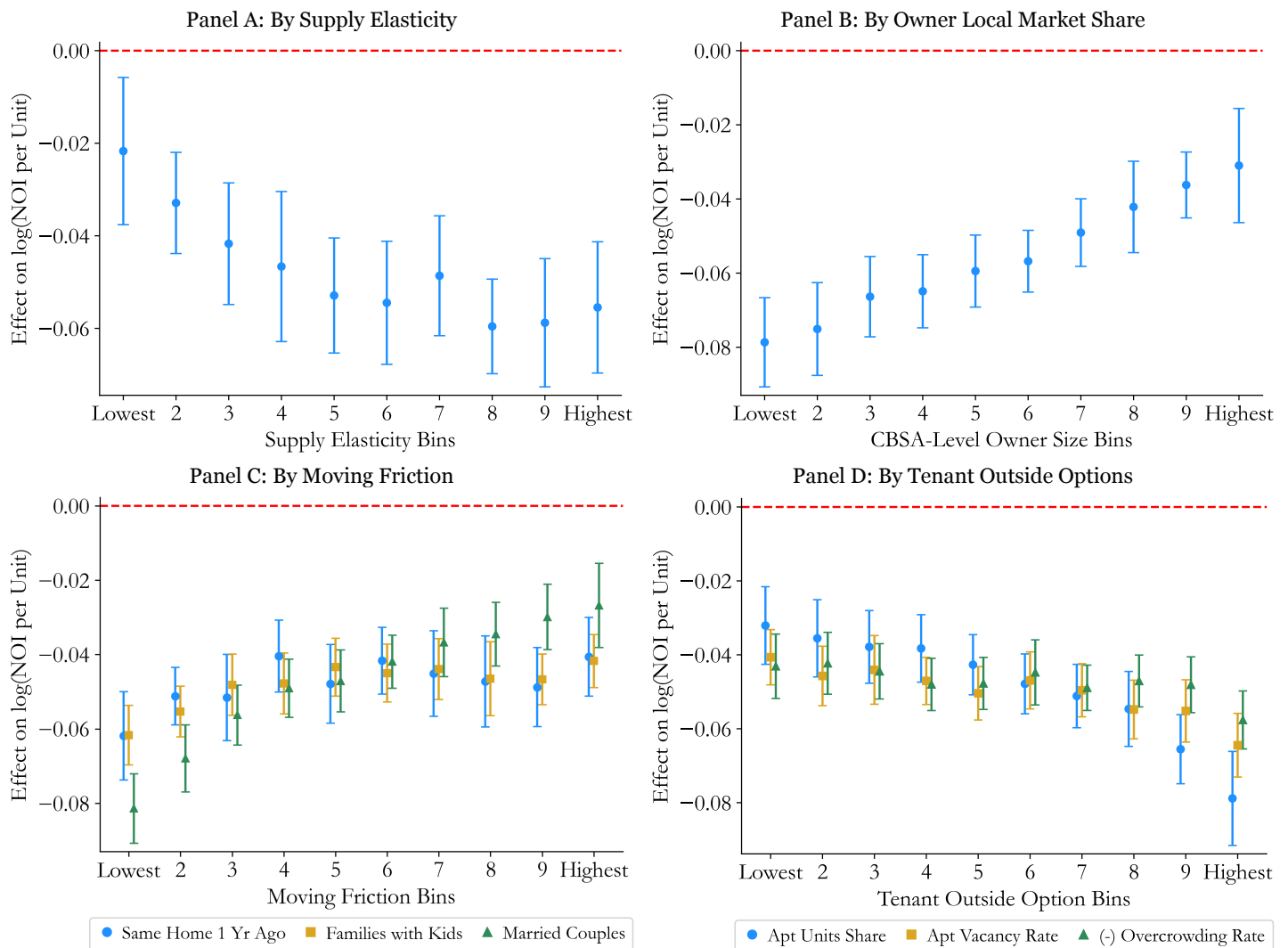


### Figure IA.20: Owner Size and Insurance Costs, Split by Expected Annual Losses

This figure replicates Figure 8, Panel B using expected annual losses rather than risk scores to measure local disaster risk.

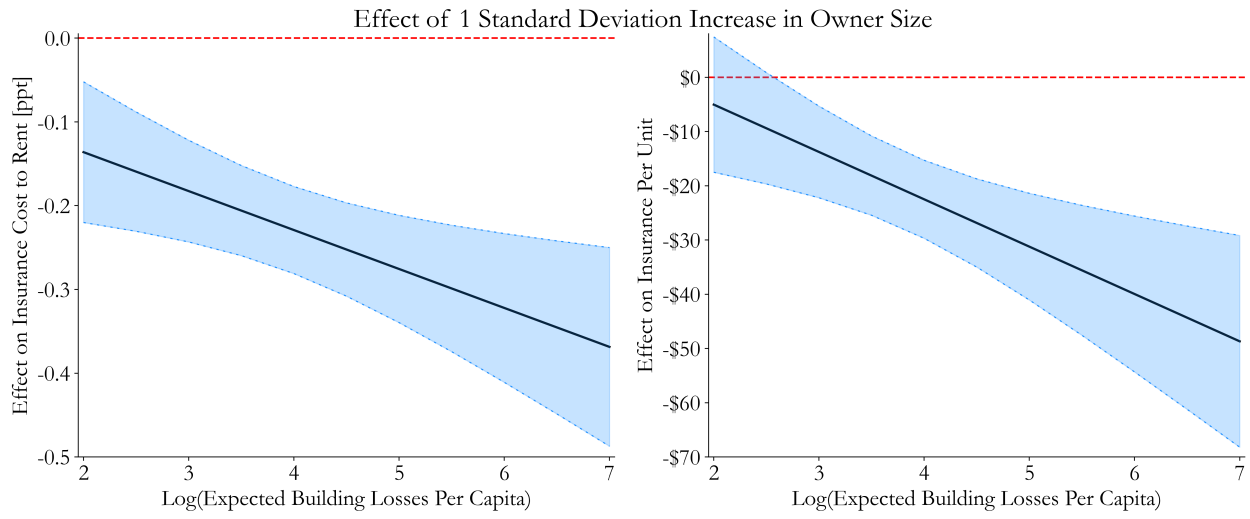


**Figure IA.21: Owner Portfolio Risk Using Weighted Expected Annual Losses**

This figure replicates Figure 9, Panel A using unit-weighted expected annual losses across the owner's portfolio rather than the unit-weighted portfolio risk score.

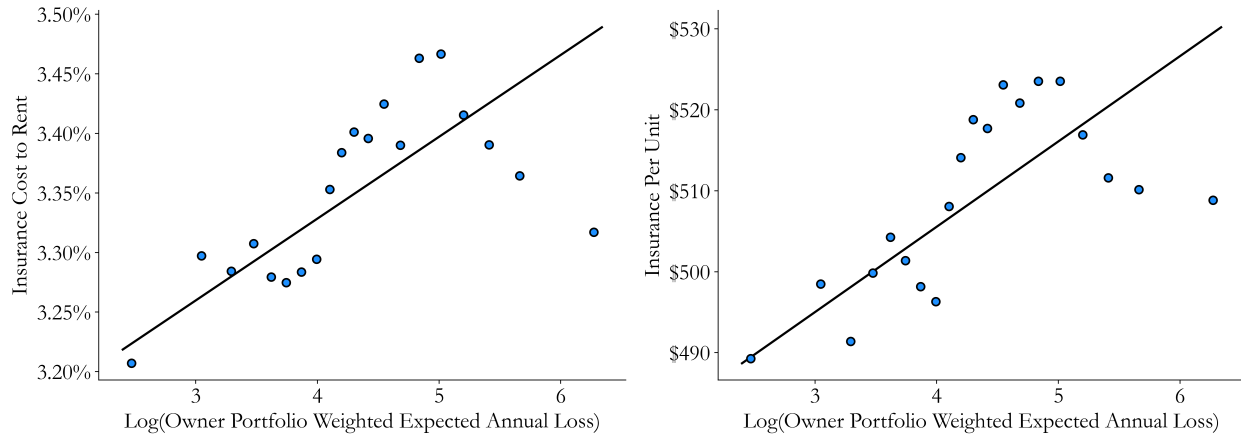


**Figure IA.22: Renovation Activity Around M&A Events**

This figure plots dynamic stacked difference-in-differences estimates of renovation activity around portfolio-level M&A events. Event time is measured in years relative to the M&A transaction, with the year immediately before the event ( $t = -1$ ) omitted as the reference period. The dependent variable is an indicator for whether the property is renovated, and property-by-cohort fixed effects and CBSA-by-year-by-cohort fixed effects are included. Error bars denote 95% confidence intervals based on owner-clustered standard errors.

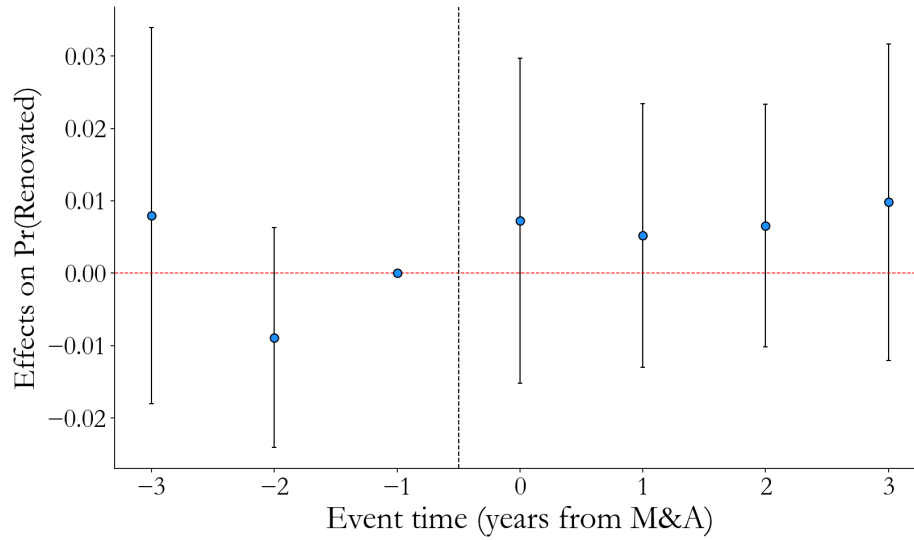


### Figure IA.23: Building-Permit Activity Around M&A Events

This figure plots dynamic stacked difference-in-differences estimates of building-permit activity around portfolio-level M&A events. Event time is measured in years relative to the M&A transaction, with the year immediately before the event ( $t = -1$ ) omitted as the reference period. The dependent variable is an annual property-level indicator for whether a permit is issued: in Panel A, for any building permit; in Panel B, for insurance-relevant work—roof, exterior envelope, windows and doors, structural and seismic work, fire protection, new construction, and additions. Property-by-cohort fixed effects and CBSA-by-year-by-cohort fixed effects are included. Error bars denote 95% confidence intervals based on owner-clustered standard errors.

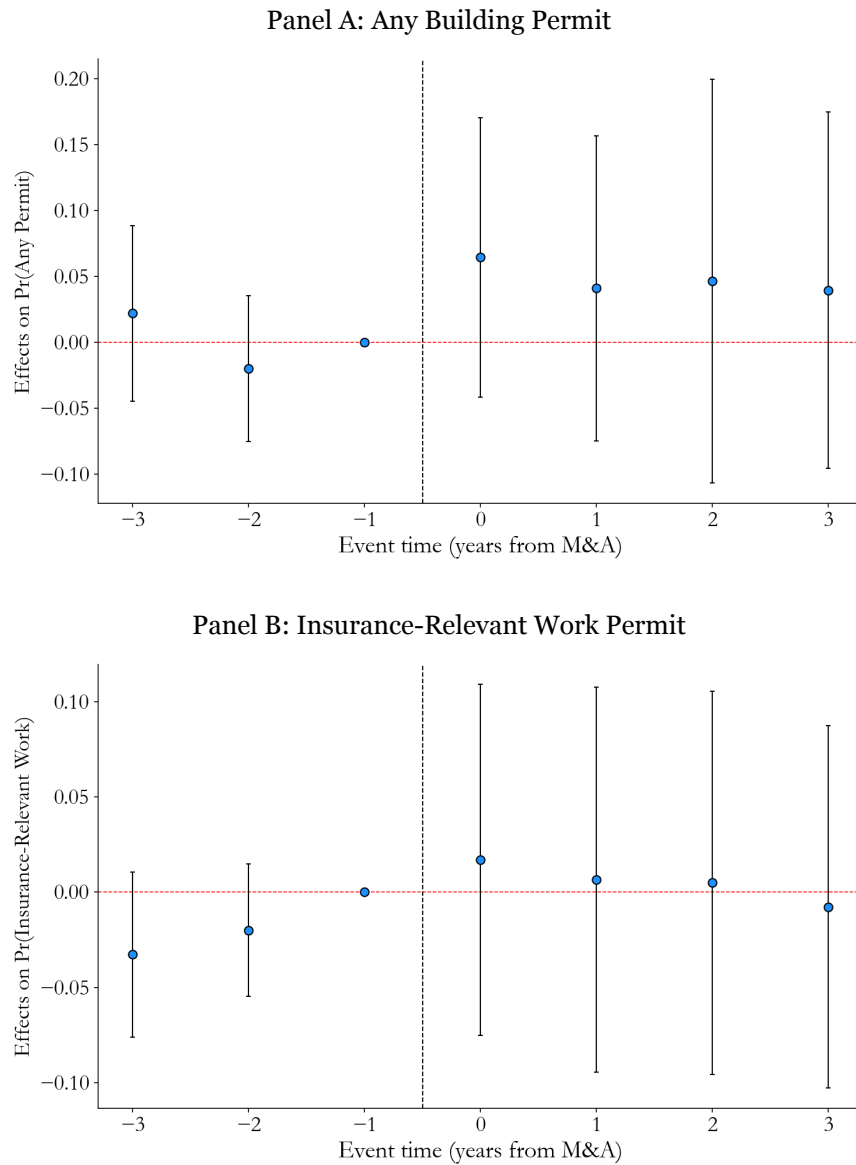


**Figure IA.24: Property Risk, Owner Size, and Property Sales Over Time**

This figure plots the annual estimated effect of being in a high-risk location on the probability that a property is sold by owners in size deciles 1–2 relative to the omitted owner-size decile 5. For each year, the regression relates a transaction indicator to interactions between the high-risk indicator and owner-size deciles, controlling for CBSA fixed effects. High risk is defined as above-median expected annual building losses. Error bars denote 95% confidence intervals based on standard errors clustered by owner.

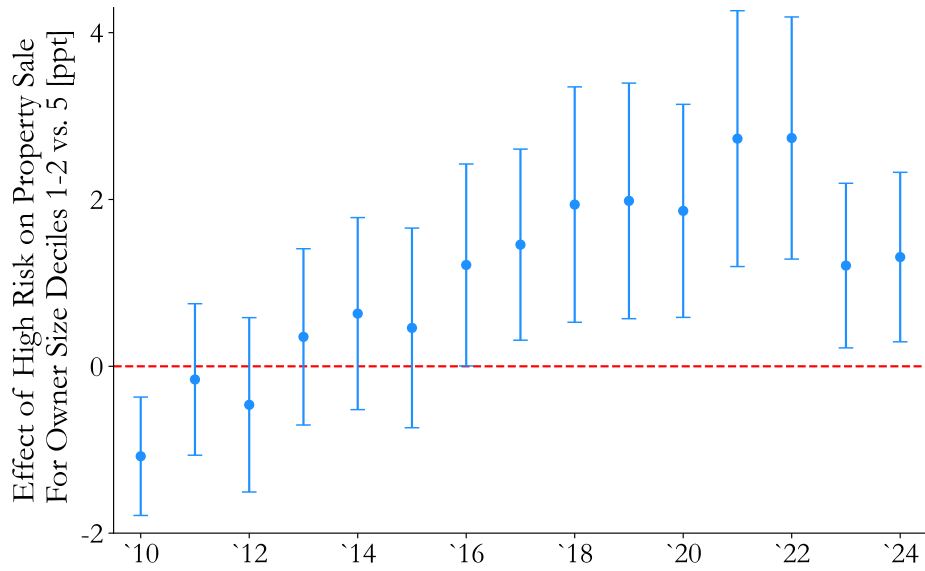


**Table IA.1: Reinsurance Exposure and Insurance Cost Increases, Expected Losses**

This table replicates Columns (4)–(7) of Table 1 using expected annual losses per capita instead of risk scores. The dependent variable is the change in insurance cost per unit for property  $i$  in state  $s$  and year  $t$ . Reinsurance exposure is measured at the state level as the weighted average share of direct premiums ceded to unaffiliated reinsurers by insurers operating in the state, following [Keys and Mulder \(2025\)](#).  $\Delta$ Reins. Cost denotes the annual change in the Guy Carpenter Rate-On-Line Index. Robust standard errors are double-clustered by state and year.

Dep. Variable:	$\Delta$ Insurance Cost Per Unit			
	(1)	(2)	(3)	(4)
Reins. Exposure	34.88 (0.28)			
$\Delta$ Reins. Cost $\times$ Reins. Exposure	-955.8* (-1.94)	-1044.9 (-1.37)	-699.7 (-0.86)	
$\log(\text{Expected Annual Losses Per Capita})$	-0.738 (-0.21)	2.974 (0.43)		
$\Delta$ Reins. Cost $\times \log(\text{Expected Annual Losses Per Capita})$	-43.96** (-2.33)	-47.05* (-2.13)	-34.44 (-1.42)	
Reins. Exposure $\times \log(\text{Expected Annual Losses Per Capita})$	5.769 (0.22)	-16.43 (-0.37)		
$\Delta$ Reins. Cost $\times$ Reins. Exposure $\times \log(\text{Expected Annual Losses Per Capita})$	531.7*** (5.99)	551.5*** (4.06)	455.5*** (3.22)	457.8*** (3.23)
Year FE	✓	✓	✓	✓
State FE		✓		
Property FE			✓	✓
Year $\times \log(\text{Expected Annual Losses Per Capita})$				✓
Year $\times$ Reins. Exposure				✓
Observations	325,705	325,705	312,920	312,920
Adjusted $R^2$	0.0878	0.0941	0.0430	0.0436

$t$ -statistics in parentheses.

\* $p < 0.10$ , \*\* $p < 0.05$ , \*\*\* $p < 0.01$

**Table IA.2: Losses and the Commercial-Homeowners Insurance Cost Wedge**

This table examines whether the relative-pricing wedge between commercial and homeowners insurance costs rises more steeply following insurer losses in states with greater homeowners insurance market frictions. The commercial-homeowners ratio is not a matched-contract premium ratio. ZIP-code-by-year homeowners insurance premiums and loss ratios are from [U.S. Department of the Treasury \(2025\)](#). The dependent variable in all columns is the ratio of each commercial property's insurance cost per unit to homeowners insurance costs in the property's ZIP code.  $\mathbb{1}(\text{Low Friction})$  and  $\mathbb{1}(\text{High Friction})$  are based on the state-level homeowners insurance market friction measures from [Oh, Sen, and Tenekedjieva \(2025\)](#), with low friction defined as the bottom two terciles and high friction defined as the top tercile. Columns (3) and (4) split the sample by friction level. Fixed effects are specified at the bottom of each column. Robust standard errors are clustered at the state level.

Dep. Variable:	Commercial to Homeowners Insurance Cost Ratio			
	(1)	(2)	(3)	(4)
Lagged Loss Ratio	0.00238*** (2.76)			
$\mathbb{1}(\text{Low Friction}) \times \text{Lagged Loss Ratio}$		0.000862 (0.58)		
$\mathbb{1}(\text{High Friction}) \times \text{Lagged Loss Ratio}$		0.00342*** (4.14)		
$\mathbb{1}(\text{Low Risk Score}) \times \text{Lagged Loss Ratio}$			0.00230 (0.92)	0.000888 (0.36)
$\mathbb{1}(\text{High Risk Score}) \times \text{Lagged Loss Ratio}$			-0.000911 (-0.58)	0.00513*** (4.84)
States Included	All	All	Low	High
Property FE	✓	✓	✓	✓
State $\times$ Year FE	✓	✓	✓	✓
Observations	158,047	158,047	80,519	77,528
Adjusted $R^2$	0.823	0.823	0.840	0.801

*t*-statistics in parentheses.

\* $p < 0.10$ , \*\* $p < 0.05$ , \*\*\* $p < 0.01$

**Table IA.3: Claims and the Commercial-Homeowners Insurance Cost Ratio**

This table replicates Table IA.2 using the percentage of homeowners policies with claims instead of loss ratios. The dependent variable is the ratio of each commercial property's insurance cost per unit to homeowners insurance costs in the property's ZIP code. Fixed effects are specified at the bottom of each column. Robust standard errors are clustered at the state level.

Dep. Variable:	Commercial to Homeowners Insurance Cost			
	(1)	(2)	(3)	(4)
Lagged Pct. Claims	0.0201 (1.29)			
1(Low Friction) × Lagged Pct. Claims		-0.0164 (-0.61)		
1(High Friction) × Lagged Pct. Claims		0.0451*** (4.39)		
1(Low Risk Score) × Lagged Pct. Claims			-0.000554 (-0.01)	0.0265 (1.23)
1(High Risk Score) × Lagged Pct. Claims			-0.0297 (-1.36)	0.0628*** (3.18)
States Included	All	All	Low	High
Property FE	✓	✓	✓	✓
State × Year FE	✓	✓	✓	✓
Observations	158,047	158,047	80,519	77,528
Adjusted $R^2$	0.823	0.823	0.840	0.801

*t*-statistics in parentheses.

\* $p < 0.10$ , \*\* $p < 0.05$ , \*\*\* $p < 0.01$

**Table IA.4: Incidence of Insurance Cost Increases on Rents and NOI, Other Class Proxies**

This table replicates the rent and NOI incidence specifications from Columns (3)–(4) and (7)–(8) of Table 3, Panel A using alternative property-class proxies. The dependent variables are log rent per unit in Columns (1)–(4) and log NOI per unit in Columns (5)–(8). Each column uses a different proxy for class, with Columns (1) and (5) using property age, Columns (2) and (6) using rent per unit, Columns (3) and (7) using occupancy rate, and Columns (4) and (8) using all three proxies at the same time. Each class proxy is determined by splitting properties within a given CBSA  $\times$  year into terciles. Panel B additionally includes property-level controls used in Columns (4) and (8) of Table 3, Panel A (occupancy, log(Operating Expenses Excluding Insurance Cost Per Unit), log(Capital Expenses), an indicator for renovations in the previous year, an indicator for renovations in the previous five years, log(Property Age), and log(Effective Property Age)). Dependent and independent variables are winsorized at the 1% tails within each year. Fixed effects and controls are indicated at the bottom of each column. Robust standard errors are clustered by CBSA.

Panel A: Columns (3) and (7) of Table 3, Panel A

Dep. Variable:	log(Rent Per Unit)				log(NOI Per Unit)			
	(1)	(2)	(3)	(4)	(5)	(6)	(7)	(8)
log(Insurance Cost Per Unit)	0.0150*** (9.74)	0.0127*** (10.26)	0.0148*** (10.84)	0.0109*** (10.61)	-0.0476*** (-13.26)	-0.0511*** (-14.66)	-0.0474*** (-14.32)	-0.0527*** (-14.42)
Property FE	✓	✓	✓	✓	✓	✓	✓	✓
CBSA $\times$ Age Class $\times$ Year FE	✓			✓	✓			✓
CBSA $\times$ Rent Class $\times$ Year FE		✓		✓		✓		✓
CBSA $\times$ Occupancy Class $\times$ Year FE			✓	✓			✓	✓
Observations	401,996	407,134	403,769	392,302	401,996	407,134	403,769	392,302
Adjusted $R^2$	0.980	0.984	0.980	0.984	0.926	0.932	0.925	0.933

Panel B: Columns (4) and (8) of Table 3, Panel A

Dep. Variable:	log(Rent Per Unit)				log(NOI Per Unit)			
	(1)	(2)	(3)	(4)	(5)	(6)	(7)	(8)
log(Insurance Cost Per Unit)	0.0144*** (7.91)	0.0122*** (9.16)	0.0154*** (9.28)	0.0112*** (7.73)	-0.0418*** (-8.89)	-0.0462*** (-10.87)	-0.0401*** (-8.60)	-0.0477*** (-11.00)
Property FE	✓	✓	✓	✓	✓	✓	✓	✓
CBSA $\times$ Age Class $\times$ Year FE	✓			✓	✓			✓
CBSA $\times$ Rent Class $\times$ Year FE		✓		✓		✓		✓
CBSA $\times$ Occupancy Class $\times$ Year FE			✓	✓			✓	✓
Additional Controls	✓	✓	✓	✓	✓	✓	✓	✓
Observations	170,237	170,246	171,480	166,798	170,237	170,246	171,480	166,798
Adjusted $R^2$	0.976	0.981	0.976	0.980	0.929	0.941	0.928	0.938

$t$ -statistics in parentheses.

\*  $p < 0.10$ , \*\*  $p < 0.05$ , \*\*\*  $p < 0.01$

**Table IA.5: Incidence of Insurance Cost Increases on Operating Margin and DSCR**

This table replicates Table 3, Panel A for additional dependent variables. The dependent variable is operating margin [NOI / total revenue] in Columns (1)–(4) and debt service coverage ratio [NOI / debt service] in Columns (5)–(8). Dependent and independent variables are winsorized at the 1% tails within each year. Fixed effects and controls are indicated at the bottom of each column. Robust standard errors are clustered by CBSA.

Dep. Variable:	Operating Margin				Debt Service Coverage Ratio			
	(1)	(2)	(3)	(4)	(5)	(6)	(7)	(8)
log(Insurance Cost Per Unit)	-0.0303*** (-24.94)	-0.0301*** (-26.55)	-0.0308*** (-25.20)	-0.0295*** (-21.12)	-0.104*** (-8.78)	-0.107*** (-12.07)	-0.113*** (-11.61)	-0.107*** (-11.75)
Property FE	✓	✓	✓	✓	✓	✓	✓	✓
Year FE	✓				✓			
CBSA × Year FE		✓				✓		
CBSA × Class × Year FE			✓	✓			✓	✓
Additional Controls				✓				✓
Observations	410,023	410,023	405,204	170,791	410,104	410,104	405,284	170,791
Adjusted $R^2$	0.859	0.865	0.874	0.921	0.747	0.763	0.779	0.755
Mean of Dep. Variable	0.536	0.536	0.536	0.549	2.030	2.030	2.031	1.938

*t*-statistics in parentheses.

\*  $p < 0.10$ , \*\*  $p < 0.05$ , \*\*\*  $p < 0.01$

**Table IA.6: Owner Size and Insurance Costs, Expected Annual Losses**

This table replicates Columns (2) and (3) of Table 5, Panel A using expected annual losses instead of risk scores. The dependent variable is the insurance-cost-to-rent ratio. Owner size is the log of the total number of multifamily units owned nationally by each owner in a given year. All regressions include CBSA-by-year fixed effects and property fixed effects. Expected annual losses are from FEMA's National Risk Index, and property ownership is from Real Capital Analytics. Robust standard errors are clustered by owner.

Dep. Variable:	Insurance Cost to Rent	
	(1)	(2)
log(Owner Size)	0.0000105 (0.03)	-0.000450 (-1.29)
log(Owner Size) × log(Expected Annual Losses Per Capita)	-0.000255*** (-3.19)	-0.000171** (-2.06)
1(2018 or Later) × log(Owner Size)		0.000563*** (4.01)
1(2018 or Later) × log(Expected Annual Losses Per Capita)		0.000492* (1.92)
1(2018 or Later) × log(Owner Size) × log(Expected Annual Losses Per Capita)		-0.000101*** (-3.16)
CBSA × Year FE	✓	✓
Property FE	✓	✓
Observations	301,853	301,853
Adjusted $R^2$	0.767	0.767
Mean of Dep. Variable	0.0335	0.0335

*t*-statistics in parentheses.

\*  $p < 0.10$ , \*\*  $p < 0.05$ , \*\*\*  $p < 0.01$

**Table IA.7: Insurance Costs Around M&A Events, Heterogeneity Using Insurance to OpEx**

This table replicates the heterogeneity analysis in Table 7 with the insurance-cost-to-operating-expenses ratio as the dependent variable. See Table 7 for more details regarding the estimation and specification. Fixed effects and controls are indicated at the bottom of the table. Robust standard errors are clustered by owner. In both panels, the Wald  $t$ -statistics and  $p$ -values reported at the bottom of each panel test whether the estimated treatment effects differ between the high and low groups, both unconditionally and within each owner-size-gap subsample.

Panel A: Heterogeneity by Property Risk						
Dep. Variable:	Insurance Cost to OpEx					
Owner-Size Gap:	Unconditional		High		Low	
Property Risk:	High	Low	High	Low	High	Low
$\mathbb{1}(\text{Treated}) \times \mathbb{1}(\text{Post})$	-0.0232*** (-3.01)	-0.0075* (-1.65)	-0.0377*** (-8.58)	-0.0123* (-1.75)	-0.0053 (-1.45)	-0.0025 (-0.50)
Property $\times$ Cohort FE	✓	✓	✓	✓	✓	✓
CBSA $\times$ Year $\times$ Cohort FE	✓	✓	✓	✓	✓	✓
Observations	279,249	266,648	266,928	277,050	282,406	262,053
Adjusted $R^2$	0.826	0.835	0.825	0.836	0.826	0.835
Wald $t$ -stat ( $p$ -value)	-1.76 (0.079)		-3.07 (0.002)		-0.44 (0.661)	

Panel B: Heterogeneity by Portfolio-Risk Reduction						
Dep. Variable:	Insurance Cost to OpEx					
Owner-Size Gap:	Unconditional		High		Low	
Portfolio-Risk Reduction:	High	Low	High	Low	High	Low
$\mathbb{1}(\text{Treated}) \times \mathbb{1}(\text{Post})$	-0.0250*** (-3.23)	-0.0065** (-2.37)	-0.0343*** (-12.37)	-0.0104* (-1.87)	+0.0002 (0.05)	-0.0062* (-1.79)
Property $\times$ Cohort FE	✓	✓	✓	✓	✓	✓
CBSA $\times$ Year $\times$ Cohort FE	✓	✓	✓	✓	✓	✓
Observations	549,311	549,104	548,373	548,132	548,476	548,517
Adjusted $R^2$	0.831	0.831	0.831	0.831	0.831	0.831
Wald $t$ -stat ( $p$ -value)	-2.24 (0.025)		-3.82 (0.000)		1.20 (0.231)	

$t$ -statistics in parentheses.

\*  $p < 0.10$ , \*\*  $p < 0.05$ , \*\*\*  $p < 0.01$

**Table IA.8: Insurance Costs Around M&A Events, Heterogeneity Using Insurance Per Unit**

This table replicates the heterogeneity analysis in Table 7 with  $\log(\text{Insurance Cost Per Unit})$  as the dependent variable. See Table 7 for more details regarding the estimation and specification. Fixed effects and controls are indicated at the bottom of the table. Robust standard errors are clustered by owner. In both panels, the Wald  $t$ -statistics and  $p$ -values reported at the bottom of each panel test whether the estimated treatment effects differ between the high and low groups, both unconditionally and within each owner-size-gap subsample.

Panel A: Heterogeneity by Property Risk						
Dep. Variable:	log(Insurance Cost Per Unit)					
Owner-Size Gap:	(1) Unconditional		(3) High		(5) Low	
Property Risk:	High	Low	High	Low	High	Low
$\mathbb{1}(\text{Treated}) \times \mathbb{1}(\text{Post})$	-0.1863*** (-2.87)	-0.0714 (-0.91)	-0.3049*** (-5.67)	-0.0830 (-0.70)	-0.0358 (-0.89)	-0.0485 (-0.44)
Property $\times$ Cohort FE	✓	✓	✓	✓	✓	✓
CBSA $\times$ Year $\times$ Cohort FE	✓	✓	✓	✓	✓	✓
Observations	279,274	266,581	266,962	276,954	282,437	261,980
Adjusted $R^2$	0.872	0.901	0.871	0.901	0.872	0.901
Wald $t$ -stat ( $p$ -value)	-1.13 (0.258)		-1.70 (0.088)		0.11 (0.914)	

Panel B: Heterogeneity by Portfolio-Risk Reduction						
Dep. Variable:	log(Insurance Cost Per Unit)					
Owner-Size Gap:	(1) Unconditional		(3) High		(5) Low	
Portfolio-Risk Reduction:	High	Low	High	Low	High	Low
$\mathbb{1}(\text{Treated}) \times \mathbb{1}(\text{Post})$	-0.2038*** (-3.03)	-0.0616 (-0.86)	-0.2392*** (-2.98)	-0.1724 (-1.14)	-0.0844* (-1.65)	-0.0326 (-0.38)
Property $\times$ Cohort FE	✓	✓	✓	✓	✓	✓
CBSA $\times$ Year $\times$ Cohort FE	✓	✓	✓	✓	✓	✓
Observations	549,236	549,029	548,298	548,057	548,401	548,442
Adjusted $R^2$	0.887	0.887	0.887	0.887	0.887	0.887
Wald $t$ -stat ( $p$ -value)	-1.45 (0.148)		-0.39 (0.697)		-0.52 (0.604)	

$t$ -statistics in parentheses.

\*  $p < 0.10$ , \*\*  $p < 0.05$ , \*\*\*  $p < 0.01$



The mission of the Hutchins Center on Fiscal and Monetary Policy is to improve the quality and efficacy of fiscal and monetary policies and public understanding of them.

Questions about the research? Email [ESmedia@brookings.edu](mailto:ESmedia@brookings.edu).  
Be sure to include the title of this paper in your inquiry.